VULNERABILITY OF SLOPES WITH BUILDING LOADS IN AIZAWL

A THESIS SUBMITTED IN PARTIAL FULFILMENT OF THE REQUIREMENTS FOR THE DEGREE OF DOCTOR OF PHILOSOPHY

K. ZIRSANGZELI

MZU REGISTRATION NO: 1900352

Ph.D REGISTRATION NO: MZU/PhD/1616 of 01.08.2019

GREATER DEEDS REMAIN

ESTD MIZORAM UNIVERSITY 2001

DEPARTMENT OF CIVIL ENGINEERING

SCHOOL OF ENGINEERING AND TECHNOLOGY

NOVEMBER, 2024

VULNERABILITY OF SLOPES WITH BUILDING LOADS IN AIZAWL

By
K. Zirsangzeli
Department of Civil Engineering

Supervisor
Dr. Rebecca Ramhmachhuani

Co-Supervisor
Dr. Ruhul Amin Mozumder

SUBMITTED
IN PARTIAL FULFILMENT OF THE REQUIREMENT OF THE DEGREE OF DOCTOR OF PHILOSOPHY IN CIVIL ENGINEERING,
MIZORAM UNIVERSITY, AIZAWL

Department of Civil Engineering
School of Engineering and Technology
MIZORAM UNIVERSITY
(*A Central University*)
Tanhril, Aizawl - 796 004, Mizoram

SUPERVISOR'S CERTIFICATE

This is to certify that the thesis entitled "**Vulnerability of slopes with building loads in Aizawl**" submitted to Mizoram University for the award of the degree of **Doctor of Philosophy, Civil Engineering** by **K. Zirsangzeli**, Ph.D. Registration No. **MZU/PhD/1616 of 01.08.2019**, is Ph.D. scholar in the Department of Civil Engineering, under my guidance and supervision and has not been previously submitted for the award of any degree in any Indian or foreign University. She has fulfilled all criteria prescribed by the UGC (Minimum Standard and Procedure governing Ph.D. Regulations). She has fulfilled the mandatory publication (Publication enclosed) and completed Ph. D course work. It is also certified that the scholar has been admitted in the Department through an entrance test, followed by an interview as per UGC Regulation of 2018.

Date:
Place: Aizawl

(DR. REBECCA RAMHMACHHUANI)
Supervisor

Department of Civil Engineering
School of Engineering and Technology
MIZORAM UNIVERSITY
(*A Central University*)
Tanhril, Aizawl - 796 004, Mizoram

DECLARATION

I, **K. Zirsangzeli,** hereby declare that the subject matter of this thesis entitled "**Vulnerability of slopes with building loads in Aizawl"** is the record of work done by me, that the contents of this thesis did not form basis of the award of any previous degree to me or to do the best of my knowledge to anybody else, and that the thesis has not been submitted by me for any research degree in any other University/Institute.

This is being submitted to the Mizoram University for the degree of Doctor of Philosophy in **Civil Engineering.**

(K. ZIRSANGZELI)
Candidate

Head of the Department

(Dr. REBECCA RAMHMACHHUANI)
Supervisor

(Dr. RUHUL AMIN MOZUMDER)
Co-Supervisor

ACKNOWLEDGEMENT

Praise be to GOD for His countless blessings, wisdom, strength, and good health that have enabled me to complete this research work.

I would like to express my deepest appreciation and gratitude to my supervisors **Dr. Rebecca Ramhmachhuani** and Dr. **Ruhul Amin Mozumder**, Assistant Professor in the Department of Civil Engineering at Mizoram University. Their unwavering support, effective guidance, timely motivation, constant encouragement, and valuable suggestions have been instrumental throughout this research.

I am also grateful to the members of the Research Advisory Committee (RAC) - **Prof. Sudipta Chattopadhyay**, **Prof. K. Srinivasa Rao**, and **Dr. Lalsangzela Sailo**. Their insightful comments, encouragement, and challenging questions spurred me to broaden my research perspectives and contributed to the completion of my research work.

I am grateful for the love, support, and sacrifices my parents have made in my education and for shaping my future. I would like to extend a special thanks to my mother, **Mrs. Lalronghinglovi**, whose unwavering support and prayers have provided me with strength and good health throughout my research journey.

Last but not least, I wish to convey my heartfelt appreciation to everyone who has contributed to this endeavor, both directly and indirectly.

(K. ZIRSANGZELI)

Table of Contents

Acknowledgement			i
Table of Contents			ii
List of Figures			v
List of Tables			vii
List of Abbreviations			viii
CHAPTER			**PAGE**
Chapter 1	**Introduction**		1 - 22
	1.1	Introduction	1
	1.2	Types of slopes	3
		1.2.1 Types of slopes according to construction of slope	4
		1.2.2 Types of slopes according to its extent	5
	1.3	Causes of slope failure	5
	1.4	Types of slope failure	6
	1.5	Need for study	9
	1.6	Study area	9
		1.6.1 Lithology of the Study Area	13
		1.6.2 Structural features of the Study Area	14
		1.6.3 Slope of the Study Area	14
		1.6.4 Annual rainfall of the Study Area	14
	1.7	Objectives	18
	1.8	Methodology for assessing slope vulnerability and mapping	18
	1.9	Organization of the Thesis	22
Chapter 2	**Literature Review**		23 - 31
	2.1	Introduction	23
	2.2	Bearing capacity of soil	23
	2.3	Slope stability analysis	27
	2.4	Vulnerability zonation of slope with building loads and other factors	30
Chapter 3	**Application of regression techniques for bearing capacity prediction in Aizawl City**		32-57
	3.1	Introduction	32
	3.2	Study area	34

	3.3	Materials and Methods	34
	3.3.1	Data collection and preparation of databases	34
	3.3.2	Linear Regression Methods	38
	3.4	Regression model development	40
	3.5	Results and Discussion	42
	3.5.1	Geotechnical properties and bearing capacity of soil	42
	3.5.2	Stepwise regression	42
	3.5.3	Lasso regression	47
	3.5.4	Comparison between Stepwise and Lasso regression	54
	3.6	Summary	55
Chapter 4		**Slope stability analysis with impact of building topologies on hill slope**	57 - 84
	4.1	Introduction	57
	4.2	Study Area	58
	4.3	Materials and Methods	58
	4.3.1	Preparation of databases	58
	4.3.2	Method of slope stability assessment	59
	4.3.3	Model development	62
	4.4	Results and Discussions	65
	4.4.1	Free slope stability analysis	65
	4.4.2	Stability of slope with step back building	67
	4.4.3	Stability of slope with step back setback building	73
	4.4.4	Sensitivity analysis of soil properties (cohesion and angle of internal friction)	75
	4.4.5	Comparison of step back and step back setback building in the analysis of slope stability	79
	4.4.6	Influence of building types on the shape of the critical slip surface of the slope	80
	4.4.7	Influence of slope geometry on the shape of the critical slip failure	82
	4.5	Summary	83
Chapter 5		**Zonation mapping of slope vulnerability with building loads in Aizawl city**	85- 102

	5.1 Introduction	85
	5.2 Study Area	86
	5.3 Materials and Methods	86
	5.3.1 Data used	86
	5.4 Data Analysis	96
	5.5 Results and Discussions	97
	5.5.1 Very High Vulnerability Zone	98
	5.5.2 High Vulnerability Zone	98
	5.5.3 Moderate Vulnerability Zone	98
	5.5.4 Low Vulnerability Zone	99
	5.6 Summary	101
Chapter 6	**Conclusions**	103 - 106
	6.1 Conclusions	103
	6.2 Scope for Further Studies	106
Appendices		107-114
References		115-128
Brief Bio-data of candidate		129
List of Publications		130
Particulars of the candidate		131

List of Figures

Fig. No	Caption	Page
1.1	Images showing slope failure due to construction activities in Aizawl city	3
1.2	a) Natural slope b) Man made slope	4
1.3	a) Finite slope b) Infinite slope	5
1.4	a) Translational failure	6
	b) Rotational failure	7
	c) Compound failure	8
	d) Wedge failure	8
	e) Toppling failure	8
1.5	Map of the study area	11
1.6	Lithology map of the study area	13
1.7	Slope map of the study area	15
1.8	Annual rainfall of the study area	17
1.9	Methodology for zonation of slope vulnerability of the study area	21
2.1	The Prandtl wedge failure mechanism	24
3.1	a) Morh's circle diagram for CU type triaxial test for S24 b) Morh's circle diagram for CU type triaxial test for S34 c) Morh's circle diagram for CU type triaxial test for S55	35 36 36
3.2	Plot showing correlation of plasticity index with cohesion of soil samples collected at different sites	37
3.3	Stepwise predicted and IS 6403:1981 calculated bearing capacity for (a)strip footing (b)square footing (c) rectangular footing and (d) circular footing.	47
3.4	Performance of stepwise regression for developing model of bearing capacity of soil in terms of (a) RMSE (b) MAPE	48
3.5	Lasso predicted and IS 6403:1981 calculated bearing capacity for (a)strip footing (b)square footing (c) rectangular footing and (d) circular footing	51
3.6	Lasso regression performance for bearing capacity prediction in	52

	terms of MAPE	
3.7	Cross validation for minimum mean square error (a)strip footing (b)square footing (c) rectangular footing and (d) circular footing	53
4.1	Step back building model adopted for different slope angle	63
4.2	Step back setback building model adopted for different slope angle	64
4.3	Free slope analysis showing its factor of safety for various slope such as a) 20° b) 25° c) 30° d) 35° e) 40° f) 45°	68
4.4	Slope stability analysis with step back building under static condition showing its factor of safety for various slope such as a) 20° b) 25° c) 30° d) 35° e) 40° f) 45°.	71
4.5	Slope stability analysis with step back building under seismic conditions showing its factor of safety for various slope such as a) 20° b) 25° c) 30° d) 35° e) 40° f) 45°	76
4.6	Slope stability analysis with step back setback building under static condition showing its factor of safety for various slope such as a) 20° b) 25° c) 30° d) 35° e) 40° f) 45°	76
4.7	Slope stability analysis with step back setback building under seismic conditions showing its factor of safety for various slope such as a) 20° b) 25° c) 30° d) 35° e) 40° f) 45°	77
4.8	The resulting factor of safety for S42 with β =20°, ϕ=8° and c = (41.27,82.54,123.81) kN/m^2	78
4.9	The resulting factor of safety for S42 when β =20°, c=41.27 kN/m^2 and ϕ= (8,16,24) °	78
5.1	Comparison of the Factor of Safety obtained with step back building and step back setback building (a), (b)	81
5.2	Impact of varying factor of safety on the lowest five critical slip surface due to step back and step back setback building loads under static conditions and seismic conditions	82
5.3	Comparison of shape of the critical slip surface for varied slope angle with similar soil properties	83
5.4	SBC map of the study area	88
5.5	FoS map of the study area	90
5.6	A map showing bedrock orientation of the study area	92
5.7	A map showing vulnerability of slope with building loads (G+6) of the study area	100

List of Tables

Table No.	Title	Page
1.1	Location of the selected sites	12
1.2	Characteristics of the selected sites	16
2.1	Formulae for bearing capacity calculation	25
2.2	Minimum factor of safety in hilly area [as per IS 14243 (part 1):1995]	28
2.3	Duncan (1996) review of LEM with their assumptions, limitations, FoS and forces considered	29
3.1	Statistical analysis of parameters in the database of the study	40
3.2	Geotechnical properties and bearing capacity of soil	43
3.3	*P* values for predicted model parameter	48
3.4	Results of sensitivity analysis using stepwise regression method	54
4.1	Column loads obtained for various slope angle	65
4.2	FoS obtained in free slope analysis	66
4.3	FoS obtained with step back building	70
4.4	FoS obtained with step back setback building	74
4.5	Comparison of FoS obtained with two building topologies	79
5.1	Statistics of SBC value obtained in the study area	89
5.2	Statistics of FoS value obtained in the study area	91
5.3	Statistics of bedrock in the study area	93
5.4	Statistics of slope of the study area	93
5.5	Statistics of lithology of the study area	94
5.6	Statistics of annual rainfall of the study area	95
5.7	Parameters and their ranking in terms of their influence to slope vulnerability.	97
5.8	Statistics of vulnerability class of the study area	101
6.1	Soil properties and other related parameters of slope vulnerability assessment	107

List of Abbreviations

RCC	=	Reinforced Cement Concrete
SBC	=	Safe Bearing Capacity
FoS	=	Factor of Safety
ASTM	=	American Society for Testing and Materials
MIRSAC	=	Mizoram Remote Sensing Application Centre
Sc & Tech	=	Science and Technology
IS	=	Indian Standard
MATLAB	=	Matrix Laboratory
GIS	=	Geographic Information System
LEM	=	Limit Equilibrium Method
FEM	=	Finite Element Method
G+6	=	Ground with Six Story Building
SF	=	Safety Factor
Eq.	=	Equation
Fig.	=	Figure
q_{ult}	=	Ultimate Bearing Capacity
c	=	Cohesion of soil
γ	=	Unit weight of soil
ϕ	=	Angle of internal friction of soil
q	=	Overburden pressure
B	=	Width of foundation

D	=	Depth of foundation
N_c	=	Bearing Capacity Factors
N_q	=	Bearing Capacity Factors
N_γ	=	Bearing Capacity Factors
D_f	=	Depth of footing
s_c	=	Shape factors
d_c	=	Depth factors
i_c	=	Inclination factors
GPS	=	Generalized procedure of slices
SSI	=	Soil-structure interactions
PI	=	Plasticity Index
R^2	=	Coefficient of determination
RMSE	=	Root Mean Square Error
MAPE	=	Mean Absolute Percentage Error
ML	=	Machine Learning
AI	=	Artificial Intelligence
R	=	Pearson Correlation Coefficient
AIC	=	Akaike Information criterion
BIC	=	Bayesian Information Criterion
λ	=	Lasso Regularization Coefficient
MSE	=	Mean Squared Error
H	=	Slope height
β	=	Slope angle

AMC	=	Aizawl Municipal Corporation
LHZ	=	Landslide Hazard Zonation
SPT	=	Standard Penetration Test

CHAPTER 1

INTRODUCTION

1.1 Introduction

The surge in population worldwide is driving a surge in demand for infrastructure development yielding both favorable and adverse outcomes for inhabitants. Infrastructure advancements in both plain areas and hilly areas have brought significant benefits, including better transportation, enhanced public services, and increased economic opportunities [1]. While these developments have greatly benefited those living in plain areas, it poses significant risks to hilly regions [2]. The construction of roads, buildings, and other infrastructure often involves extensive alteration of the natural slope, which destabilizes the slopes and makes them more vulnerable to landslide induced failures [3]. As a results, assessing the vulnerability of slopes is essential before altering or modifying the natural terrain.

The vulnerability of slopes is a critical issue in geotechnical engineering, as it involves the potential for slope failure, which can lead to significant environmental, economic, and social impacts [4]. Several factors contribute to slope vulnerability, including geological (i.e., soil and rock types), slope morphology (i.e., slope angle and slope height), and human activities (i.e., excavation and loading) [5]. Different types of soils and rocks have distinct shear strengths characteristics. For instance, clayey soils can be prone to landslides due to their low permeability and high plasticity, while soils containing sand fraction are typically more prone to erosion leading to change in slope geometry and consequently may fail under certain conditions [6]. Moreover, the slope angle and slope height can influence slope stability by elevating the driving forces and increasing the soil mass causing the soil to move downward. As a result, slopes with adverse geological structures are more vulnerable to failure [7]. The human-induced factors such as excavation can remove support from the base of the slope, while adding loads from buildings or other structures can increase the driving forces acting on the slope, leading to instability and making the slopes more vulnerable. Human-induced factors are crucial contributors to slope vulnerability such as landslides, but they are also controllable with proper planning, design, and construction practices [8]. By understanding the impacts of construction practices and implementing appropriate mitigation measures, engineers can significantly reduce the risk of slope failure and enhance the stability of slopes. Therefore, assessing the vulnerability of slopes with building loads is of critical importance, mainly for hilly areas where construction of building takes place on the face of the slope or near the slope.

A hilly area like Aizawl city which often referred to as the "Land of Mountains" situated in the midst of scenic beauty of Mizoram has experienced a tremendous development in the past decades. Among these developments, the rapid increase in building construction can pose severe challenges, particularly in relation to slope failures or landslides. The construction activities such as excavation, altering natural landscape and improper land management practices can disrupt the stability of slopes and increase the risk of landslides. Figure 1.1 shows the real time images showing slope failure due to construction activities. One of the major factors contributing to this issue includes construction on steep slopes. Construction of Reinforcement Cement Concrete (RCC) structures are designed to distribute the loads from the building foundation to the underlying ground soil or rock strata. RCC buildings constructed on hill slope transfers loads to the soil in the form of vertical loads. With all these loads, the shear stress imposed on the slope can exceed the shear strength of the soil or rock strata leading to instability of slopes [9-10]. Moreover, one of the predominant cause of landslides in Mizoram also appears to be rainfall, particularly noticeable due to a sharp rise in landslide occurrences during the monsoon season. Mizoram, situated along the trajectory of the southeast monsoon, receives excessive rainfall during this period. The infiltration of rainwater heightens the pore water pressure within soil and rocks, consequently reducing their shear resistance and triggering landslides [11]. As a result, the vulnerability assessment of the slopes under building loads and rainfall infiltration is crucial, with significant implications for construction safety and sustainability. Understanding the slope and analyzing the stability of the slopes is the first and foremost steps in the assessment of vulnerability of slopes.

Fig.1.1: Images showing slope failure due to construction activities in Aizawl city.

1.2 Types of Slopes

According to geotechnical engineering, types of slopes can be determined based on the construction of slope and based on the extent of slope. According to the construction of the slope we have natural and artificial slope whereas according to the slope extent, the types of slopes can be divided into finite slope and infinite slope.

1.2.1 Types of slopes according to construction of slope.

(a) Natural slope: The slopes formed due to geological and geomorphological processes in nature as such slopes found in hilly areas as shown in figure 1.2(a).

Fig. 1.2(a): Images showing natural slope

(b) Artificial slope: Artificial slopes are created or modified by human activities to achieve specific goals, such as land development for construction of roads, railways, canals, dams and buildings respectively as shown in figure 1.2(b). Such types of slopes are also called man-made slope. Man-made slopes may be in the form of either elevated fills or excavated depressions.

Fig. 1.2(b): Images showing man-made slope. (nativerevegetation.org)

1.2.2 Types of slopes according to its extent.

(a) Finite slope: A finite slope refers to a slope with a specific, limited length or extent. In practical terms, it's a slope where the length of the slope is finite and bounded. A finite slope model is shown in figure 1.3(a).

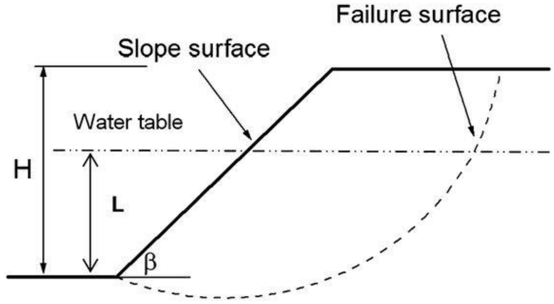

Fig.1.3(a): Finite slope [12]

(b) Infinite slope: An infinite slope refers to a slope that extends infinitely in one or more directions. This type of slope extends infinitely, or up to an extent whose boundaries are not well defined. An infinite slope model is shown in figure 1.3(b).

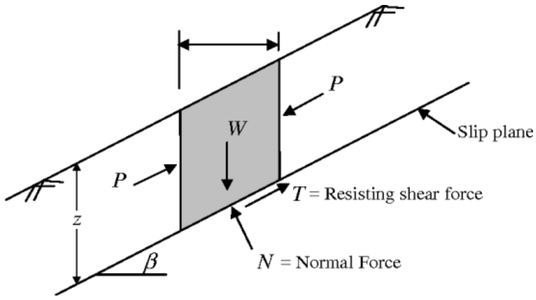

Fig.1.3(b): Infinite slope [12]

1.3 Causes of Slope Failure

Slope failure occurs when the driving force of gravity exceeds the resisting force of the slope material. Some of the causes of slope failure includes-

(a) Soil erosion: Erosion occurs when wind or rainwater carries away soil particles. It changes the shape of the slope and makes it less stable, increasing the risk of slope failure. In some cases, erosion can cause landslides, where large amounts of soil suddenly move downhill.

(b) Rainfall: When rainwater infiltrates the soil, it increases the water content within the slope. This can raise the pore water pressure, reducing the effective stress that holds the soil particles together, making the slope more susceptible to failure.

(c) Earthquakes: Earthquakes induce the dynamic forces that reduce the shear strength and stiffness of the soil. The vibrations formed by the earthquake can cause soil particles to lose contact with each other, leading to reduction in friction and consequently leads to slope failure.

(d) Geological conditions: Geological conditions of the slope such as rock type, layering, faults, and the presence of weak or fractured materials significantly influence the stability of the slope. These conditions can create zones of weakness or reduce the overall strength of the slope, leading to an increased risk of slope failure.

(e) External loading: External loading on the slope such as construction activities, traffic load, water accumulation or other activities can increase the stress on a slope, reducing its stability and can lead to slope failure. Proper engineering and slope management practices are essential to mitigate these risks when working on or near the slopes.

1.4 Types of slope failure

Slope failure is broadly classified into five types:

(a) Translational failure: Translational failure occurs where the form of the failure surface is influenced by the presence of an adjacent stratum of significantly different strength. Translational slips tend to occur where the adjacent stratum is at a relatively shallow depth below the surface of the slope. Moreover, the failure surface tends to be plane and roughly parallel to the slope as given in figure 1.4(a).

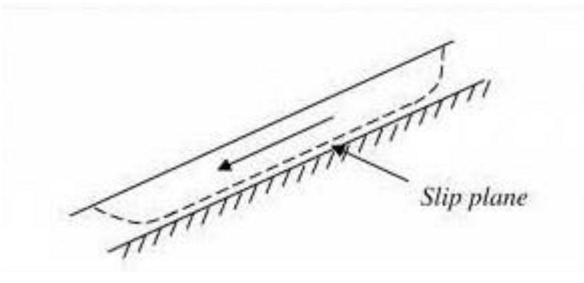

Fig:1.4(a) Translational failure [13]

(b) Rotational failure: This type of failure occurs when a mass of earth or rock moves downward and outward along a curved surface. In rotational slips, the shape of the failure surface in section may be a circular or a non-circular curve. In general, circular slips are associated with homogeneous soil conditions and non-circular slips with non-homogeneous conditions. Three different types of failure can occur under rotational failure such as face failure, toe failure and base failure. Figure 1.4(b) shows the details of different types of rotational failure.

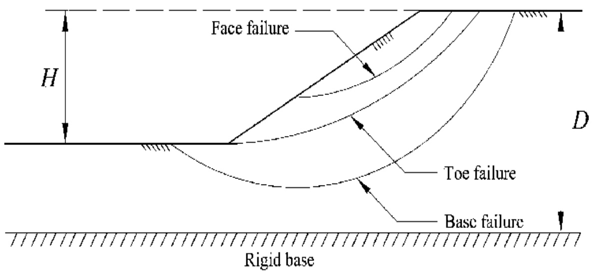

Fig:1.4(b) Rotational failure [14]

(i) Face failure: Face failure occurs when the slope or retaining wall fails near the surface or face, resulting in material slumping or sliding off the slope. This type of failure typically involves shallow surface layers and does not necessarily affect the entire structure.

(ii) Toe Failure: Toe failure occurs when the failure plane emerges near the toe of the slope, which is the bottom part where the slope meets the ground. This type of failure typically involves deeper soil layers and can be more significant, potentially affecting the stability of the entire slope or structure.

(iii) Base failure: Base failure involves the failure plane passing through the base of the slope or underneath the entire slope mass. This is often the most critical and catastrophic type of failure, as it usually involves the movement of the entire slope or structure. This failure can occur when the underlying soil or rock cannot support the weight of the slope.

(c) Compound failure: This type of failure is a combination of translational failure and rotational failure. In this type of failure, the slip surface is curved at two ends like rotational slip surface and flat at central portion like in translational failure. The image showing compound failure is given in figure 1.4(c).

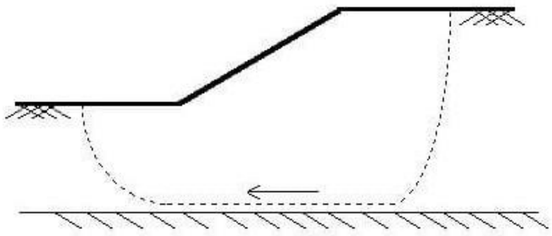

Fig:1.4(c) Compound failure [15]

(d) Wedge Failure: It occurs when two or more intersecting discontinuities within the slope create a wedge of material that can slide out. Wedge failure can occur in rock mass with two or more sets of discontinuities whose lines of intersection are approximately perpendicular to the strike of the slope and dip towards the plane of the slope. The image showing wedge failure is given in figure 1.4(d).

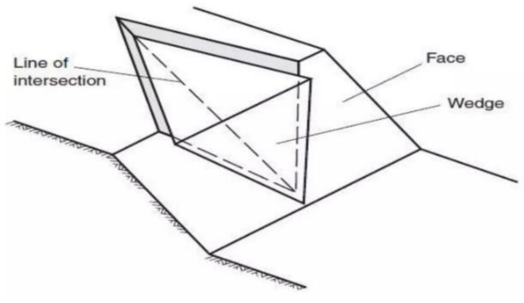

Fig:1.4(d) Wedge failure [16]

(e) Toppling failure: It is a type of failure occurs when the rock columns, blocks, or slabs rotate forward and fall due to gravity. This failure mechanism is common in steep rock slope where the rock layers or joints are oriented in such a way that they dip away from the slope face. The image showing toppling failure is given in figure 1.4(e).

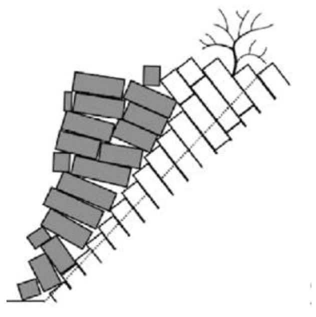

Fig: 1.4(e) Toppling failure [17]

1.5 Need for study

A hilly area like Aizawl city has experienced recently a rapid growth in development. Growing requirement in building construction in hilly slopes also brings along with it the challenges of slope failure or landslides. The construction activities such as excavation, altering natural landscape and improper land management practices can disrupt the stability of slopes and increase the risk of landslides.

The major factors contributing to this issue include construction on steep slopes. Construction of Reinforcement Cement Concrete (RCC) structures are designed to distribute the loads from the building foundation to the underlying ground soil or rock strata. RCC buildings constructed on hill slope transfers loads to the soil in the form of vertical loads. With all these loads, the shear stress imposed on the slope can exceed the shear strength of the soil or rock strata leading to instability of slopes [1,2]. Moreover, one of the predominant causes of landslides in Mizoram also appears to be rainfall, particularly noticeable due to a sharp rise in landslide occurrences during the monsoon season. Mizoram, situated along the trajectory of the southeast monsoon, receives excessive rainfall during this period. The infiltration of rainwater heightens the pore water pressure within soil and rocks, consequently reducing their shear resistance and triggering landslides. As a results, studying the vulnerability of slopes in Aizawl city by considering building loads and rainfall infiltration is crucial for ensuring construction safety and sustainability. In summary, developing a comprehensive vulnerability map of Aizawl city, considering all these factors such as building loads, safe bearing capacity (SBC) of the soil, factor of safety (FoS) of the slope, lithology, rainfall, slope morphology and bed rock respectively are crucial for ensuring the safety and sustainability of construction practices and urban development.

1.6 Study Area

Aizawl district is located in the northern part of Mizoram, in the north-east corner of India. Aizawl city, the state capital is situated within the district. With a total area of 3576.00 sq km the district is geographically located between 92°37’03” E to 93°11’45” E longitudes and 23°18’17” N to 24°25’16” N latitudes. The municipal areas of the vulnerable slopes in Aizawl city have been studied and identified. Among various vulnerable sites, 182 sites were randomly selected representing a various slope angle of 20°,25°,30°,35°,40° and 45° respectively in the study area after investigation of its history of slope failure in the past. Moreover, the selected sites are indeed a built-up area where people are residing and the area of each selected site ranges from 200sqm to 500sqm. Soil samples were collected from the selected sites and geotechnical investigation was carried out. Laboratory tests were conducted on the collected soil samples for determination of geotechnical properties and shear strength parameters of soil as per American Society for Testing and Materials (ASTM). The locations and characteristics of the 182 selected sites Aizawl city is shown in Table 1.1. The map for the selected sites is shown in figure 1.5.

1.6.1 Lithology of the study area

The earliest geological study of Mizoram dates back to 1891[18], when it was noted that the region was characterized by a flysch facies, comprising monotonous sequences of shale and sandstone [18]. Lithology, which refers to the physical and chemical characteristics of rocks, plays a critical role in assessing slope vulnerability because different types of rocks respond differently to environmental conditions and stress [19]. Based on the exposed rock types in the study area, four distinct lithology units have been identified in the area such as crumbled shale, shale sandstone, siltstone sandstone and sandstone respectively. Sandstone, being the hardest rock in the region, predominantly forms ridgelines due to its erosion resistance. Siltstone and shale sandstone, which are nearly inseparable, cover a large portion of the area as a combined unit. Crumbled shale which are the weakest rocks are the most common rock bed found in the study area. These unconsolidated material units are more prone to slope failure, thus receiving the highest weightage in vulnerability assessments. Siltstone and shale sandstone are particularly susceptible to landslides compared to the more stable sandstone units. Figure 1.6 shows the lithology map of the study area obtained by Mizoram Remote Sensing Application Centre (MIRSAC) which has been cross verified with the site investigation.

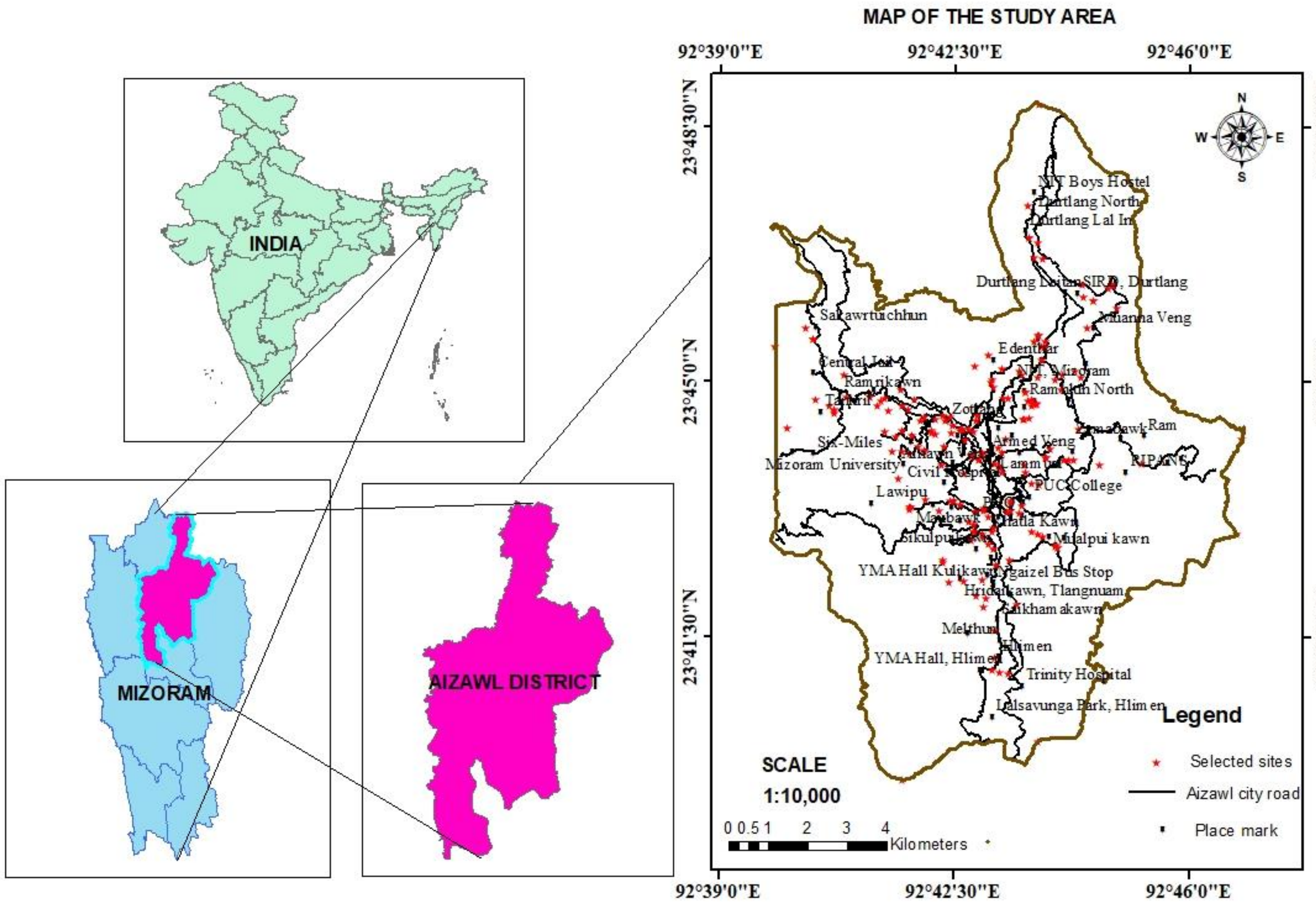

Fig.1.5: Map of the study area

Table 1.1: Locations of the selected sites.

Sites	Locations/Coordinates		Sites	Locations/Coordinates		Sites	Locations/Coordinates		Sites	Locations/Coordinates	
	Latitude (N)	Longitude (E)		Latitude (N)	Longitude (E)		Latitude (N)	Longitude (E)		Latitude (N)	Longitude (E)
S1	23.7581	92.73	S47	23.7786	92.7281	S93	23.7389	92.7028	S139	23.7206	92.7158
S2	23.7606	92.7292	S48	23.7831	92.7269	S94	23.7342	92.6953	S140	23.7228	92.7075
S3	23.7606	92.7294	S49	23.7819	92.7292	S95	23.7278	92.6946	S141	23.7202	92.7134
S4	23.7592	92.7283	S50	23.7464	92.7206	S96	23.7342	92.7008	S142	23.7219	92.7099
S5	23.7625	92.7414	S51	23.7515	92.7353	S97	23.7383	92.7028	S143	23.7228	92.7083
S6	23.7511	92.7397	S52	23.755	92.73	S98	23.7517	92.6808	S144	23.7231	92.7014
S7	23.7525	92.7383	S53	23.7578	92.7306	S99	23.7378	92.6978	S145	23.7208	92.6972
S8	23.7428	92.6783	S54	23.7517	92.7253	S100	23.7375	92.6939	S146	23.7214	92.6975
S9	23.7436	92.6786	S55	23.7525	92.7244	S101	23.7394	92.6667	S147	23.7214	92.6972
S10	23.7433	92.6786	S56	23.7461	92.7275	S102	23.7438	92.6969	S148	23.7206	92.7047
S11	23.7444	92.7275	S57	23.7461	92.7216	S103	23.7341	92.6931	S149	23.7292	92.7261
S12	23.7447	92.7283	S58	23.7478	92.7261	S104	23.7389	92.6953	S150	23.7267	92.7277
S13	23.7447	92.7289	S59	23.7458	92.7267	S105	23.7444	92.6892	S151	23.7264	92.7294
S14	23.7714	92.7467	S60	23.7453	92.7278	S106	23.7433	92.6919	S152	23.7222	92.7225
S15	23.7719	92.7478	S61	23.7453	92.7289	S107	23.7464	92.6872	S153	23.7228	92.7225
S16	23.7722	92.7475	S62	23.7504	92.7178	S108	23.7444	92.6953	S154	23.7203	92.7217
S17	23.7336	92.7153	S63	23.7537	92.7136	S109	23.7456	92.69	S155	23.7206	92.7225
S18	23.7339	92.7153	S64	23.7529	92.7203	S110	23.7464	92.6817	S156	23.7217	92.7253
S19	23.7306	92.7197	S65	23.7487	92.718	S111	23.7444	92.6773	S157	23.72	92.7247
S20	23.7308	92.7194	S66	23.7561	92.7169	S112	23.7458	92.6739	S158	23.7144	92.7156
S21	23.7292	92.7203	S67	23.7411	92.7139	S113	23.7597	92.6733	S159	23.7152	92.7154
S22	23.7327	92.7314	S68	23.7499	92.7174	S114	23.7411	92.7	S160	23.713	92.717
S23	23.7328	92.731	S69	23.7422	92.7142	S115	23.7597	92.6733	S161	23.7158	92.7133
S24	23.7417	92.7269	S70	23.7484	92.7351	S116	23.7622	92.6714	S162	23.7158	92.7133
S25	23.7414	92.7258	S71	23.7394	92.7392	S117	23.7331	92.7125	S163	23.7158	92.7178
S26	23.7414	92.7256	S72	23.7314	92.755	S118	23.7336	92.7153	S164	23.7147	92.7303
S27	23.7119	92.7342	S73	23.7322	92.7381	S119	23.7291	92.7106	S165	23.7128	92.7339
S28	23.7122	92.7336	S74	23.7311	92.7444	S120	23.7386	92.7133	S166	23.7158	92.7278
S29	23.7092	92.7056	S75	23.7322	92.7369	S121	23.7333	92.7125	S167	23.7153	92.7292
S30	23.7086	92.7056	S76	23.7311	92.7258	S122	23.7392	92.7103	S168	23.7167	92.7181
S31	23.7686	92.7431	S77	23.7369	92.7211	S123	23.7419	92.7072	S169	23.6985	92.7156
S32	23.7669	92.7486	S78	23.7346	92.7323	S124	23.7383	92.7078	S170	23.6836	92.7197
S33	23.7694	92.7406	S79	23.7322	92.7356	S125	23.7392	92.71	S171	23.6833	92.7219
S34	23.7722	92.7403	S80	23.7339	92.7203	S126	23.7393	92.7121	S172	23.7081	92.7189
S35	23.7903	92.7267	S81	23.735	92.7192	S127	23.7458	92.6983	S173	23.7004	92.7163
S36	23.7782	92.7304	S82	23.7312	92.7183	S128	23.7389	92.7097	S174	23.7011	92.7139
S37	23.7831	92.727	S83	23.7351	92.7058	S129	23.7478	92.7261	S175	23.7042	92.7072
S38	23.7511	92.7292	S84	23.7308	92.7053	S130	23.7481	92.695	S176	23.6869	92.7186
S39	23.7504	92.7334	S85	23.7344	92.7008	S131	23.7422	92.7056	S177	23.6842	92.7178
S40	23.7461	92.691	S86	23.7351	92.6994	S132	23.74	92.7081	S178	23.6931	92.7186
S41	23.7594	92.7309	S87	23.7384	92.691	S133	23.7367	92.7111	S179	23.7044	92.7108
S42	23.7339	92.715	S88	23.7336	92.6972	S134	23.7136	92.7125	S180	23.7117	92.7181
S43	23.7322	92.7144	S89	23.7411	92.7061	S135	23.7175	92.7133	S181	23.7047	92.7153
S44	23.7119	92.7342	S90	23.7414	92.7036	S136	23.7181	92.7119	S182	23.6992	92.7239
S45	23.7092	92.7222	S91	23.7381	92.7036	S137	23.7192	92.7169			
S46	23.7686	92.7431	S92	23.7421	92.701	S138	23.7211	92.7156			

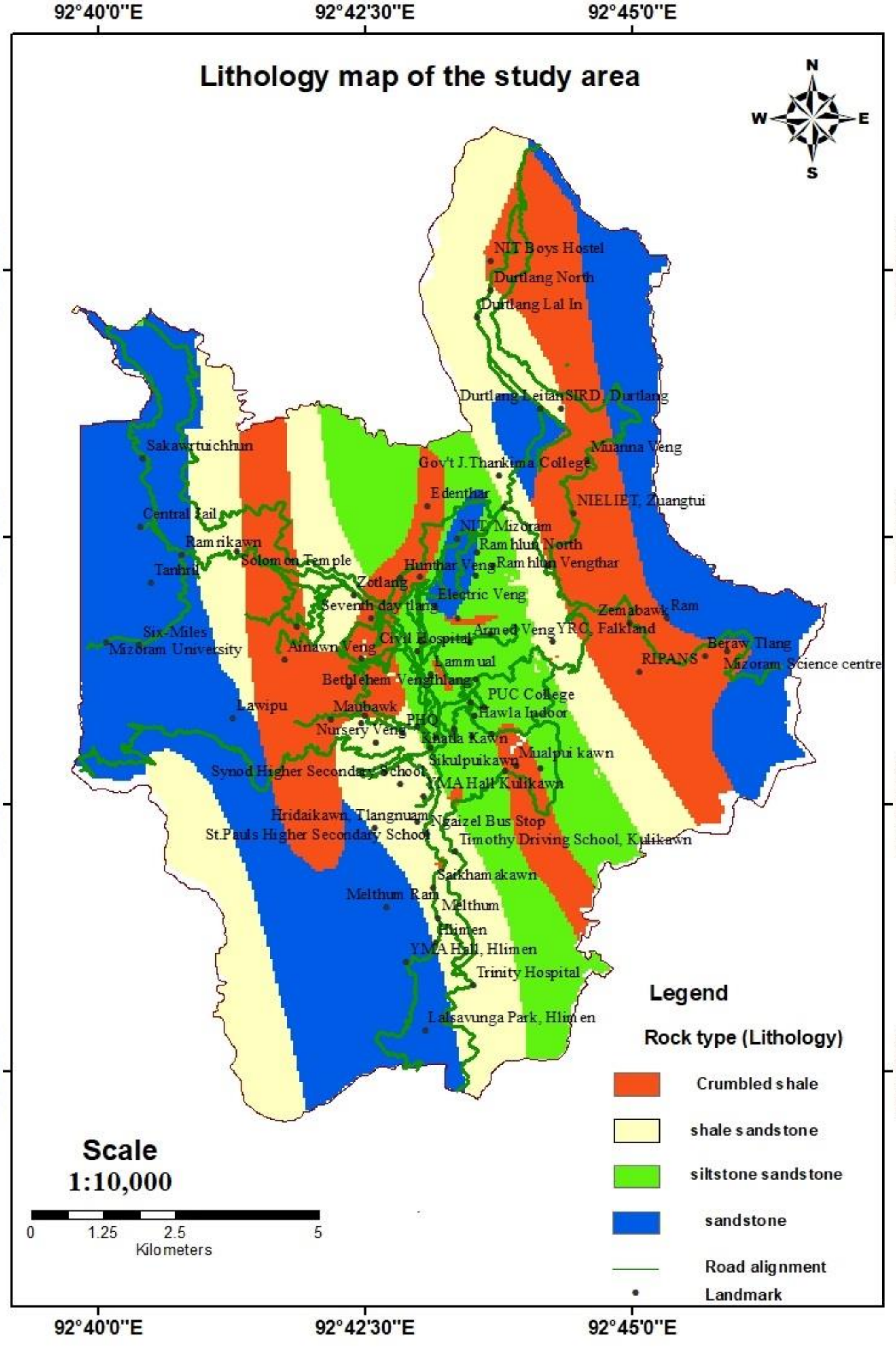

Fig.1.6: Lithology map of the study area (MIRSAC)

1.6.2 Structural features of the study area

The study area falls within the Bhuban Formation from the Miocene age and consists of shale, siltstone, and sandstone. The region is characterized by these rock types from the Surma Formation, also of Miocene age. Structural features, such as the bedding of the rock, are critical in evaluating slope vulnerability. In particular, the interaction between the slope and the bed rock is a key factor influencing slope stability. Consequently, the relationship between the slope and the bedded rocks was examined at each site and categorized into four types: anti-dip (opposite) slope, homo-clinal (parallel) slope, strike (perpendicular) slope, and oblique slope. The details of the map that illustrates the structural features by highlighting the relationship between the slope and the bedded rock has been described in Chapter 5.

1.6.3 Slope of the study area

Shear stress in soil and other loose materials tends to increase with the slope angle, making slope one of the key factors in assessing vulnerability. Landslides are more likely to occur on steeper slopes compared to moderate or gentle slopes. The slope map of the study area, produced by MIRSAC and validated through site investigations and actual slope measurements, is shown in figure 1.7. This map categorizes slopes into six ranges: 15°-25°, 25°-30°, 30°-35°, 35°-40°, 40°-45°, and 45°-60°. Weightage values are assigned based on these slope ranges to evaluate slope vulnerability. Detailed slope morphology of the selected sites is provided in Table 1.2.

1.6.4 Annual rainfall of the study area

Aizawl experiences significant amounts of rainfall each year. The city sits on steep mountains ridges that are prone to frequent landslides, especially during the monsoon season (Government of Mizoram, 2012). Rainfall indeed is one of the most important factors for assessing the vulnerability of slope. Rainfall infiltration, particularly in soil slope can lead to slope failure such as landslides. As a result, to evaluate rainfall-induced slope vulnerability, the annual rainfall map produced by State Meteorological Centre (Sc & Tech), shown in figure 1.8, is utilized. This map classifies the average annual rainfall into five categories: very low, low, moderate, high, and very high. The rainfall intensity for each category is as follows: very low (2061mm to 2205mm), low (2205mm to 2294mm), moderate (2294mm to 2376mm), high (2376mm to 2462mm), and very high (2462mm to 2611mm).

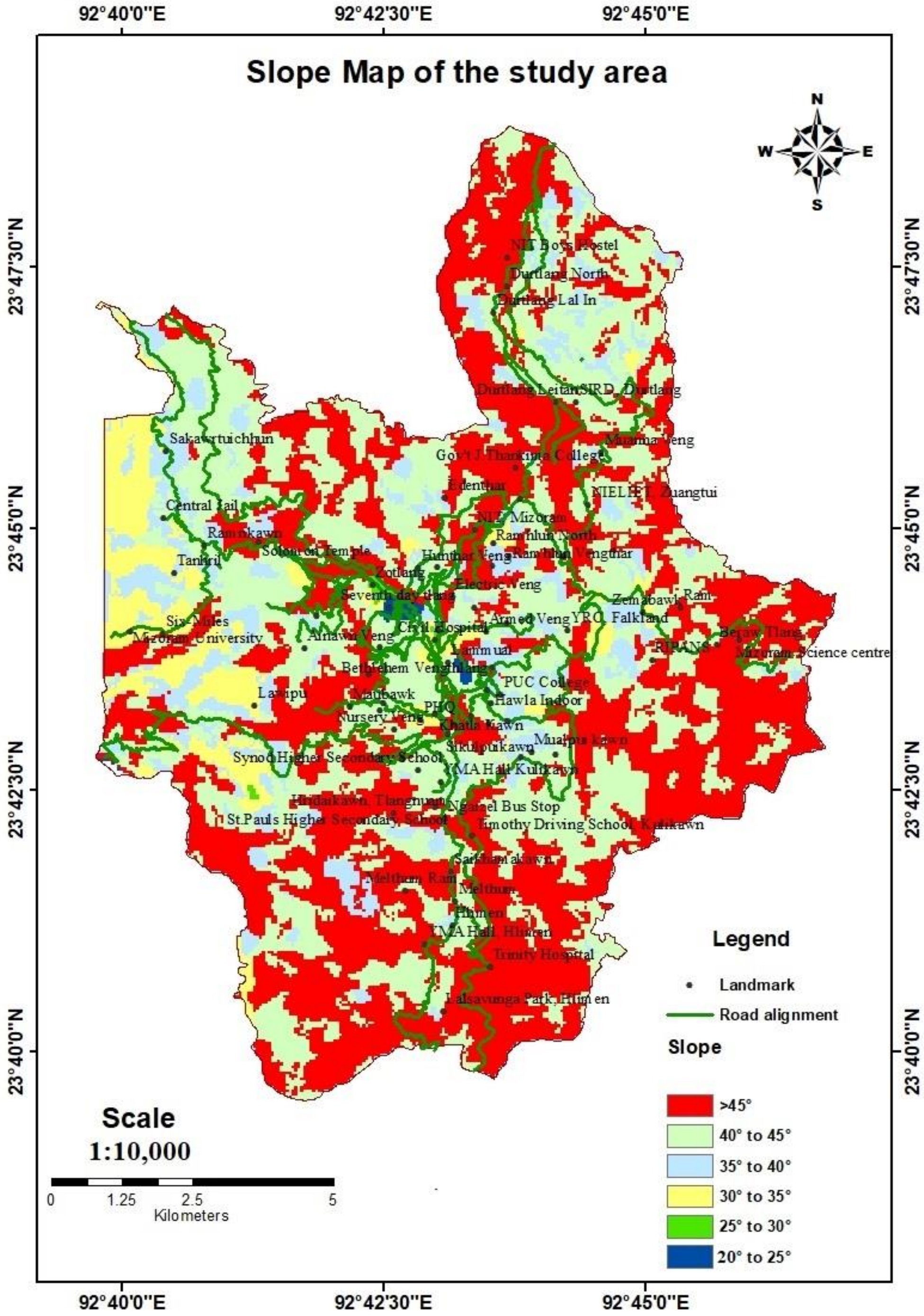

Fig.1.7: Slope map of the study area

Table:1.2 Characteristics of the selected sites

Sites	Slope morphology		Sites	Slope morphology		Sites	Slope morphology		Sites	Slope morphology	
	Slope angle (degrees)	Slope height (m)		Slope angle (degrees)	Slope height (m)		Slope angle (degrees)	Slope height (m)		Slope angle (degrees)	Slope height (m)
S1	30°	14	S47	20°	11	S93	30°	14	S139	35°	15
S2	30°	14	S48	40°	17	S94	36°	15	S140	40°	17
S3	30°	14	S49	40°	17	S95	35°	15	S141	35°	15
S4	30°	14	S50	35°	15	S96	35°	15	S142	25°	12
S5	30°	14	S51	40°	17	S97	35°	15	S143	35°	15
S6	40°	17	S52	30°	14	S98	35°	15	S144	40°	17
S7	40°	17	S53	38°	17	S99	44°	18	S145	30°	14
S8	40°	17	S54	30°	14	S100	35°	15	S146	35°	15
S9	25°	12	S55	30°	14	S101	35°	15	S147	30°	14
S10	25°	12	S56	30°	14	S102	25°	12	S148	40°	17
S11	25°	12	S57	35°	15	S103	36°	15	S149	20°	11
S12	30°	14	S58	40°	17	S104	40°	17	S150	30°	14
S13	30°	14	S59	30°	14	S105	35°	15	S151	25°	12
S14	30°	14	S60	37°	17	S106	30°	14	S152	30°	14
S15	20°	11	S61	37°	17	S107	30°	14	S153	30°	14
S16	20°	11	S62	40°	17	S108	40°	17	S154	39°	17
S17	20°	11	S63	30°	14	S109	30°	14	S155	30°	14
S18	35°	15	S64	40°	17	S110	40°	17	S156	35°	15
S19	35°	15	S65	25°	12	S111	32°	14	S157	30°	14
S20	35°	15	S66	30°	14	S112	30°	14	S158	45°	18
S21	35°	15	S67	25°	12	S113	35°	15	S159	35°	15
S22	35°	15	S68	35°	15	S114	30°	14	S160	40°	17
S23	35°	15	S69	30°	14	S115	35°	15	S161	25°	12
S24	40°	17	S70	35°	15	S116	30°	14	S162	35°	15
S25	40°	17	S71	40°	17	S117	30°	14	S163	35°	15
S26	40°	17	S72	25°	12	S118	30°	14	S164	38°	17
S27	40°	17	S73	25°	12	S119	32°	14	S165	25°	12
S28	40°	17	S74	25°	12	S120	25°	12	S166	35°	15
S29	40°	17	S75	30°	14	S121	36°	15	S167	30°	14
S30	35°	15	S76	25°	12	S122	40°	17	S168	35°	15
S31	35°	15	S77	40°	17	S123	40°	17	S169	30°	14
S32	35°	15	S78	30°	14	S124	35°	15	S170	33°	15
S33	25°	14	S79	30°	14	S125	40°	17	S171	30°	14
S34	30°	14	S80	40°	17	S126	40°	17	S172	30°	14
S35	30°	14	S81	45°	18	S127	30°	14	S173	40°	17
S36	35°	15	S82	30°	14	S128	38°	17	S174	30°	14
S37	30°	14	S83	30°	14	S129	30°	14	S175	38°	17
S38	40°	14	S84	30°	14	S130	40°	17	S176	25°	12
S39	25°	12	S85	30°	14	S131	40°	17	S177	30°	14
S40	30°	14	S86	40°	17	S132	35°	15	S178	35°	15
S41	20°	11	S87	45°	18	S133	30°	14	S179	40°	17
S42	20°	11	S88	35°	15	S134	35°	15	S180	30°	14
S43	45°	18	S89	35°	15	S135	35°	15	S181	38°	17
S44	25°	12	S90	30°	14	S136	35°	15	S182	25°	12
S45	30°	14	S91	30°	14	S137	40°	17			
S46	20°	11	S92	45°	18	S138	35°	15			

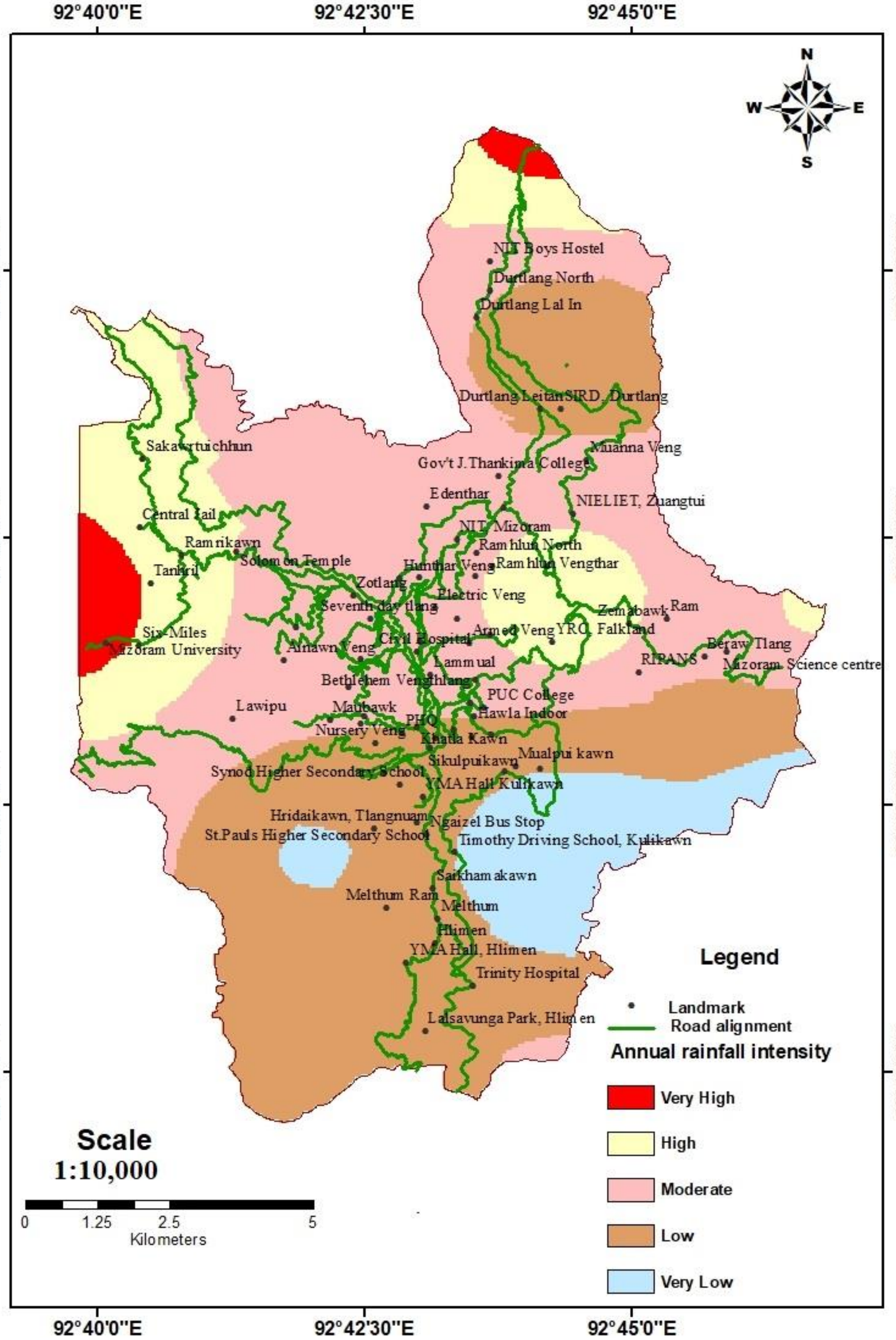

Fig.1.8: A map showing annual rainfall data (MIRSAC)

1.7 Objectives

The primary goal of this study is to identify vulnerable sites within the study area, assessing the vulnerability of various factors and conduct a comprehensive vulnerability assessment. Moreover, constructing a slope vulnerability map of the study area by incorporating the relevant causative factors. To accomplish this, the following objectives have been drafted:

1. To study land-use topology in the selected area.
2. To carry out Geotechnical investigations of the slopes.
3. To analyze Slope Stability and Vulnerability Assessment.
4. To generate a slope vulnerability map.

Firstly, examining the land-use topology within the selected area to identify how land uses may influence slope stability.

Secondly, conduct thorough geotechnical investigations to gather data on soil properties by laboratory testing such as Atterberg's Limit Test, Specific gravity Test, Compaction Test, Triaxial Test and other relevant factors that affect slope stability.

Thirdly, analyse the stability of slopes using established methodologies to evaluate potential risks and identify vulnerable areas based on geotechnical and environmental data. Lastly, generate a comprehensive slope vulnerability map of the study area, integrating all causative factors to visualize and highlight zones at risk.

1.8 Methodology

The vulnerability assessment of slopes can be carried out by evaluating various factors relevant to the objectives of the study. Additionally, a vulnerability map of the slopes can be produced by taking into account different parameters specific to the location of the study area. These parameters may include land use, geological conditions, surcharge load, soil types, lithology, slope morphology, and rainfall etc. A systematic approach should be employed to achieve the objectives of the study, which are outlined in the following steps:

1. To select endangered areas of landslides at different places in Aizawl and investigate the potential failure mechanisms.

2. Detailed in-situ investigations which include mapping topography and collection of soil samples from selected sites to determine the slope sensitivity to different triggering mechanisms.

3. Laboratory investigation of the soil samples collected from the sites to evaluate physical and engineering parameters of the soil.

4. Determination of shear strength parameters of the soil i.e., cohesion ‘c’ and angle of internal friction ‘ϕ’ for all the selected sites.

5. Using the laboratory results, determination of safe bearing capacity (SBC) of the soil by Indian Standard (IS) code IS 6403:1981 for all the selected sites.

6. Developing regression model equation of soil bearing capacity (SBC) based on varied soil properties using MATLAB software.

7. Performing free slope stability analysis without any external loads using Slope/W software.

8. Performing slope stability analysis with building loads subjected to static and seismic conditions using Slope/W software in all the selected sites.

9. Vulnerability assessment depending on the probability of occurrence of a slope failure. Developing a vulnerability map for slopes in the study area, considering building loads and various other factors using ArcGIS software.

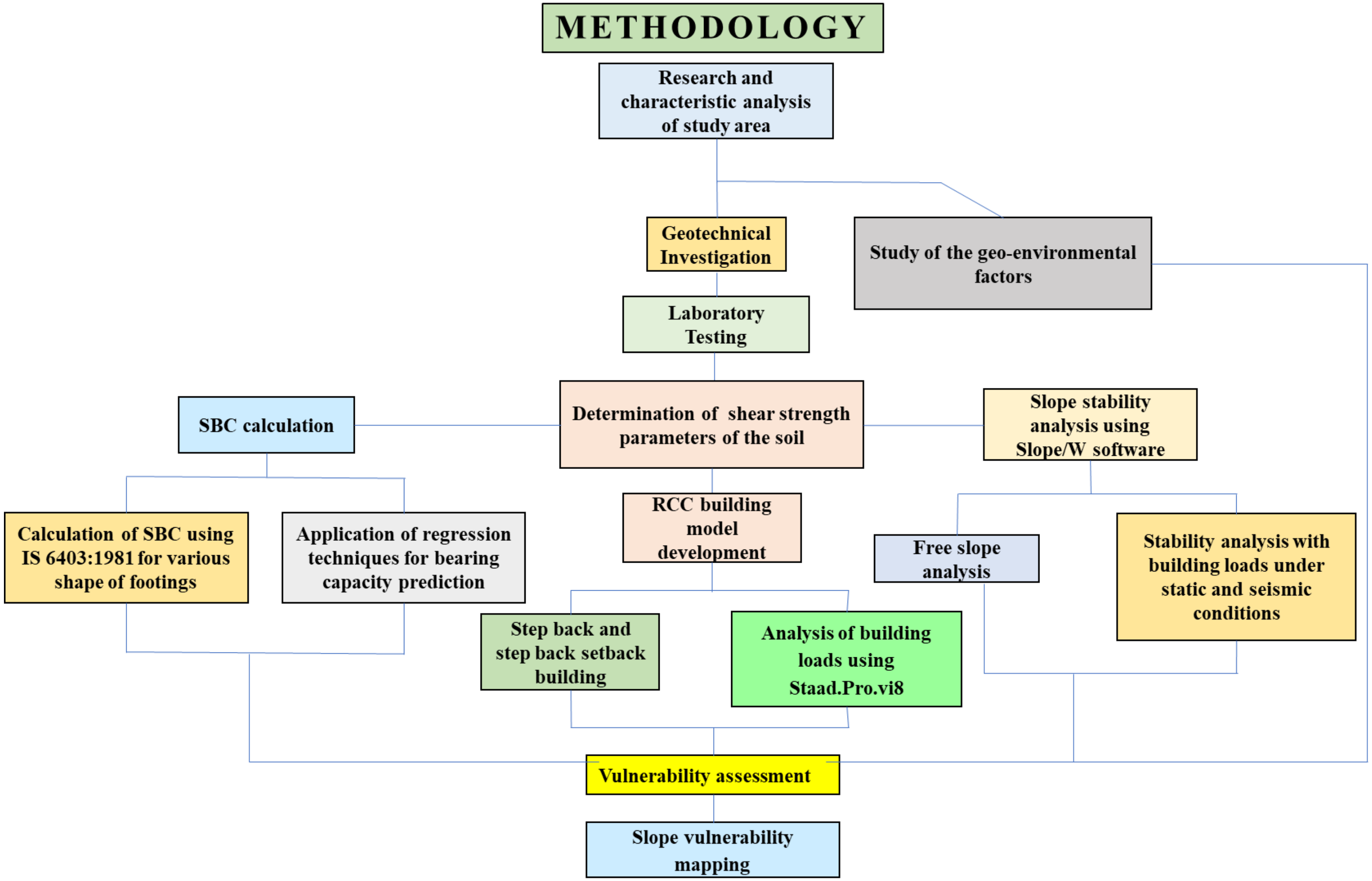

Fig.1.9: Methodology for zonation of slope vulnerability of the study area

1.9 Organization of the thesis

Chapter 1: Introduction.

This chapter outlines the necessity and importance of assessing slope vulnerability, particularly in hill regions such as Aizawl city. It examines the various factors that contribute to slope instability and potential failure, which further leads to landslides. The chapter also describes different types of slopes, potential causes of slope failure, and various types of slope failures, supported by schematic diagrams. It highlights the necessity of the study, details the locations and coordinates of the selected sites within the study area. Moreover, the chapter provides information on the existing data and maps collected and generated for the research. The chapter concludes with the aims and objectives of the research and outlines the methodology to be used in the study.

Chapter 2: Literature Review.

This chapter provides a comprehensive review of existing literature related to the prediction of soil bearing capacity, slope stability analysis, and vulnerability mapping of slopes. The objective is to contextualize the study within the current body of knowledge and identify key research trends, methodologies, and findings in these areas. The chapter contains different methods of soil bearing capacity prediction, Slope stability analysis using Limit Equilibrium Method (LEM) and Finite Element Method (FEM) and generation of vulnerability mapping by considering various factors such as rainfall data, lithology, soil types, geological conditions of the sites etc.

Chapter 3: Application of regression techniques for bearing capacity prediction in Aizawl city.

This chapter focuses on the various methods for calculating the bearing capacity of soil for different shape of footings including strip, square, rectangular, and circular footings respectively. It emphasizes the importance of accurately predicting the bearing capacity of soil, particularly in hilly regions where soil properties can vary significantly over short distances. This chapter presents a regression model developed using the IS 6403:1981 code, which incorporates regression techniques such as stepwise and Lasso regression to predict soil bearing capacity. Additionally, it includes a comparison of the performance of the two regression methods.

Chapter 4: Impact of building topologies on hill slope stability in Aizawl city

This chapter examines how different building topologies affect slope stability in the study area, focusing on two types: step-back and step-back setback buildings respectively. It details the analysis of building loads and includes a slope stability analysis for both free (unmodified) slopes and slopes affected by building loads. The analysis considers both static and seismic conditions. This chapter provides a comparison of the two building types in terms of their impact on slope stability. Additionally, this chapter explained the study on how different building types affect the critical slip failure of the slopes.

Chapter 5: Zonation mapping of slope vulnerability with building loads in Aizawl city.

This chapter outlines the various factors affecting slope vulnerability, including the Safe Bearing Capacity (SBC) of Soil, the Factor of Safety (FoS) in Slope Analysis with step-back building (G+6), Structural features such as bedrock, Slope morphometry, Lithology, and Rainfall Intensity respectively. A study map was created, incorporating each causative factor with appropriate classification and weightage values. By using these thematic layers, a final vulnerability map for slopes, considering building loads in Aizawl city, was generated. The map categorizes the area into four hazard zones: Very High, High, Moderate, and Low. The extent of each zone is provided in square kilometres, with proper weightage assigned to each causative factor.

Chapter 6: Conclusions.

This chapter provides a summary of the work conducted across each chapter of the thesis, along with the conclusions drawn from the investigations. It consolidates the findings and offers an overview of the key results obtained. Additionally, this chapter includes recommendations for future research directions in this field, suggesting areas where further exploration could be beneficial.

CHAPTER 2

LITERATURE REVIEW

2.1 Introduction

The study of slope vulnerability has been conducted by numerous researchers, with results varying based on the factors each author or researcher considers. In geotechnical engineering, slope vulnerability is often assessed based on land use, soil properties, rock characteristics, and geological conditions of the site. When assessing the vulnerability of slopes for building construction, the focus is on predicting the bearing capacity of soil and conducting slope stability analyses with building loads under both static and seismic conditions. The safe bearing capacity (SBC) of soil is crucial for designing appropriate building loads, while slope stability analysis determines the safety factor (SF) of the slope. A vulnerability map for the study area has been generated by incorporating various factors such as SBC, factor of safety (FoS), slope morphology, annual rainfall data, lithology, and structural features of the slope.

2.2 Bearing capacity of soil.

An analytical solution for calculation of bearing capacity of soil under strip load was first developed by Prandtl's in 1920 [20] as shown in Eq. (1). The assumption was made that kinematic failure of the weightless soil was caused by the strip load. The strength of the soil was determined by using the angle of internal friction, ϕ, and the cohesion, *c*. The figure 1 shows the original failure mechanism drawn by Prandtl.

$$q_{ult} = \frac{c}{\tan\emptyset}\left[\left\{tan^2\left(45+\frac{\emptyset}{2}\right)e^{\pi\tan\emptyset}\right\}-1\right] \qquad (1)$$

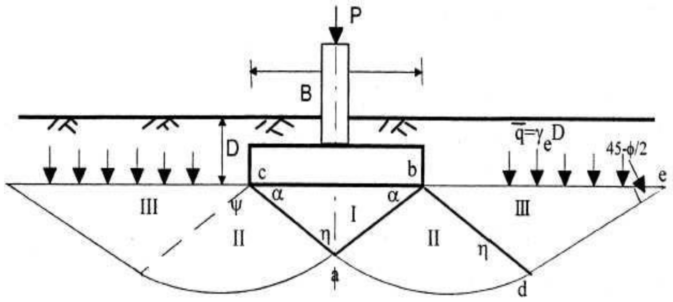

Fig: 2.1 The Prandtl wedge failure mechanism [18]

Later in 1943, Terzaghi's developed the bearing capacity calculation of soil for various footing shapes such as strip, square, circular and rectangular footings as illustrated in Eq. (1,2,3, and 4) respectively. Terzaghi's (1943) was the first to develop equations for calculating soil bearing capacity for various footing shapes. The equations developed was based on plastic theory and the superposition principle, including the weight of the soil [21].

For strip footing, $$\mathrm{q_{ult}} = 1.3\mathrm{cN_c} + \mathrm{qN_q} + 0.4\gamma\mathrm{BN_\gamma} \quad (2)$$

For square footing, $$\mathrm{q_{ult}} = 1.3\mathrm{cN_c} + \mathrm{qN_q} + 0.4\gamma\mathrm{BN_\gamma} \quad (3)$$

For circular footing, $$\mathrm{q_{ult}} = 1.3\mathrm{cN_c} + \mathrm{qN_q} + 0.3\gamma\mathrm{BN_\gamma} \quad (4)$$

For rectangular footing, $$\mathrm{q_{ult}} = (1 + 0.3\frac{\mathrm{B}}{\mathrm{L}})\mathrm{cN_c} + \mathrm{qN_q} + (1 - 0.2\frac{\mathrm{B}}{\mathrm{L}})\gamma\mathrm{BN_\gamma} \quad (5)$$

in which q_{ult} is the ultimate bearing capacity of soil, c is the cohesion of soil, γ is the unit weight of soil, q is the overburden pressure, B is the foundation width, N_c is the bearing capacity factors concerning the cohesion of soil c, N_q is the bearing capacity factors concerning the depth of foundation, N_γ is the bearing capacity factors concerning the internal friction angle of soil, ϕ.

Skempton (1951) interpreting the bearing capacity calculation of saturated clayey soil assuming undrained conditions based on Terzaghi's bearing capacity factor given in Eq. (6) [22]

$$q_{ult} = cN_c + \gamma D_f \quad (6)$$

where c is cohesion, D_f is the depth of footing, γ is the unit weight of soil and N_c is the bearing capacity factors. Meyerhof (1951) proposed a bearing capacity equation similar to that of Terzaghi wherein shape factor s_c, depth factors d_c and inclination factors i_c were taking into account [23]. Hansen (1970) provided an extension to Meyerhof (1963) by considering both the shape and depth factors which helps in capturing the influence of foundation size and embedment depth on the bearing capacity [24]. Vesic (1973) also developed an equation same as Hansen in which the bearing capacity factors for depth of foundation, N_γ was slightly changed [25]. With these methods of bearing capacity calculation along with other relevant factors and considerations, the IS 6403:1981 provides an equation of bearing capacity considerations which later on modified by so many researchers as shown in Table 2.1.

Table 2.1: Formulae for bearing capacity calculation

Authors &Codes	**Formula**	**Remarks**
Skempton, 1948 [35]	$q_{uilt(unsat)} = \left[\frac{q_{u(unsat)}}{2}\right]\left[1 + 0.2\left(\frac{B}{L}\right)\right] N_{unsat}$	Using Terzaghi's bearing capacity factor, the bearing capacity of saturated fine-grained soils are determined by considering undrained conditions.
Skempton, 1951 [22]	$q_{ult} = cN_c + \gamma D_f$	Design for clayey soil.
Meyerhof,1963 [27]		Using the shear strength of the soil, the expression for bearing capacity was derived for both shallow and deep foundations.
(i)	$q_{ult} = cN_c.s_c.d_c + \gamma.D.N_q d_q + 0.5\gamma B' N_\gamma s_\gamma d_\gamma$	
(ii)	$q_{ult} = cN_c.s_c.i_c + \gamma.D.N_q i_q + 0.5\gamma B' N_\gamma s_\gamma i_\gamma$	
Meyerhof , 1957 [36] For Shallow foundation	$q_{ult} = cN_c\lambda_{c\beta} + qN_q\lambda_{q\beta} + 0.5\gamma BN_\gamma\lambda_{\gamma\beta}$	This equation was developed for a shallow foundation near the slope edge.
Hansen, 1970 [24] *(i)*	$q_{ult} = cN_c.s_c.i_c.d_c.g_c.b_c + \gamma.D.N_q.i_q.d_q.g_q.b_q + 0.5\gamma B' N_\gamma.s_\gamma.i_\gamma.d_\gamma.b_\gamma$	Hasen equation is further the extension of Meyerhof's equation. This equation can be used for any types of foundations for calculating bearing capacity.
(ii)	$q_{ult} = 5.14.c_u(1 + s_c' + d_c' - i_c' - g_c' - b_c') + \gamma.D$	
Meyerhof, 1974 [37]	$q_{ult} = C_{uo}N_c + q_o + 2(H^2\gamma' + 2H_{qo})$	Based on the punching shear method for sand overlaying clay

Vesic, 1975 [38]	$q_{ult} = (5.14 - 2\beta)c + \gamma D_f(1 - \tan\beta)^2 - \gamma B \sin\beta\,(1 - \tan\beta)^2 - 2\beta$	Vesic concluded that the bearing capacity factor N_γ has a below zero value for frictionless soil when the weight of the soil is not considered. Considering,$N_c = 5.14$ and $N_q = 1$
IS 6403:1981 [39] 1)General shear failure	$q_{ult} = cN_c.s_c.d_c.i_c + q.(N_q - 1)s_q d_q i_q + B\gamma' N_\gamma s_\gamma d_\gamma i_\gamma W'$	Based on shear and allowable settlement criteria by taking into consideration the footing's shape, the loading's inclination, the embedment's depth, and the water table's impact.
2)Local shear failure	$q_{ult} = cN'_c.s_c.d_c.i_c + q.(N'_q - 1)s_q d_q i_q + B\gamma' N'_\gamma s_\gamma d_\gamma i_\gamma W'$	
Rankine's,1885 [40]	$q_{ult} = \gamma D_f \left[\frac{1 + \sin\emptyset}{1 - \sin\emptyset}\right]^2$	Design based on loose earth, dry granular sandy soil
Eurocode 7, 1996 [41] *For pile foundation*	$q_{ult} = (N_q \times q)A_B + \left(L \times \frac{\gamma}{2} k_s \tan\gamma\right) A_s$	The Eurocode 7 bearing capacity method follows the Vesic method with a few minor alterations. It uses Chen's equation for Nγ, which assumes a rough base.
Huang & Meng, 1997 [42]	$q_{ult} = \eta\gamma + (B + \Delta B)N_\gamma + \gamma d N_q$	An analysis of maximum bearing capacity of a ground improvement foundation by employing the deep-footing and wide-slab failure technique.
Oloo et .al, 1997 [43]	$q_{ult} = [c' + (u_a - u_w)\tan\emptyset^b]N_c\varepsilon_c + qN_q\varepsilon_c + 0.5B\gamma\varepsilon_\gamma N_\gamma$	The equations developed according to the supposition that the bi-linearity of unsaturated soil ultimate bearing capacity failure envelope.
Wayne et al., 1998 [44] *Square footing*	$q_{u(R)} = q_b + \frac{4c_a s_a d}{B} + 2\gamma_1 d^2 \left(1 + \frac{2D_f}{d}\right)\frac{k_s S_s \tan\emptyset_t}{B} + \frac{4\sum_{i=1}^{n} T_i S_t \tan\delta}{B} - \gamma_t d$	Based on the failure modes of reinforcement an analytical approach for assessing the ultimate bearing capacity of reinforced soil foundations.
Yang et al., 2005 [45]	$q_{ult} = 2C_t B_o(f_4 + f_5 + f_6) - \frac{\gamma B_o^2}{2}(f_1 + f_2) - q_o B_o f_3$	Using upper bound solution with modified Hoek-Brown failure.
Cerato et al., 2006 [46] For square and circular footing on cohesionless soil	$q_{ult} = 0.5\gamma B N_\gamma^*$	Modified SBC factors of Terzaghi's. The bearing capacity factors depend on relative density, shape factors and width of footings.

Vanapalli & Mohammed, 2007 [47]	$q_{ult} = \{c' + (u_a - u_w)b[1 - S^{\varphi_{BC}} \tan \emptyset'] + (u_a - u_w)_{AVR} S^{(\varphi_{BC})} \tan \emptyset'\} N_c \varepsilon_c + 0.5 B\gamma \varepsilon_\gamma N_\gamma$	The equations were developed by employing the effective shear-strength parameters and the soil and water relationships curve.
Sherif et al., 2007 [48]	$q_{ult} = cN_c + D\gamma_x N_q + 0.5B \tan \beta_m \gamma_\gamma N_\gamma$	Based on Terzaghi's equation ($\alpha - method$)
Chen, 2008 [49]	$q_{ult} = cN_c + qN_q + 0.5\gamma B N_\gamma + \Delta_{qr}$	Bearing factors are the same as Taraghi's (1943), whereas $\Delta_{qr}$is greater bearing capacity as a result of tensile force
Kalindi et al., 2010 [50]	$q_{ult} = x_1 \gamma D^{x_2}. N_q. F_{aqs}. F_{qd} + x_3 \gamma B^{x_4} N_\gamma F_{\gamma s} F_{\gamma d}$	Modified Meyerhof's (1963) equation.

In the context of India, current practice for estimation of bearing capacity of shallow foundation is based on the provisions laid by Indian Standard (IS) code IS 6403:1981. The IS code includes the shape factors, depth factors, inclination factors and water table following the equation given by Vesic (1973). For footing located near or on the slope, due to the constrained zone of passive resistance that develops towards the slope face, it is assume that the foundation will have less bearing capacity [26]. Meyerhof (1963) proposed an equation which includes the slope height and the slope angle for shallow continuous foundation located on the slope or near the slope for purely cohesive and cohesionless soil [27]. Several researchers have conducted studies on an extension of Meyerhof equation for calculating bearing capacity on or near slope ground mainly for strip footing [28-34].

2.3 Slope Stability Analysis

The purpose of slope stability analysis is to assess the stability of natural or man-made slopes such as hillsides, embankments or excavations. The analysis aims to determine whether the slope is prone to failure or can safely withstand the forces acting upon on it. Slope stability is normally assessed using the safety factor (SF) which is defined as the ratio of average shear strength of soil to the average shear stress acting along the potential failure surface. The average shear strength of the soil greater than the average shear stress acting on slope implies stability of a slope. Conversely, a slope is considered unstable if the average shear stress exceeds the shear strength of the soil, suggesting potential instability and an increased risk of slope failure [51-55]. Table 2.2 shows the value of factor of safety for slope stability analysis. According to IS 14243 (part 2):1995 shown in Table 2.2, for analyzing the stability of soil slope, the minimum factor of safety in hilly area should be 1.5 and 1.2 under static and seismic conditions [56].

Table 2.2: Minimum factor of safety in hilly area [as per IS 14243 (part 1):1995]

Type of soil	**Static factor of safety**	**Dynamic factor of safety**
Soil slope/Talus/debris slope	1.5	1.2
Rock slope	1.2	1.0

Several researchers have conducted the slope stability analysis involving multiple problems with variant soil properties using different methods of slope stability analysis [57-62]. Of all the methods, the Limit Equilibrium Method (LEM) and the Finite Element Method (FEM) are the two most commonly used methods for slope stability analysis. The LEM is a traditional method and is widely used due to its simplicity and quick calculation. It is based on the assumption of a predefined failure surface and evaluates the equilibrium conditions along the surface. LEM for slope stability analysis require evaluating the driving forces (shear stress) and the resisting forces (shear strength) to assess the safety factor. The LEM is a typical approach used in slope stability analysis to analyze the slopes and embankments. The concept implies that a slope will fail when the driving force (gravity, applied loads or external pressures) exceeds the resisting force (soil shear strength). When the driving forces equal the resisting forces, the equilibrium condition is attained, and any further rise in driving forces results in slope failure [63-66]. Various LEM approaches presented by Duncan [67] include Fellenius method, 1927 [68], Modified Bishop Method, 1955 [69], Janbu Simplified Method, 1968 [70], Morgenstern- Price method, 1965 [71] and Spencer method, 1967 [72]. Fellenius [68] developed the first method for a circular slip surface, known as the Ordinary or Swedish method. Bishop

[69] proposed the first technique, which introduced an entirely novel equation for the base normal force. As a result, the FoS equation became non-linear. Simultaneously, Janbu [70] developed a simplified approach for non-circular failure surfaces that involved separating a possible sliding mass into numerous vertical slices. The generalized procedure of slices (GPS) was created concurrently with the advancement of the simpler approach. Morgenstern-Price [71], Spencer [72], Sarma [73], and others later contributed with alternative assumptions for the interslice forces. All these methods of LEM are based on the assumption that the slope is divided into slices and each slice is analyzing separately. This assumption allows the analysis to simplify the complex problem of slope stability into smaller and manageable parts. Each method of LEM has its own set of assumptions and limitations, and the choice of method depend on the specific characteristics of the slope and the level of accuracy required for the analysis as shown in Table 2.3 [74-75].

Table 2.3**:** Duncan (1996) review of LEM with their assumptions, limitations, FoS and forces considered.

Methods	Equilibrium conditions, Assumptions and Limitations	Forces considered	Factor of safety (FoS) equations
Ordinary method of slices, 1927 [68]	Based on static equilibrium, satisfies only vertical force equilibrium, neglect interslice forces, applies only in circular slip surfaces, low FoS.	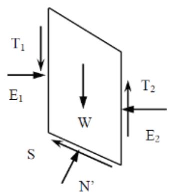	$F_m = \frac{\sum(c'l + \tan\emptyset' W \cos\alpha)}{\sum W \sin\alpha}$
Modified Bishop method,1955 [69]	Based on static equilibrium, satisfies vertical force equilibrium and overall moment equilibrium, consider normal interslice forces but neglect interslice shear force, applies only in circular slip surfaces, accurate FoS.	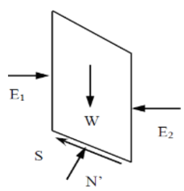	$F_m = \frac{\sum(c'l + N' \tan\emptyset')}{\sum W \sin\alpha}$
Janbu Simplified method, 1968 [70]	Based on static equilibrium, satisfies all conditions of equilibrium, considers both the normal interslice forces and interslice shear force, applies for any shape of slip surfaces, accurate FoS.	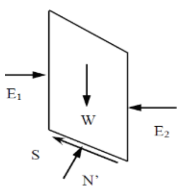	$F_m = \frac{\sum(c'l + (N - ul)\tan\emptyset')\sec\alpha}{\sum W \tan\alpha + \sum \Delta E}$

Morgenstern-Price method, 1965 [71]	Based on static equilibrium, satisfies all conditions of equilibrium, considers both interslice forces including interslice shear force and normal force, applies for any shape of slip surfaces, accurate FoS.	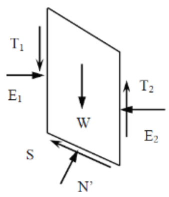	$F_m = \dfrac{\sum(c'l + (N - ul)\tan\emptyset')}{\sum W \sin\alpha}$
Spencer method, 1967 [72]	Based on static equilibrium, it satisfies all equilibrium criteria, takes into account both interslice forces, including interslice shear force and normal force, and can be applied to any shape of slip surface, accurate FoS.	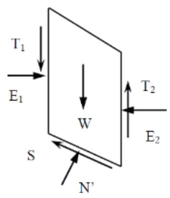	$F_m = \dfrac{\sum(c'l + \sigma'\tan\emptyset')}{\sum W \sin\alpha + P \sin\alpha}$

The main issue of the slope instability experienced in Aizawl city can be attributed to the interplay between soil conditions and construction practices where inadequate slope management has been followed with the non-engineered building construction. A study of Soil-structure interactions (SSI) in hilly area defines that building topology play a substantial effect in the stability of the slope. Furthermore, the location of the foundation has an impact on the slope stability analysis due to the intensity of the load [9,10]. There is, however, a scarcity of research on how different building topologies affect the slope instability at various slope angles, particularly in Aizawl, where buildings of 15m to 21m height are situated on a 20° to 45° slope angle. The majority of structures in Aizawl City have been constructed without having the knowledge on how the building configuration affects slope instability, resulting in numerous slope failures. As a result, the overall safety of the building on hill slope also depends on the stability of slope [76,77]. Buildings constructed on sloping ground can be designed with various structural configurations to ensure safety, provided that appropriate structural design principles are followed and high-quality materials are used. However, with the unstable slope, the proper structural design with good quality of materials can collapse [78]. Therefore, analyzing the impact of different building topologies on hill slope stability is crucial.

2.4 Vulnerability zonation of slopes with building loads and other factors

A landslide vulnerability of slopes zonation map has been developed by several researchers depending on various factors such as land use, slope geometry, rainfall, drainage density, lithology, fault density and soil properties [79-83]. The study of zonation of landslide susceptibility and risk assessment are mainly carried out by direct and indirect method [84]. Certainly, direct approaches encompass methods like distribution analysis (or inventory analysis), geomorphic analysis, and heuristic evaluation techniques, which rely on the expertise and judgment of evaluators which is also referred to as qualitative approaches. On the other hand, indirect method involves statistical, deterministic, probabilistic, and distribution-free techniques which is also referred to as quantitative approaches [85-91]. Qualitative methods are inherently subjective, influenced by the perspectives and interpretations of those conducting the analysis, while quantitative methods are objective, relying on numerical data, measurements and statistical analysis to derive insights and draw conclusions. The landslide zonation map of various districts of Mizoram has been developed by a very few researchers using Remote sensing and Geographical Information System (GIS). These zonation maps of landslide were developed mainly based on geoenvironmental factors such as socio-economics, slope morphometry, geomorphology, lithology, geological structure, physical footprint, land use, relative relief [79, 92]. Moreover, the landslide hazard zonation map was also developed for Siaha, Champhai, Saitual, Aizawl, Hnahthial and Lunglei district based on qualitative approach with the detailed geological survey of the study area from the satellite imaginary, aerial photographs, topographic map and ground reality [93- 96].

CHAPTER 3

APPLICATION OF REGRESSION TECHNIQUES FOR BEARING CAPACITY PREDICTION IN AIZAWL CITY

3.1 Introduction

The bearing capacity of the soil is an important criterion in foundation design. Terzaghi's method is a commonly used method for determining the bearing capacity of soil. However, the need for a bearing capacity model in terms of index properties of soil remains critical. In this regard, the present study aims to develop a data driven regression techniques-based bearing capacity prediction model using index properties of soil as its input parameters. To this end, two different methods namely stepwise linear regression and Lasso regression were adopted for developing the bearing capacity prediction model. From 50 different locations in Aizawl City, soil samples were collected and tested in the laboratory. Thus, obtained geotechnical properties from laboratory test were used for determining the bearing capacity of each location for various types of footing such as strip, square, rectangular and circular footing respectively. These 50 data points contain bearing capacity as output and geotechnical index properties such as plasticity index (PI), dry unit weight of soil (γ), cohesion (c) and angle of internal friction (ϕ), the width of foundation (B) and depth of the foundation (D) constitute the dataset and were fed into regression models for training and testing. Performance comparison of stepwise regression with Lasso regression suggested that stepwise regression performed marginally better than Lasso regression in terms of R^2 value. RMSE and MAPE values of both the models were comparable. Also, stepwise performed better than Lasso regression from model complexity point of view with eight (8) predictor terms in comparison to the nine (9) terms in Lasso regression equation. However, based on the input parameters included in the model equation, it may be concluded that Lasso regression has an edge over stepwise regression in simulating the physical process in bearing capacity prediction for our data set. In each site, the square footing has the maximum bearing capacity when compared to the other types of footings. The combination of low PI, higher unit weight of soil and high shear strength parameters can influence high bearing capacity.

The main purpose of this study was to develop a model equation for assessing soil bearing capacity using regression techniques such as stepwise regression and Lasso regression. In geotechnical engineering, Machine Learning (ML) were employed to estimate the bearing capacity of foundations by establishing empirical relationships between bearing capacity and various soil parameters [97]. Few researchers have also used Machine learning to forecast the pile load capacity (both axial load capacity and lateral load capacity) [98-99]. Some studies also focused on bearing capacity prediction using machine learning techniques for soil subjected to some treatment by ground improvement methods [100-102].

The existing publications as stated in the literature review mainly focused for prediction of bearing capacity for pile foundation in a plane region using ML. According to a compilation of the catalogue of the building typologies in India, the majority of the building structures in hilly north-eastern regions are supported by shallow isolated footings [103]. As a result, model prediction of bearing capacity of shallow foundation in hilly areas using ML is crucial as most buildings in Aizawl City are constructed without considering the bearing capacity of the soil, resulting in numerous slope failures. To these consequences, for hilly areas where the soil properties vary significantly over short distances due to topography, erosion and the influence of water drainage, there should be a specific equation for calculation of bearing capacity for various shapes of footing based on the soil properties. There are, however, limited papers on developing regression model based on varied soil properties, particularly in hilly areas.

Keeping the research gap from existing studies in mind, a regression model based on IS 6403:1981 [39] was developed by implementing a stepwise regression and Lasso regression for computation of bearing capacity of shallow foundation for various shapes of footing such as strip, square, rectangular and circular footing respectively. Furthermore, the developed models were tested and validated. Sensitivity analysis was also performed to see how changes the input parameters affect the model predictions.

3.2 Study area

The municipal areas of the vulnerable slopes in Aizawl city have been studied and identified. Among various vulnerable sites, 50 sites (S1 to S50) were selected as the study area after investigation of its history of slope failure in the past. Moreover, the selected sites are indeed a built-up area where people are residing and the area of each selected site ranges from 200sqm to 500sqm. Soil samples were collected from the selected sites and geotechnical investigation was carried out. Laboratory tests were conducted on the collected soil samples for determination of geotechnical properties and shear strength parameters of soil as per American Society for Testing and Materials (ASTM). The locations and characteristics of the 50 selected sites in Aizawl city are shown in Table 1.1. The map for the selected sites is shown in Figure 1.3.

3.3 Materials and methods

3.3.1 Data collection and preparation of databases

The undisturbed soil samples were collected using a thin-walled sampler (IS 2132-1972, ASTM D1587) [121,122] from various sites in Aizawl Municipal area for this study. The samples were collected within a depth of 2m from ground surface or occurrence of rocky strata, whichever happened earlier depends on the thickness of overburden of soil. The soil samples were transported in an airtight container to the laboratory for testing. The soil samples were first tested using the triaxial test directly from airtight containers. After oven-drying at 105–110°C for 24 hours, the samples were used for other tests such as specific gravity, liquid limit, plastic limit, and the Standard Proctor test.

The triaxial compression test was carried out on cylindrical soil specimens prepared from field samples. Each specimen was subjected to a combination of axial stress (applied vertically through the loading ram) and confining stress (applied laterally through a cell fluid). The test was conducted under consolidated undrained (CU) conditions with pore water pressure measurement, in accordance with the provisions of ASTM D4767-11 (2020) [123].

The samples were tested at their natural field moisture content without prior oven-drying. For each soil specimen, the confining pressures applied ranged between 50 kPa and 200 kPa, representing the anticipated in-situ stress conditions of the sites. The strain rate was maintained at approximately 0.5–1.0 mm/min, ensuring uniform loading and adherence to the standard recommendations. Drainage was not permitted during shearing, consistent with undrained test requirements.

Three specimens were tested for each site, and the average values of cohesion (c) and angle of internal friction (ϕ) were reported as the representative shear strength parameters. The stress–strain data obtained were used to construct Mohr's circles for selected critical sites (S24, S34, and S55) shown in figures 3.1(a), 3.1(b) and 3.1(c) respectively. From these, the failure envelope was plotted, and the shear strength parameters were estimated.

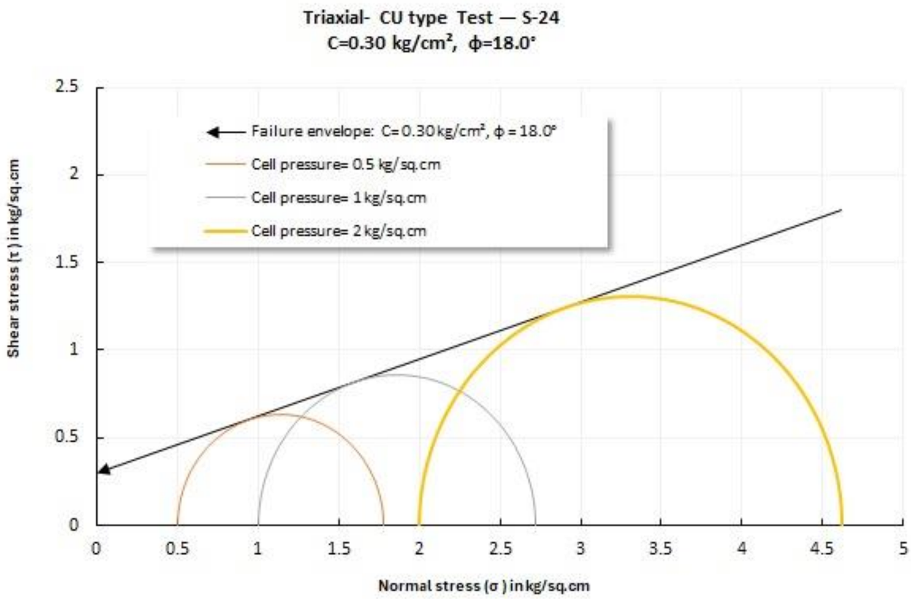

Fig.3.1(a): Morh's circle for CU type triaxial test for S24.

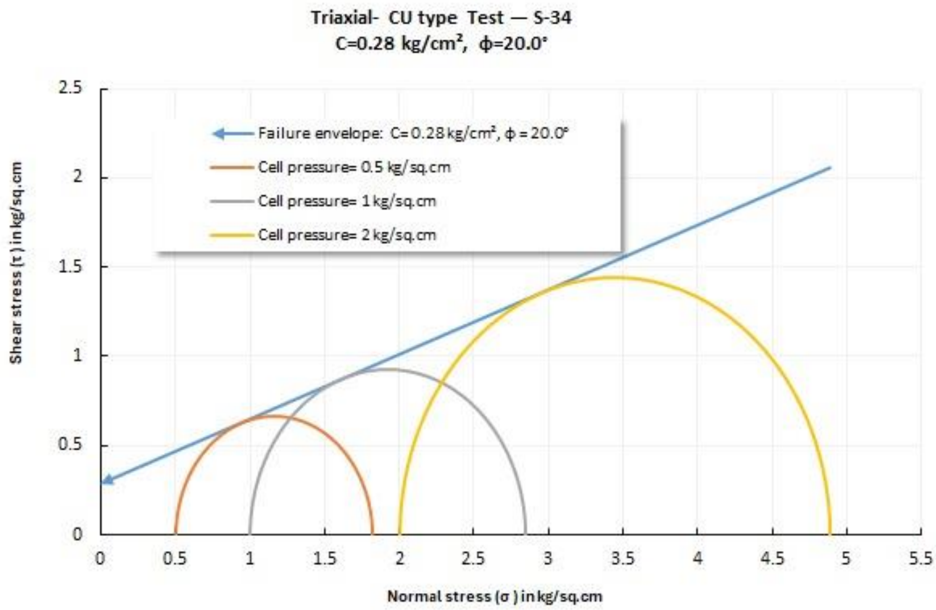

Fig.3.1(b): Morh's circle for CU type triaxial test for S34.

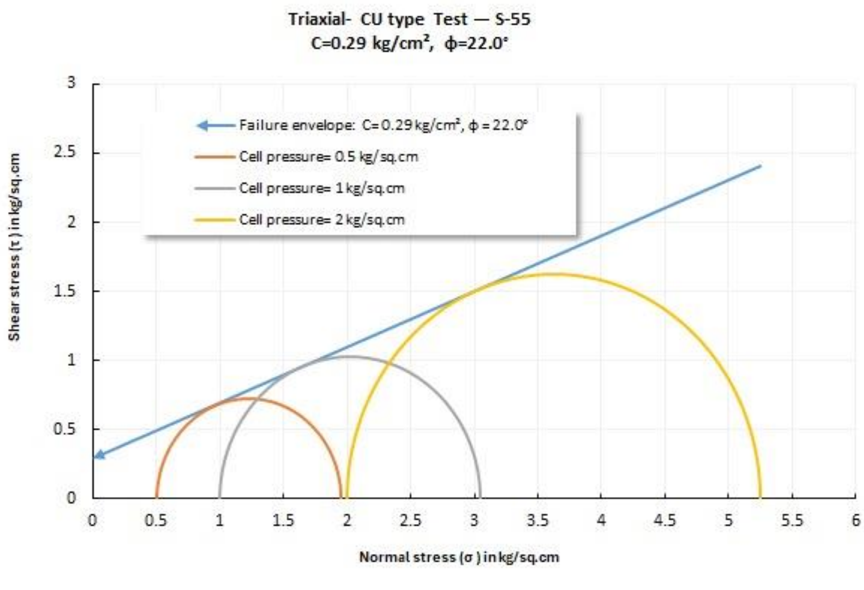

Fig.3.1(c): Morh's circle for CU type triaxial test for S55.

The Standard Proctor test was performed to determine the optimum moisture content and density of the compacted soil sample by using proctor compaction apparatus. This was conducted based on following the guidelines of ASTM D698-12 (2021) [124]. The specific gravity test was conducted using Pycnometer method as per ASTM D854-23 (2023) [125], the Atterberg's limit test includes Liquid Limit test and Plastic Limit test which was conducted using Casagrande's liquid device and rolling thread method as per ASTM D4318-17e1 (2018) [126]. The plasticity index was calculated as the difference between the liquid limit and plastic limit. Based on the laboratory results, the soil types were categorized according to USCS soil classification referring IS 1498(1970) [127]. Using the obtained geotechnical properties, the bearing capacity of soil for different types of footing such as strip, square, rectangular and circular footings respectively were calculated based on IS 6403:1981 [128]. For each site, the type of shear failure mechanism (General or Local) was determined based on soil consistency, classification, and strength parameters, as recommended in IS 6403:1981. Specifically, soils exhibiting low cohesion and high friction angles (such as ML, MI, and soft clays) were treated as undergoing local shear failure, while soils with moderate to high cohesion and lower friction angles (such as CL, CI) were assumed to fail by general shear. The selected failure mode for each site was then used to guide the bearing capacity calculations, with strength parameter reductions applied for local shear cases as per IS 6403.

In order to check for any inconsistency in the soil sample data collected from both site and laboratory which essentially forms the major component of the database for regression technique-based models, following figure 3.1 is provided.

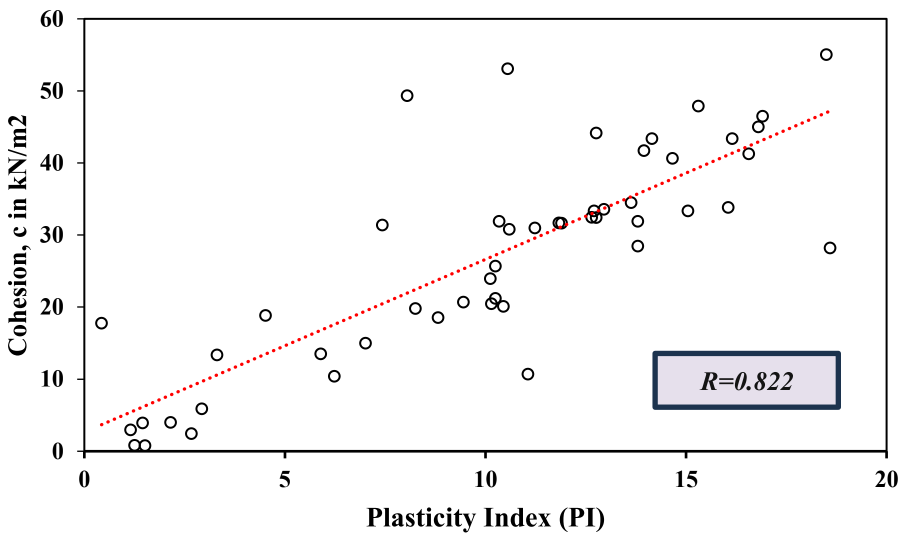

Fig.3.2: Plot showing correlation of plasticity index with cohesion of soil samples collected at different sites.

The figure 3.2 shows the variation of cohesion with plasticity index, PI and it may be observed that both are strongly and positively correlated. In general, plasticity index among other factors depends on surface area of soil [104]. Plasticity index increases with increase in surface area which is also an indicator of increase in cohesive bonding resulting in an increase in cohesion of the soil [105]. Thus, formed database was subsequently used for developing regression method-based bearing capacity models, details of which are discussed below.

3.3.2 Linear Regression methods

(i) Stepwise linear regression:

Stepwise regression is a method used in statistical modelling and machine learning to select a subset of features or predictors that have the most significant impact on the dependent variable. It is an iterative process that starts with an empty model and adds or remove features based on their statistically significant [106]. The stepwise regression typically follows one of the two approaches i.e.; forward selection or backward elimination. Both the forward selection and backward elimination can utilize the AIC (Akaike Information criterion) or the BIC (Bayesian Information Criterion) as criteria for selecting features [107].

The forward selection starts with an empty model and evaluate each feature's individual relationship with the dependent variable using a predetermined criterion, such as p-values or a measure like the AIC or BIC. The forward selection adds the feature that has the strongest relationship with the dependent variable, based on the chosen criterion. It continues adding the features one by one, evaluating their significance at each step, until no more features meet the predetermined criterion. Similarly, the backward elimination starts with a model that includes all available features and then evaluating the significance of each feature using the chosen criterion, such as p-values, AIC or BIC. It removes the feature with the weakest relationship with the dependent variable, based on the chosen criterion (i.e., AIC or BIC), This process is repeated by evaluating the significance of the remaining features and removing the least significant one until no more features meet the predetermined criterion [108].

The two methods of stepwise regression can be further refined with variations like bidirectional elimination, which combines both forward selection and backward elimination. Stepwise regression aims to strike a balance between model complexity and predictive accuracy. Additionally, the stepwise regression procedures incorporate validation such as coefficient of determination (R^2), root mean square error (RMSE) and mean absolute percentage error (MAPE) to help preventing overfitting the model [109]. Both the AIC and BIC takes into account of the likelihood of the data given the model and the numbers of the parameters in the model as shown in Eq. (7) and Eq. (8).

$$\text{AIC} = -2\log L(\hat{\theta}) + 2k \tag{7}$$

$$\text{BIC} = -2\log L(\hat{\theta}) + k\log(T) \tag{8}$$

where, $\log L(\hat{\theta})$ is the log-likelihood algorithm of the data given the model; k is the number of parameters in the model to fit a sample size of T data points.

(ii) Regularized Polynomial regression: LASSO Regression

Lasso regression also known as L^1 regularization is a regularized version of polynomial regression. It introduces a penalty term based on the sum of the absolute values of the regression coefficients, which helps to promote sparsity in the model by encouraging some coefficients to become exactly zero. This promotes feature selection and can improve the model generalization ability. [110]

In Polynomial regression, the relationship between the input variables (X) and the target variables (Y) is modelled using polynomial functions of the input variables. The standard polynomial regression model can be expressed as:[111]

$$y = \beta_0 + \beta_1 X + \beta_2 X^2 + \cdots + \beta_p X^p + \varepsilon \tag{9}$$

where, Y is the target variable, X is the input variable $\beta_0, \beta_1, \beta_2, \ldots \beta_p$ are the coefficients to be estimated, X^p represents the higher order terns in the polynomial equation with p representing the maximum degree of the polynomial and ε is the error term. The coefficient in regularized Lasso regression is estimated by a loss function with an additional regularization term. The loss function used in the regularized polynomial regression is a combination of the mean squared error (MSE) term and a penalty term based on the L^1 norm of the coefficients as given in Eq. (10)

$$Loss\ function = MSE + \lambda \sum_{j=1}^{m} |\beta|^q \qquad (10)$$

In the above equation, λ is the regularization parameter that controls the amount of regularization applied. A higher value of λ leads to more coefficients being pushed towards zero, promoting sparsity and feature selection. A lower value of λ allows more coefficients to remain non-zero, potentially capturing more complex relationships. By minimizing the loss function, regularized polynomial regression finds the optimal values for the coefficients that balance the fit to the training data and the regularization term. The regularization in the Lasso regression encourages a sparse model by shrinkage less important features towards zero, effectively performing feature selection and producing a simpler and more interpretable model.[112]

3.4 Regression model development

In the present study, it is proposed to develop regression technique-based models for bearing capacity prediction of different sites in Aizawl city. To this effect, a data base containing soil data from 50 different sites (S1 to S50) as given in Table 3.2 were used. Different statistical parameters i.e., mean, standard deviation, maximum and minimum of the parameters considered in the database are presented in the Table 3.1.

Table 3.1: Statistical analysis of parameters in the database of the study

Model variable	Mean	Standard Deviation	Maximum	Minimum
Plasticity index (PI)	10.18	4.98	18.59	0.43
Cohesion, kN/m^2	27.05	14.52	55.03	0.76
Angle of internal friction (ϕ°)	23.78	8.38	43.77	8.00
Unit weight, (kN/m^3)	16.50	0.87	17.97	15.18
Depth of foundation, D (m)	1.51	0.41	2.00	1.00
Width of foundation, B (m)	1.51	0.41	2.00	1.00
SBC in kN/m^2 (Square footing)	364.92	363.46	2087.41	93.63

Two different regression techniques namely stepwise linear regression and Lasso regression method were adopted to simulate the bearing capacity of soil. Depth of the foundation, D (m), width of the foundation, B(m), bulk unit weight of soil, γ(kN/m^3), plasticity index of the soil, PI (%) and shear strength parameters such as angle of internal friction of soil (ϕ°) and cohesion, c (kN/m^3) were served as input variables for the regression models. For development of any data driven regression, it is imperative to divide the data into training and testing sets. While training set is used for calibrating and developing a regression model, on the other hand, efficacy of the developed regression model is evaluated by feeding an independent unseen data i.e., testing data set into the model. In general, 70-80% of data is used for training while remaining data points are used for testing. In addition to this, for some cases wherein applicable, cross validation technique is also used for optimizing some of the regression model parameters which will be discussed in subsequent sections. In cross-validation technique, a data set is divided into certain number (say, k) of subsets or folds. In each run of the model, k-1 folds are used for training while remaining 1-fold for testing. In this way till k-th run is achieved, all the folds are iteratively used both for training and testing. In general model performance during training and testing is assessed via using some statistical criterions. Thereafter, criterions used in the present study are R^2, RMSE and MAPE as defined in Eq. (11-13). Each of these criterions evaluates a different measure of the prediction performance thus, enabling a comprehensive evaluation of model efficiency.

$$R^2 = 1 - \frac{\sum_{i=1}^{m}(t_i - y_i)^2}{\sum_{i=1}^{m}\left(t_i - \frac{1}{m}\sum_{i=1}^{m} t_i\right)^2} \tag{11}$$

$$RMSE = \sqrt{\frac{\sum_{i=1}^{m}(y_i - t_i)^2}{m}} \tag{12}$$

$$MAPE = \frac{100}{m}\sum_{i=1}^{m}\left|\frac{y_i - t_i}{t_i}\right| \tag{13}$$

Where, t_i is the target bearing capacity; y_i is the predicted bearing capacity; m is the number of observations.

3.5 Results and discussion

3.5.1 Geotechnical properties and bearing capacity of soil

Table 3.2 presents the laboratory test results in which the geotechnical properties such as plasticity index, cohesion, angle of internal friction and unit weight of the soil samples from the selected sites were obtained as per American Society for Testing and Materials (ASTM). From the obtained results, the soil samples were classified based on ASTM D2487-17e1 (2020) as shown in Table 3.2. According to the classification of soil using USCS classification, the most dominating soil observed in the selected sites are clay of low plasticity (CL). The bearing capacities for various types of footings were determined using IS 6402:1981 and are shown in Table 3.2 along with the foundation dimension (i.e., B and D). The square footing has the maximum bearing capacity in each of the selected sites when compared to the other types of footings. The combination of a low PI value, higher unit weight of soil and a high shear strength value (i.e., c and ϕ) influences the high bearing capacity. Soils with low PI values are generally recommended for foundations and load bearing structures in geotechnical engineering, particularly for foundation design, considering they are less susceptible to rapid settlement or volume changes. The higher unit weight of soil indicates the greater density which means there are more solid particles per unit volume resulting in better load bearing capacity. As a results, higher shear strength parameters in combination with a low PI value and higher unit weight of soil provide greater stability and load bearing capacity. The geotechnical properties and the calculated bearing capacity are the input parameters for model development using regression techniques such as stepwise and Lasso regression.

3.5.2 Stepwise regression

This section presents the results of stepwise regression model for bearing capacity simulation. Scheme of stepwise regression adopted in the study starts with no input variable but a constant term to an upper bound of including maximum quadratic terms of input variables in the regression equation. By this process, stepwise regression is designed to select only those terms with highest significance in influencing the model output (i.e., bearing capacity) by making use of a certain statistical criterion which is *p*-value in the present case.

Table 3.2: Geotechnical properties and bearing capacity of soil

Sites	Plasticity index (PI)	Cohesion kN/m^2	Angle of internal friction (ϕ°)	Unit weight (kN/m^3)	UCS Classi-fication	D (m)	B (m)	Safe Bearing capacity of soil (kN/m^2)				Shear Failure Type
								Strip footing	Square footing	Rectangular footing	Circular footing	
S1	5.89	13.5	32	17.46	ML	1	1	533.21	592.89	538.74	560.96	General
S2	1.25	0.8	35	15.4	ML or OL	1	1	426.46	426.78	394.26	385.07	General
S3	16.053	33.84	20	15.59	CL	1	1	131.81	160.39	144.89	158.45	Local
S4	11.832	31.68	15	15.69	ML	1	1	443.73	513.20	463.98	493.66	Local
S5	12.76	32.43	12	17.51	CL	1	1	98.34	98.34	98.34	98.34	Local
S6	18.5	55.034	11	17.97	CL	1	1	93.63	93.63	93.63	93.63	Local
S7	15.306	47.87	7	15.18	CL	1	1	133.65	133.65	133.65	133.65	Local
S8	1.51	0.76	35	17.02	ML or OL	1	1	148.62	148.62	148.62	148.62	General
S9	14.66	40.64	7	15.89	CL	1	1	461.42	461.42	461.42	461.42	Local
S10	13.63	34.5	18	15.45	CL	1	1	139.07	139.07	139.07	139.07	Local
S11	6.23	10.39	29	16.52	ML	1.5	1.5	121.95	148.75	134.37	147.17	Local
S12	13.796	31.88	18	16.18	ML	1.5	1.5	410.73	410.73	410.73	410.73	Local
S13	10.25	25.67	26	15.79	ML	1.5	1.5	136.18	162.90	150.96	160.92	Local
S14	10.15	20.45	24	15.49	ML	1.5	1.5	183.56	215.86	199.74	211.19	Local
S15	10.45	20.1	25	15.79	ML	1.5	1.5	145.31	169.13	157.06	165.34	Local
S16	10.25	21.2	29	16.87	ML	1.5	1.5	154.75	179.54	166.69	175.22	Local
S17	11.895	31.65	22	16.97	CL	1.5	1.5	549.79	633.87	581.55	610.67	Local
S18	2.15	3.98	34	16.77	ML or OL	1.5	1.5	168.05	199.92	185.10	196.72	General
S19	12.95	33.57	23	16.97	CL	1.5	1.5	648.44	678.01	622.16	626.72	Local
S20	1.15	2.95	35	17.65	ML or OL	1.5	1.5	105.65	128.00	118.74	127.44	General
S21	1.45	3.92	34	17.26	ML or OL	1.5	1.5	185.45	221.00	204.36	217.34	General
S22	16.91	46.49	19	17.95	CL	2	2	729.26	754.55	692.07	693.92	Local
S23	8.253	19.81	28	17.95	ML	2	2	664.08	693.51	636.43	640.73	Local
S24	10.59	30.8	18	16.97	CL	2	2	208.63	250.99	232.93	248.47	Local
S25	14.15	43.38	24	16.48	CL	2	2	258.26	310.18	287.48	306.17	Local
S26	13.95	41.69	23	16.48	CL	2	2	591.57	676.25	628.23	651.43	Local

Sites	Plasticity index (PI)	Cohesion kN/m^2	Angle of internal friction (ϕ°)	Unit weight (kN/m^3)	USCS Classi-fication	D (m)	B (m)	Safe Bearing capacity of soil (kN/m^2)				Shear Failure Type
								Strip footing	Square footing	Rectangular footing	Circular footing	
S27	16.8	44.99	11	16.18	CL	2	2	156.77	184.85	174.12	182.44	Local
S28	10.12	23.93	29	16.38	ML	2	2	256.74	307.94	288.06	303.47	Local
S29	9.45	20.69	35	16.87	MH	2	2	235.85	282.57	264.56	278.62	General
S30	10.34	31.88	22	17.85	ML	2	2	192.96	228.29	214.43	224.80	Local
S31	4.52	18.84	26.65	15.4	CL	1	1	141.25	170.21	160.04	169.22	Local
S32	0.43	17.76	34	15.59	ML or OL	1	1	656.75	761.68	706.5	736.66	Local
S33	18.59	28.203	20	15.64	CL	1	1	1228.92	1383.19	1274.78	1318.8	Local
S34	10.55	53.07	12	15.69	ML	1	1	197.39	232.45	218.53	228.72	Local
S35	12.71	33.35	21	17.51	ML	1.5	1.5	173.87	204.87	192.8	201.89	Local
S36	13.8	28.45	10.96	15.18	CL	1.5	1.5	550.36	577.5	517.24	530.94	Local
S37	15.05	33.35	19.25	15.45	CL	2	2	315.7	344.95	312.33	324.08	Local
S38	12.76	44.15	9.51	16.18	ML	2	2	651.24	690.33	613.1	636.4	Local
S39	2.93	5.88	43.77	15.79	ML or OL	2	2	117.84	139.4	130.5	136.51	General
S40	11.06	10.69	36.61	15.49	ML	2	2	127.09	157.13	147.94	156.02	General
S41	8.816	18.54	30	15.64	ML	1	1	159.77	189.88	178.91	186.65	General
S42	16.56	41.27	8	16.38	CL	1.5	1.5	697.72	701.7	625.15	634.89	Local
S43	16.15	43.38	13	17.95	CL	2	2	96.06	113.1	107.57	111.95	Local
S44	12.65	32.47	22	16.67	ML	2	2	154.47	186.53	176.52	184.83	Local
S45	11.23	30.97	20	17.26	CL	2	2	131.29	147.6	138.92	142.56	Local
S46	3.31	13.35	32.78	17.46	ML or OL	1	1	179.89	210.51	201.4	206.98	General
S47	2.67	2.45	34.89	17.97	ML	1.5	1.5	525.85	599.06	559.97	575.74	General
S48	8.05	49.34	13.7	17.02	CL	1.5	1.5	128.46	155.31	149.32	154.52	Local
S49	7.01	15	24.23	15.89	ML	1.5	1.5	987.41	1121.18	877.56	926.21	Local
S50	7.43	31.39	26.84	16.52	CL	2	2	1210.66	1267.1	1139.14	1168.6	Local

It is to be emphasized that higher order effect of input features is preserved provided they capture the key pattern in data. Since stepwise regression selects terms based on their significance level, therefore, entry order of terms in a stepwise regression equation also may be related to the sensitivity of the input parameters. In this way, stepwise regression method also performs sensitivity analysis alongside regression. Stepwise regression used in the present study was implemented in MATLAB R2022a environment. The predicted soil bearing capacity model developed using stepwise regression methods for strip, square, rectangular and circular footing are shown in Eq. (14,15,16 and 17) respectively.

$$q = -491.85 - 60.56\emptyset + 29.41\gamma + 36.467c - 291.42D - 11.6cD - 0.26c^2 + 2.13\phi^2 + 244.27D^2 \tag{14}$$

$$q = -433.67 - 66.43\emptyset + 17.49\gamma + 43.683c - 267.57D - 10.41cD - 0.35c^2 + 2.41\phi^2 + 232.99D^2 \tag{15}$$

$$q = -356.08 - 56.46\emptyset + 22.26\gamma + 38.543c - 402.88D - 12.66cD - 0.26c^2 + 2.0\ \phi^2 + 308.69D^2 \tag{16}$$

$$q = -518.78 - 53.50\emptyset + 20.79\gamma + 36.401c - 154.34D - 12.18cD - 0.22c^2 + 1.96\ \phi^2 + 219.82D^2 \tag{17}$$

Mathematically, a square footing could be substituted into Eq.16 by setting length by breadth ratio (L/B) as 1. However, many correlations derived from experimental or theoretical studies offer slightly different shape factors or correction factors for the square case, which can lead to minor differences in the computed safe bearing capacity. Therefore, for clarity and consistency with IS 6403:1981 and Terzaghi's bearing capacity theory, Eq.15 was used for square footings to apply the standard shape factors specifically developed for square foundations.

Comparison of the calculated bearing capacity of soil by IS 6403:1981 and the model developed for bearing capacity of soil by stepwise regression for strip, square, rectangular and circular footing are shown in figure 3.3. The performance of stepwise regression based on the statistical parameters i.e., R^2, RMSE and MAPE respectively are shown in figure 3.4. Figure 3.3 compares the estimated bearing capacity of IS 6403:1981 to the predicted stepwise regression bearing capacity for strip, square, rectangular, and circular footings. The R^2 of training data for strip, square, rectangle, and circular footings are 0.981,0.971,0.977, and 0.973 respectively, indicating a significant correlation between the calculated and predicted model for each form of footing. Similarly, the R^2 for strip, square, rectangular, and circular footings testing data are 0.971, 0.955, 0.957, and 0.955, respectively. The proposed model performance was also validated using the RMSE (root mean square error) and MAPE (mean absolute percentage error), as shown in figure 3.4. The MAPE for all types of footing was less than 20%, which matches the standard criteria, suggesting that the developed stepwise model is reasonably good and dependable.

Further validation using *P* value

P-value is a widely used parameter in the field statistics for evaluating parameters significance in regression equations. *P*-value is a measure of probability that how strongly input variables are corelated with output variable in a regression equation. Lower the *P*-value stronger is the evidence for rejecting the null hypothesis which is that no correlation exists between input and output variables. The *P*-values for all the input parameter are shown in Table 3.3, and they all met the required standards ($P \leq 0.05$ with 95% significance level) for D, ϕ and γ for all types of footing. This suggests that the values of ϕ, D and γ are the most important bearing capacity factors which have higher impact in the calculation of bearing capacity with *P*-value of ϕ being the least. Other parameters *c*, PI, and B have less impact on the proposed model of bearing capacity as the P value are found to be on higher side. This result also agrees with entry order of predictor terms in stepwise regression wherein ϕ term was first added in all the regression equations followed by terms of D, C, γ and PI.

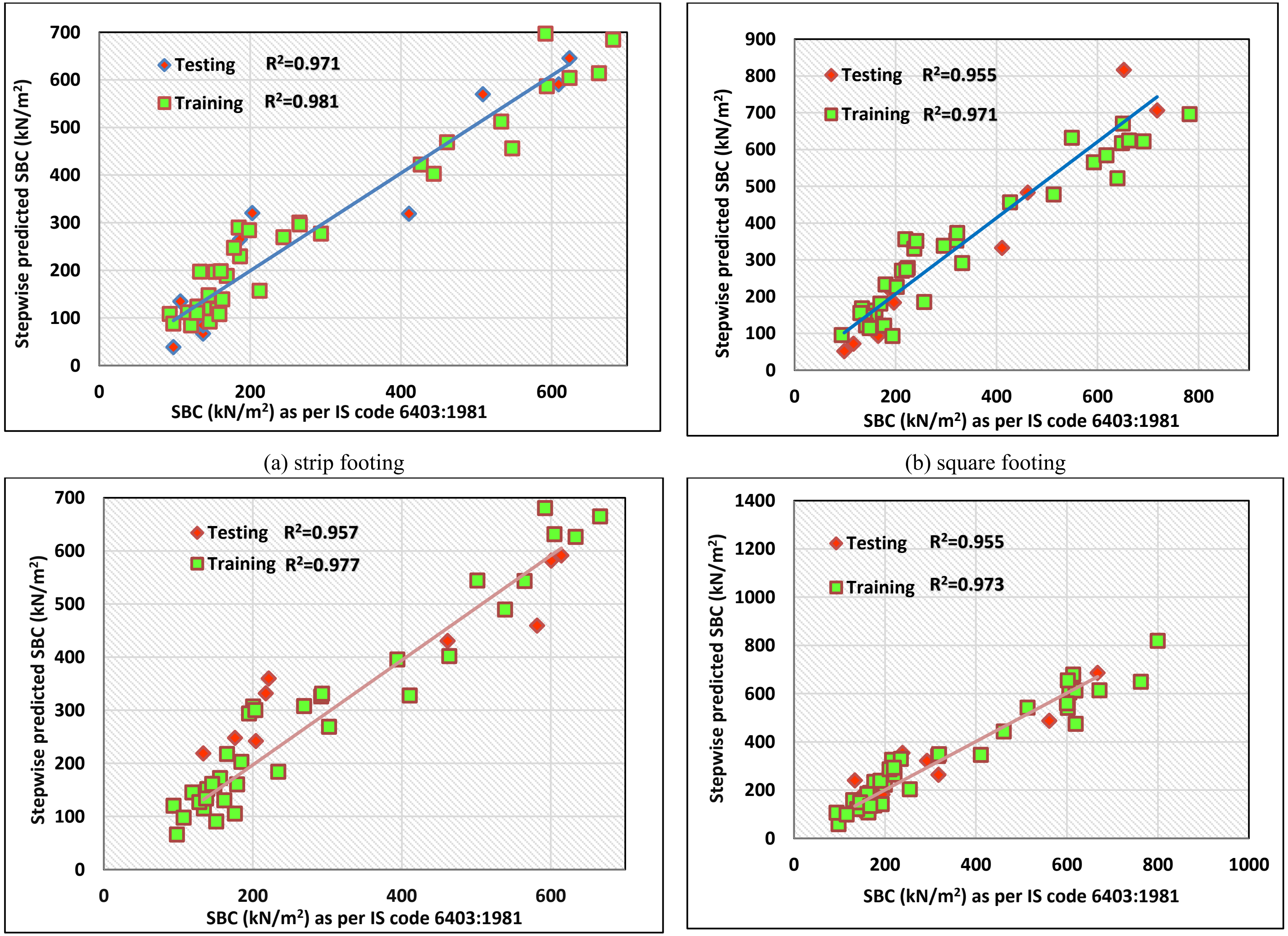

(a) strip footing

(b) square footing

(c) rectangular footing

(d) circular footing

Fig.3.3: Stepwise predicted and IS 6403:1981 calculated bearing capacity for (a)strip footing (b)square footing (c) rectangular footing and (d) circular footing

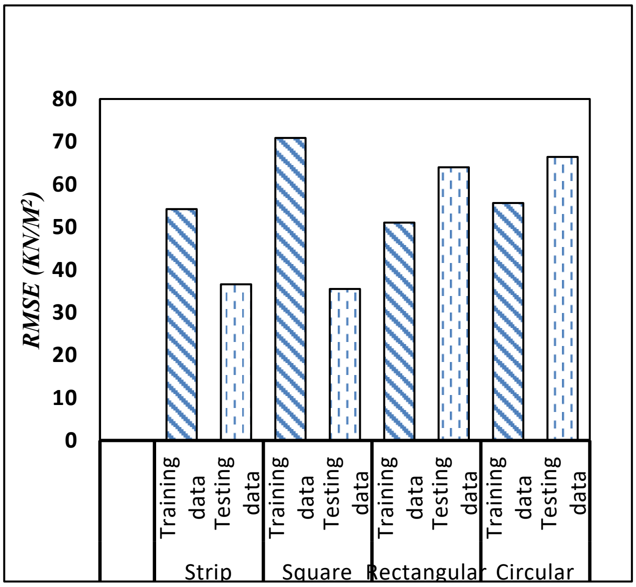

(a) RMSE (kN/m^2)

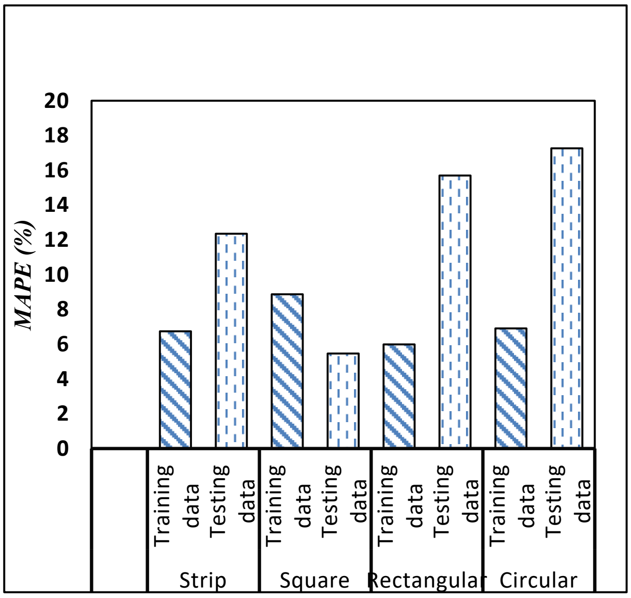

(b) MAPE (%)

Fig.3.4: Performance of stepwise regression for developing model of bearing capacity of soil in terms of (a) RMSE (kN/m^2) (b) MAPE (%)

Table 3.3: *P* values for predicted model parameter

Parameters	**Shape of footing**			
	Strip	**Square**	**Rectangular**	**Circular**
PI	0.1983	0.1434	0.81585	0.09063
c	0.097626	0.05669	0.16647	0.035806
ϕ	1.44E -09	1.77E-09	9.71E-09	2.81E-09
γ	0.041908	0.049496	0.016002	0.002141
D	0.0023246	0.0088312	0.0070731	0.031785
B	0.151	0.145	0.516	0.0675

3.5.3 Lasso regression

This section presents the results of Lasso regression for bearing capacity prediction. Lasso regression is a feature selection method wherein important features from a polynomial expansion (up to a certain order) can be identified using L^1 regularization norm as already discussed under subsection 3.3.2 (ii). One of the main tasks in implementation of Lasso regression is proper selection of regularization coefficient (λ) which in effect controls both model complexity and model performance. In this regard, optimum value of λ is found using geometric sequence technique. In this sequence the model starts with a very high λ value which renders all the model features insignificant in prediction process. Followed by this λ value is subsequently decreased in a geometric sequence till it reaches a lowest value which is in generally defined by the user. Usually, lowest value of λ is decided by maintaining a constant ratio between the largest and smallest λ value. In the process of varying λ value, Lasso regression model performance is evaluated using MSE performance criterion for each value of λ. A 5-fold cross validation technique is adopted to validate the λ value and consequently model performance. In a cross-validation technique dataset is divided in to "k" number of equal folds (k=5 in the present case). The idea is to train the data on k-1 folds wherein remaining 1-fold is used for testing the model. This process is iteratively followed till all the folds are in turn used for both training and testing. In this way 5-fold cross validated model performance is evaluated for each value of λ based on which optimum value of regularization parameter λ can be selected. The soil bearing capacity model developed using Lasso regression methods for strip, square, rectangular and circular footings are shown in Eq. (18,19,20 and 21) respectively.

$$q = -198.38 + 13.36PI + 27.07c - 78.89\emptyset - 0.51PI^2 - 0.37c^2 + 2.62\,\phi^2 + 0.80\gamma^2 + 27.2\,D^2 + 5.47\,B^2 \quad (18)$$

$$q = -489.38 + 47.67PI + 19.15c - 76.44\emptyset - 1.57PI^2 - 0.24c^2 + 2.69\,\phi^2 + 1.09\gamma^2 + 14.32\,D^2 + 22.8B^2 \quad (19)$$

$$q = -492.04 + 53.91PI + 19.12c - 74.65\emptyset - 2.05PI^2 - 0.21c^2 + 2.6\,\phi^2 + 1.07\gamma^2 + 17.26\,D^2 + 11.93B^2 \tag{20}$$

$$q = -235.87 + 46.49PI + 14.41c - 72.14\emptyset - 1.88PI^2 - 0.12c^2 + 2.53\,\phi^2 + 10.44\gamma^2 + 22.93\,D^2 + 8.8B^2 \tag{21}$$

The equations are obtained after L^1 regularization norm applied to a second order polynomial expansion of the original input space. 35 predictor terms were generated as a result of quadratic expansion of original feature space containing 7 feature variables. It may be observed that optimum number of Lasso predictor terms in all the equations were same for all footing types and is equal to 9. It is also observed that order of Lasso predictor variables was also identical in all the equations. Form and shape of Eq. (18- 21) were identical, however, varied only in terms of intercept and coefficient of the Lasso predictor variables. The comparison of the Lasso predicted bearing capacity and the IS 6403:1981 computed bearing capacity for strip, square, circular, and rectangular footings are shown in figure 3.4. Figure 3.5 shows that there is a significant correlation between the computed and predicted model for each type of footing, with the R^2 of training data for strip, square, rectangular, and circular footing being 0.918,0.959,0.935, and 0.939, respectively. Similarly, the R^2 for strip, square, rectangular, and circular footing of testing data are 0.968,0.942,0.965, and 0.962 respectively. The projected model performance was also validated using MAPE, as shown in figure 3.6. RMSE is not used here as MSE (Mean Squared Error) is already used for selection and validation of regularization parameter as discussed below.

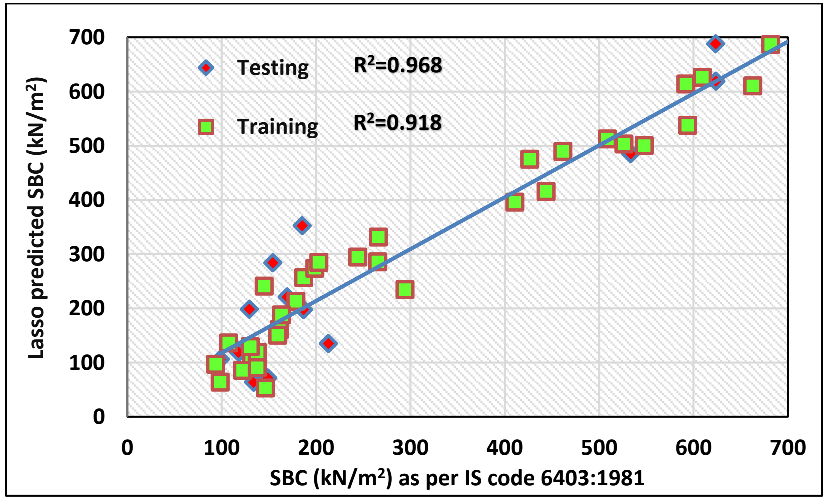

(a) strip footing

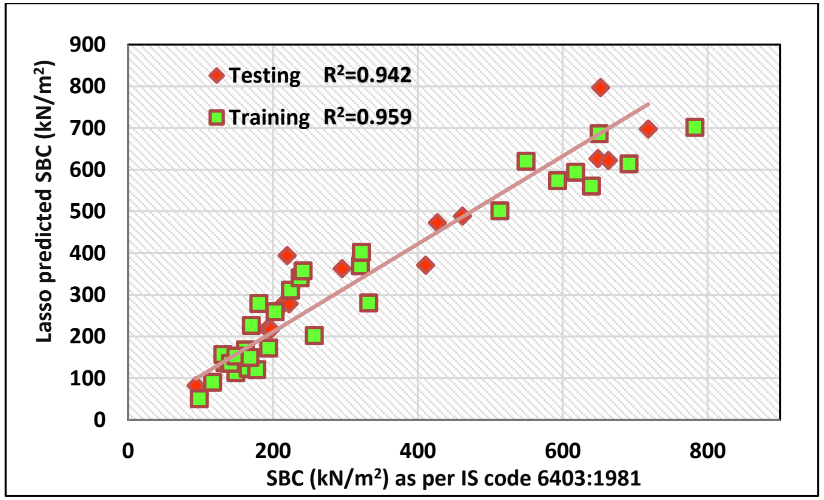

(b) square footing

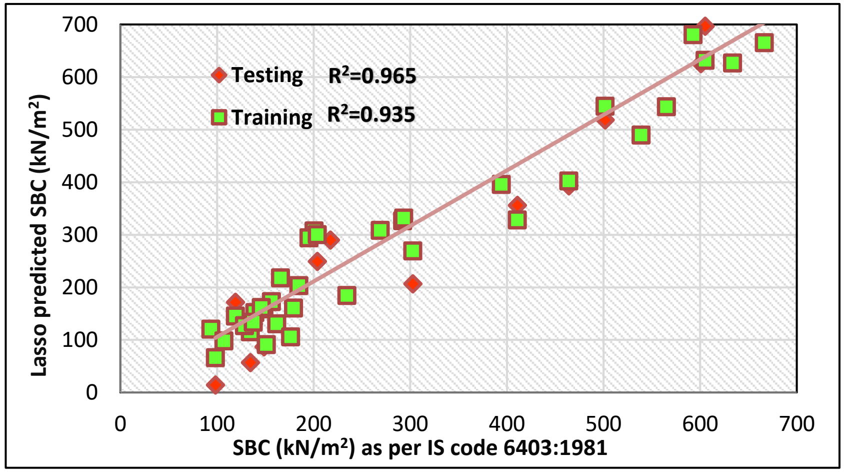

(c) rectangular footing

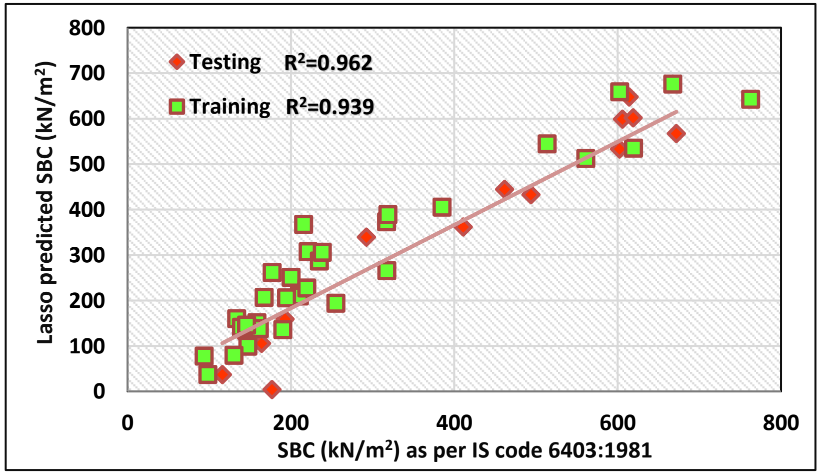

(d) circular footing

Fig.3.5: Lasso predicted and IS 6403:1981 calculated bearing capacity for (a)strip footing (b)square footing (c) rectangular footing and (d) circular footing

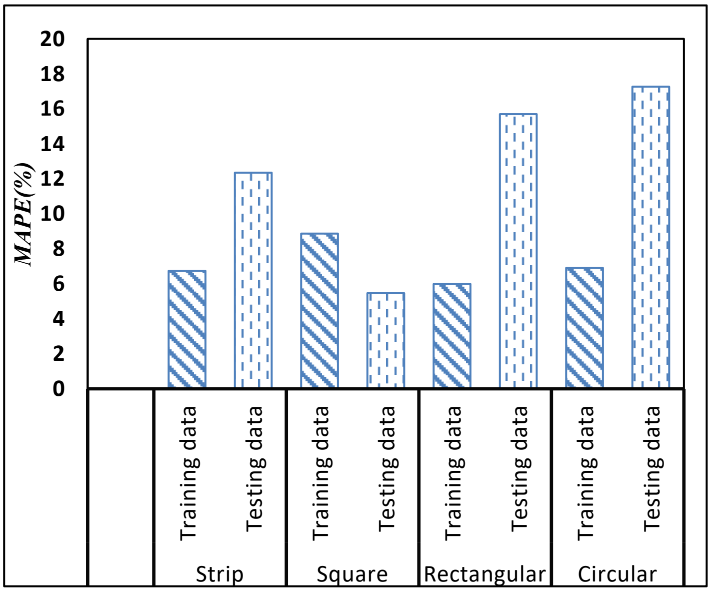

Fig.3.6: Lasso regression performance for bearing capacity prediction in terms of MAPE (%)

Selection process of optimum value of Lasso regularization parameter (λ) using MSE performance criterion and 5-fold cross validation technique is illustrated in figure.3.7. Figure 3.7(a) shows the variation of MSE with error bar for different values of λ for strip footing. λ value was varied in the range 10 to 10^{-4} in a geometric sequence as discussed earlier. Constant ratio of 10^4 is maintained between highest and lowest λ values. λ= 10 corresponds to the case of highest and starting λ value wherein all features become null variable. Optimum value of λ corresponding to minimum MSE in figure 3.7(a) is found to be 0.48 and this value is in turn used for constructing the regression equation in Eq. (18). Similarly, selection process of optimum value of λ for other footing shapes i.e., square, rectangular, and circular can be explained from figure 3.6(b), 3.6(c) and 3.6(d) respectively.

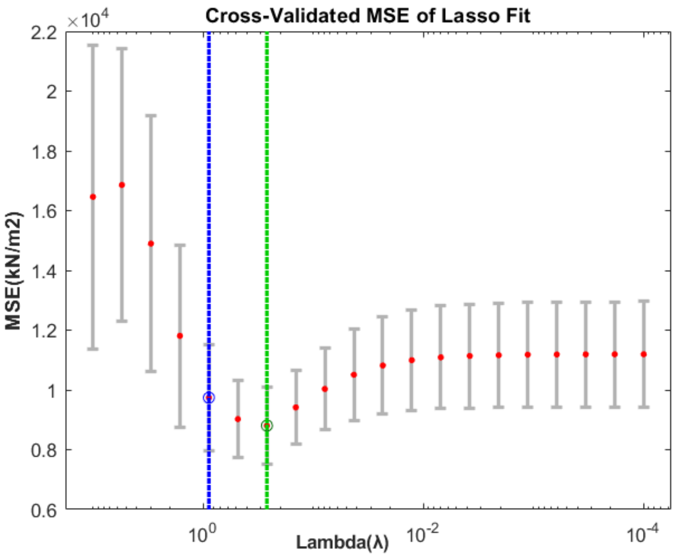

(a) strip footing

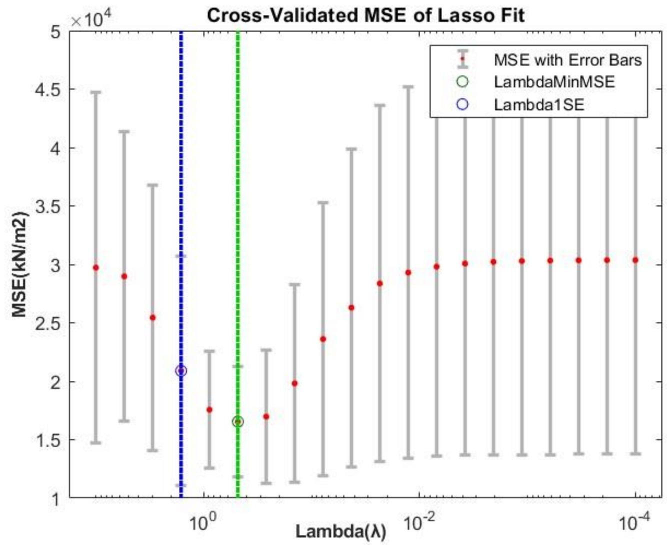

(b) square footing

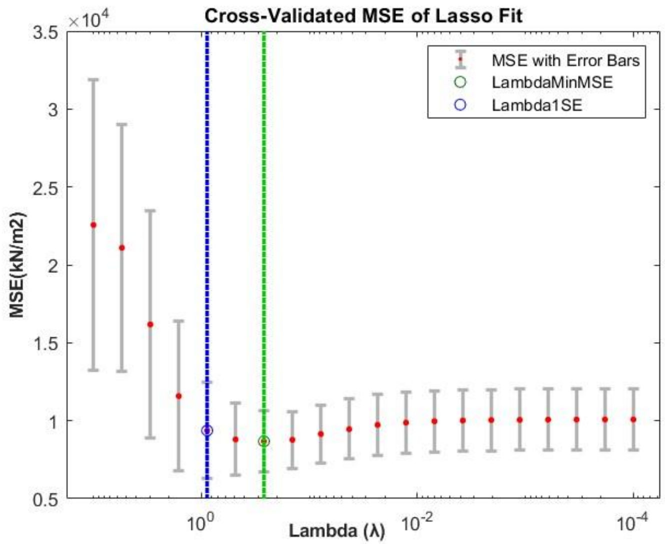

(c) rectangular footing

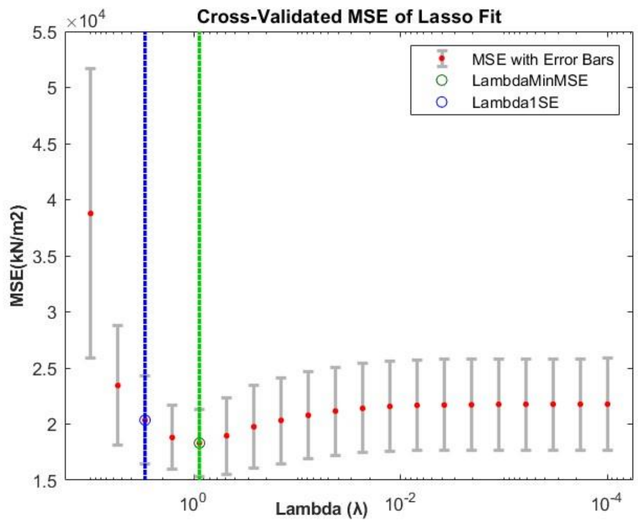

(d) circular footing

Fig.3.7: Cross validation for minimum mean square error (a)strip footing (b)square footing (c) rectangular footing and (d) circular footing

3.5.4 Comparison between stepwise and lasso regression

In the present study, two different regression techniques, namely stepwise regression and Lasso regression, have been applied for predicting the bearing capacity of soil. It may be observed that both the models have performed reasonably good in terms of all the performance indicator. Nevertheless, both training and testing performance of stepwise regression was found to be marginally better than Lasso regression in terms of R^2 value. RMSE and MAPE values of both the models were comparable. Further, from model complexity point of view stepwise regression offers a relatively less complex model with eight (8) predictor terms compared to the nine (9) predictor terms in Lasso regression. However, stepwise regression does not include width of the foundation, B as a predictor term in regression equation. This reflects the inadequacy of the stepwise regression in appropriating the physical process involved in bearing capacity estimation process. In contrast to this, Lasso regression includes width of the foundation, B as a predictor term in regression equation for all the shapes of the footing. Therefore, it may be concluded that Lasso regression has an edge over stepwise regression in simulating the physical process in bearing capacity prediction for our data set.

Further, as mentioned earlier stepwise regression selects terms based on their significance level. Thus, entry order of a terms in stepwise regression equation may be treated as sensitivity of that parameter in the model. This feature of stepwise regression can also be used as a sensitivity analysis technique of input parameters in bearing capacity prediction process. Results of sensitivity analysis using stepwise regression method is shown in Table 3.4.

Table 3.4: Results of sensitivity analysis using stepwise regression method

Entry order in model	Predictor variables entry order in model
1st	Angle of internal friction ($\phi°$)
2nd	Cohesion, kN/m^2
3rd	Depth of foundation, D (m)
4th	Unit weight, γ (kN/m^3)
5th	Width of foundation, B (m)
6th	Plasticity Index, PI (%)

Based on the entry order of the input parameters, shear strength parameters i.e., angle of internal friction (ϕ°) and cohesion (c), kN/m^2 were found to be most sensitive parameters. Similar conclusions were also found in previous literatures aimed at bearing capacity modeling using machine learning based regression techniques [26-27]. It is important to note that both the Lasso and stepwise regression techniques depend on training data sets for calibration of the regression equations. Since both training and testing in the present case is done using 5-fold cross-validation technique, this renders the regression methods are essentially an interpolation technique. This implies that for data points outside the range of input parameters as shown in Table 3.1, the developed models may not perform well. In such cases, it is always advisable to update the existing equations corresponding to the database with additional new data points.

3.6 Summary

In the present study, prediction of soil bearing capacity model was developed for strip, square, rectangular, and circular footing respectively by using stepwise and Lasso regression. A dataset consisting of bearing capacity related data from 50 different sites in and around Aizawl city was used for this purpose. The soil parameters such as depth of foundation (D), width of foundation (B), plasticity index of soil (PI), unit weight of soil (γ) and shear parameters (c & ϕ) were used as the input variables. Following general conclusion were made from the present study:

1) From the regression model developed of bearing capacity in each selected site, the strip and square footing obtained the greater bearing capacity compared to other footings. The high bearing capacity is influenced by the combination of low PI, high unit weight of soil and higher shear strength parameter (i.e., c and ϕ).
2) Both the regression methods i.e., stepwise regression and Lasso regression has performed well in predicting bearing capacity of soil in terms of all the performance indicators adopted in the present study. This suggests the flexibility and robustness of regression techniques in appropriating the bearing capacity prediction process. Similar performance of machine learning models was also reported in other literatures [18-21].

3) A comparison of predicted stepwise and calculated IS 6403:1981 shows that the regression is good, with coefficients of correlation (R^2) of training data for strip, square, rectangular, and circular footings of 0.981, 0.971, 0.977, and 0.973, respectively. Whereas, R^2 for testing data on a strip, square, rectangular, and circular footing are found to be 0.971, 0.955, 0.957, and 0.955, respectively.
4) Similarly, a comparison of predicted Lasso regression and calculated IS 6403:1981 shows that the regression is good, with R^2 of training data for strip, square, rectangular, and circular footing of 0.918, 0.959, 0.965, and 0.962, respectively. On the other hand, R^2 for testing data on a strip, square, rectangular, and circular footing are 0.968, 0.942, 0.965, and 0.962, respectively.
5) Based on the statistical performance of the models, such as R^2, RMSE, MAPE a satisfactory result was obtained for both the regression methods.
6) From the sensitivity analysis results performed in Stepwise regression using entry order and *P*-value, angle of internal friction of soil (ϕ) was found to be most dominating parameter in bearing capacity estimation followed by cohesion (c), depth of foundation (D), unit weight (γ)and plasticity index of soil (PI). Shear strength parameters i.e., c- ϕ were found to be the most dominant input parameters. Previous studies on bearing capacity modeling using ML techniques also reported to have similar findings in relation to the importance of strength parameters [102,103]. This also justifies the framework of the present study and overall acceptability of the equations presented in the paper.
7) Performance comparison of stepwise regression with Lasso regression suggested that stepwise regression performed marginally better than Lasso regression in terms of R^2 value. RMSE and MAPE values of both the models were comparable. Also, stepwise regression performed better than Lasso regression from model complexity point of view with eight (8) predictor terms in comparison to the nine (9) terms in Lasso regression equation.
8) A major inadequacy of stepwise regression found in this study is that it does not include width of the foundation, (B) as a predictor term in regression

equation wherein Lasso regression considered B as an important input parameter. Based on this it may be concluded that Lasso regression offers a more realistic bearing capacity model which can better simulate the physical process involved in bearing capacity estimation.

9) An important limitation of the present study is that developed regression models are reliable to predict with consistent accuracy only within the range of input parameters such as plasticity index (PI), dry unit weight of soil (γ), cohesion (c) and angle of internal friction (ϕ), the width of foundation (B) and depth of the foundation (D) used in the study. However, for data points outside the range considered in the study such as significantly different soil properties these regression equations may not predict well. Under such scenarios, the proposed regression equation has to be updated in light of new data points through additional training of the existing model.

CHAPTER 4

SLOPE STABILITY ANALYSIS WITH IMPACT OF BUILDING TOPOLOGIES ON HILL SLOPE

4.1 Introduction

In hilly regions like Aizawl city, wherein houses are mostly built on slopes, the layout of building plays a crucial role in slope stability. Building failures in Aizawl often results from a) non-engineered alterations of slopes b) faulty foundation construction without soil investigation or design. Many residents build and reside on slopes without considering the soil characteristics. To address this, a study was conducted to examine the impact of two common building types - step-back buildings and step-back setback buildings on slope stability in Aizawl. Fifty different sites with varying slope geometries were analyzed using Limit Equilibrium Method (LEM), considering soil parameters like cohesion, internal friction angle, unit weight, and slope geometry. The study evaluated slope stability under conditions such as free slope, slope with building loads under static and seismic conditions. The study found that sites with lower slope angles generally demonstrated greater stability, but there were cases where steeper slopes showed better stability due to superior shear strength values. Sites with higher cohesion values exhibited better stability in free slope analysis, while those with higher internal friction angles showed better stability under building loads of both static and seismic condition. To validate the above findings, a sensitivity analysis along with a comparative analysis between step-back and step-back setback building types were conducted. The results indicated that step-back setback buildings offered better stability compared to step-back buildings alone. This suggests that implementing step-back setback buildings could significantly improve slope stability in cities like Aizawl.

With the research gap mentioned in the literature review, the analysis was carried out to investigate the effects of building topologies on slope. The stability of free slope analysis as well as the analysis of slope with building loads under static and seismic conditions has been carried out for both the building topologies.

Furthermore, a comparative analysis of both the building topologies has been carried out for different slope angle. With extensive data sets, a sensitivity analysis has also been performed on how the soil properties enhance the factor of safety, resulting in better stability of the slope.

4.2 Study area

The source of the study area was similar to the previous chapter "Application of Regression Techniques for Bearing Capacity Prediction in Aizawl" where the municipal areas of the vulnerable slopes in Aizawl city have been identified and studied. Among the various vulnerable sites, 50 sites (S1 to S50) were selected as the study area after investigation of its history of slope failure. Moreover, the selected sites are indeed a built-up area where people are residing and the area of each selected site ranges from 200sqm to 500sqm. The map for the selected sites is shown in figure 1.3 of chapter-1.

4.3 Materials and methods

4.3.1 Preparation of databases

In this study, the properties of the soil such as unit weight (γ) and shear strength (c and ϕ) of the soil in all the selected sites (i.e., S1-S50) which is given in Table 3.2 of chapter -3 had taken into account. Using these data as the input parameters, the analysis of the stability of slope has been carried out to determine the factor of safety (FoS) in each site. The undisturbed soil samples collected using a thin-walled sampler (according to IS 2132-1972) from various sites in Aizawl Municipal Area were used for this study. The samples were collected within a depth of 2m from ground surface or occurrence of rocky strata, whichever happened earlier depending on the thickness of overburden of soil. The geotechnical properties of the soil in this study such as cohesion, angle of internal friction and unit weight of the soil were obtained as per American Society for Testing and Materials (ASTM). According to the classification of soil, the most dominating soil observed in the selected sites are silty clay soil.

4.3.2 Methods of slope stability assessment

The analysis of slope stability can be performed by various methods and approaches depending on the complexity of the slope and the specific requirements of the analysis. The common method used for slope stability analysis include Limit Equilibrium Method (FEM) and Finite Element Method (FEM). In this study, LEM approach was carried out for the analysis using Slope/W software, as it is best suited for the requirements and complexity of the study area. Among various approaches within LEM, the Morgenstern-Price method is often considered one of the most accurate and versatile, particularly for complex slope geometries such as hilly terrains. As per Duncan (1996) review of various LEM, Morgenstern- Price method (1965) obtained accurate FoS and considered both the interslice forces including interslice shear force and normal force. Moreover, this method can be applied for any slip surfaces of the slope [67]. Due to the stated reasons, Morgenstern- Price method was adopted among the various methods under LEM for performing the slope stability analysis in each site. The analysis of the free slope as well as the analysis of slope with two building topologies under static and seismic conditions has been carried out to study the impact of building loads on the hill slope stability.

In free slope analysis, the slope was analyzed in each site (S1 to S50) without any external loads such as building load. It entails evaluating the factor of safety (FoS) to assess the probability for landslides or collapses on natural or man-made slopes without any supports. The analysis employs an analytical method based on static equilibrium principles to model the behavior of the slope and predict its stability by evaluating the factor of safety (FoS). The geometry of the model slope in each site was defined by its dimensions (i.e., slope height and slope angle), in which the boundary conditions of the model was assigned as the actual site. A homogenous slope with c-ϕ soil was subjected to the analysis to assess the factors affecting the stability of the slope. The Mohr-Coulomb criterion has been employed as the failure criterion to simulate the shear strength of the soil. This criterion relies on two essential parameters, cohesion 'c' and the angle of internal friction 'ϕ', to characterize the behavior of the soil under shear stress. The potential failure surface, also referred to as the slip surface, was assumed based on site conditions and soil properties prior to analysis, allowing the factor of safety to be evaluated along this predefined surface. This evaluation has been influenced by various factors such as soil properties, slope geometry, and external load. To simulate the slope condition during rainwater infiltration (the most critical case), the analysis at each site was performed by considering the pore water pressure with the assumption of the piezometric line along the slope surface. In absence of actual piezometric head data available at site, conservative assumption of piezometric line along the slope surface is made and applied in the present study. Therefore, the stress governs the shear strength of the soil and the factor of safety (FoS) is expressed in terms of effective stress analysis. In this study, the strength parameters (c and ϕ), unit weight of the soil (γ), slope angle (β) and slope height (H) are the input parameters taken into account during the analysis of the slope stability.

In the analysis of slope with building loads, the free slope analysis has been taken as the parent analysis. Under the parent analysis, the analysis of the slope w.r.t building loads was performed by implementing the column loads as point loads on the slope. The column loads input for each selected sites were differed according to their slope angle as shown in Table 4.1. In addition to accounting for building loads, the slope stability analysis also includes earthquake loads, as the study area falls under seismic zone V according to IS:1893-Part I of 2016 [113]. To incorporate dynamic forces in slope stability analysis, it follows the Pseudo-static Limit Equilibrium Method, which is a simplified seismic analysis technique widely accepted for preliminary and regional slope assessments. The input seismic coefficients are considered as static equivalent forces acting on the sliding mass. The horizontal (K_h) and vertical (K_v) seismic coefficients are taken as 0.36 and 0.24 where these coefficients are calculated as per IS 1893- 2016, considering seismic zone V. Slope/W uses Pseudo-static analysis to calculate the horizontal (F_h) and vertical (F_v) forces generated by seismic motion which is as follows:

$$F_h = Kh*W$$

$$F_v = Kv*W$$

Where W is the weight of the slice.

To incorporate dynamic forces, the slope stability software Slope/W provides an option to input earthquake loads in the form of seismic coefficients. Using the response spectrum method specified in IS:1893 of 2016, the horizontal and vertical seismic coefficients for seismic zone V were calculated to be 0.36 and 0.24, respectively. Subsequently, these seismic loads were added to the slope analysis, which also included building loads, to determine the Factor of Safety (FoS) of the slope.

4.3.3 Model development

The selected sites within the study area exhibit varying soil properties and slope angles, ranging from 20° to 45°. According to the building regulations of the Aizawl Municipal Corporation (AMC), published in 2012 [114], the maximum permissible height for residential buildings is 22 meters. In compliance with this regulation, an RCC building model of G+6 story, having dimensions of 16 m in length, 12 m in width, and 21 m in height, was adopted for analysis across different slope angles ($\beta = 20°$, 25°, 30°, 35°, 40°, and 45°), as illustrated in figures 4.1 and 4.2. Each story height was taken as 3 m, and the column center-to-center spacing was maintained at 4 m for both building topologies considered in the study.

The step back and step back setback building model developed for various slope angle has been analyzed using Staad.pro v8i taking beam and column size as 300mmx400mm and 450mmx450mm respectively, which was considered to be structurally safe and stable. The structural analysis was also performed to determine the building loads in which the building loads were presented in the form of column loads. The column loads obtained for various slope angle for both the building topologies are shown in Table 4.1. The analysis of the slope stability with these obtained column loads under static and seismic conditions has been carried out to determine the factor of safety (FoS) of the slope. Moreover, by assuming the foundation depth as 2.5 meters, the point load from the building has been considered at 2.5 meters depth from the surface slope in the analysis. This assumption is critical for analyzing the stability and behavior of the slope under the building load.

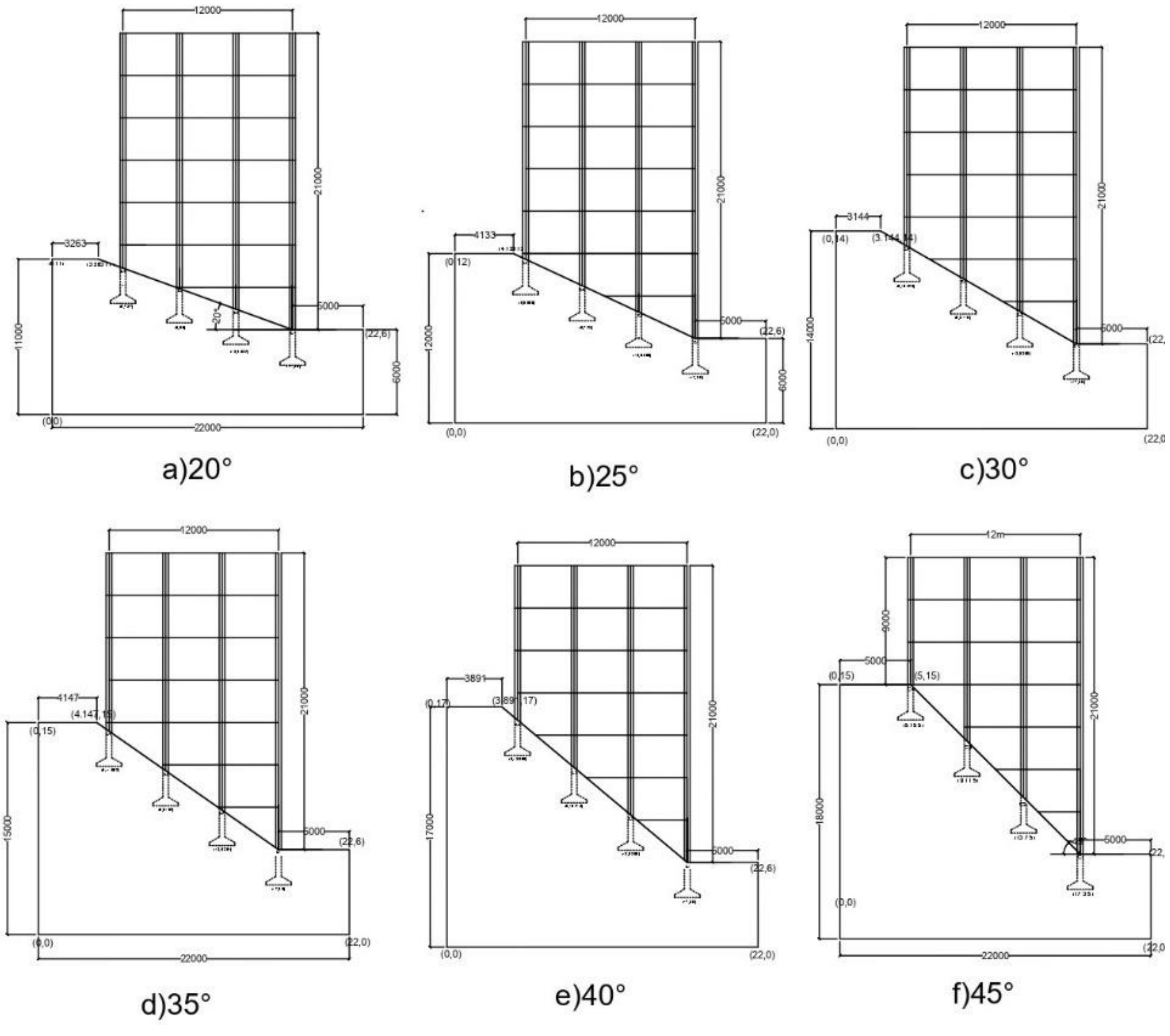

Fig:4.1: Step back building model adopted for different slope angle.

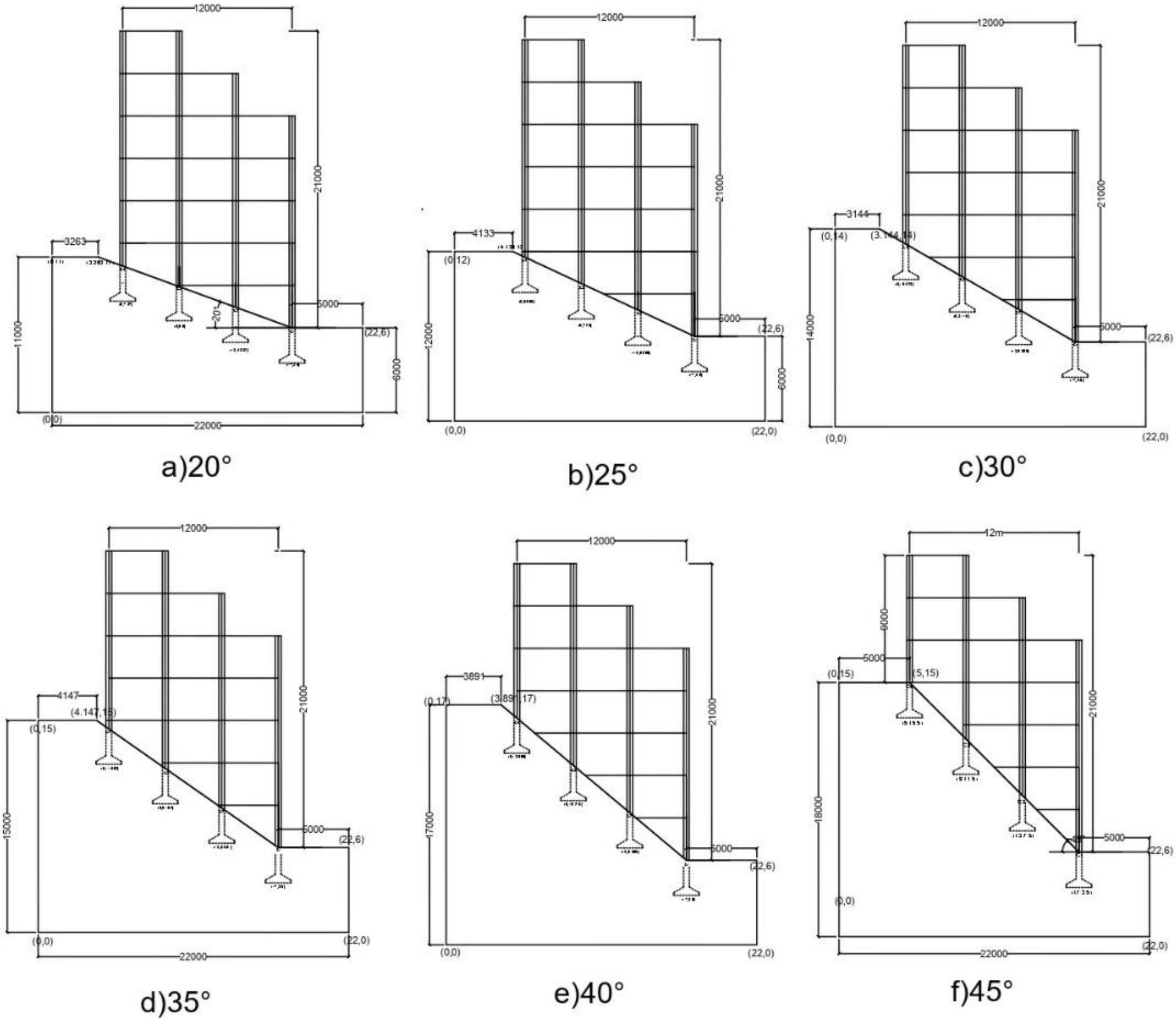

Fig:4.2: Step back setback building model adopted for different slope angle.

Table 4.1: Column loads obtained for various slope angle

Slope angle	Column no.	Loads with step back building (kN)	Loads with step back setback building (kN)
20°	1	2449.62	1833.98
	2	986.16	886.46
	3	874.56	857.69
	4	2364.77	2092.16
25°	1	2256.21	1655.43
	2	927.028	840.46
	3	900.56	895.43
	4	2037.63	1765.56
30°	1	2115.92	1522.18
	2	825.74	735.60
	3	861.80	859.34
	4	2001.45	1731.78
35°	1	1760.98	1272.68
	2	760.84	735.60
	3	688.99	735.60
	4	1488.83	1382.52
40°	1	1828.68	1256.25
	2	775.91	736.49
	3	707.17	723.601
	4	1622.23	1360.089
45°	1	1756.66	1164.405
	2	762.10	702.181
	3	684	691.011
	4	1493.45	1193.706

4.4 Results and discussions

4.4.1 Free slope stability analysis

This section presents the results of slope stability analysis without external loads including building, seismic, and wind load. The slope geometry, boundary conditions, and soil properties were defined for each site. Using cohesion, angle of internal friction, and unit weight as input parameters, the analysis was performed under static conditions. FoS was evaluated for slope angles β = 20°, 25°, 30°, 35°, 40°, and 45°, as shown in Table 4.2.

Figure 4.3 shows the free slope analysis results under static condition along with its FoS for various slope angle. Among the 50 selected sites, the most critical conditions were identified and selected as representative sites for each slope angle, based on the comprehensive dataset. Site S47 represents a slope angle of 20°, while

Table 4.2: FoS obtained in free slope analysis

Sites	Cohesion,c (kN/m²)	Angle of internal friction (ϕ°)	Unit weight (kN/m³)	Slope height (m)	Slope angle (β)	FoS	Sites	Cohesion,c (kN/m²)	Angle of internal friction (ϕ°)	Unit weight (kN/m³)	Slope height (m)	Slope angle (β)	FoS
S1	13.5	32	17.46	14	30°	1.894	S26	33.38	24	16.48	17	40°	1.983
S2	0.8	35	15.4	14	30°	1.242	S27	41.69	23	16.48	17	40°	2.162
S3	33.84	20	15.59	14	30°	2.545	S28	44.99	11	16.18	17	40°	2.034
S4	31.68	15	15.69	14	30°	2.228	S29	23.93	29	16.38	17	40°	1.749
S5	32.43	12	17.51	14	30°	2.01	S30	20.69	35	16.87	15	35°	2.149
S6	55.034	11	17.97	17	40°	2.22	S31	31.88	22	17.85	15	35°	2.047
S7	47.87	7	17.02	17	40°	2.007	S32	18.84	26.65	15.4	15	35°	1.76
S8	0.76	35	15.18	17	40°	1.046	S33	17.76	34	15.59	14	30°	2.241
S9	40.64	7	15.89	12	25°	3.397	S34	28.203	20	15.64	14	30°	2.241
S10	34.5	18	15.45	12	25°	3.206	S35	33.35	21	17.51	14	30°	2.416
S11	10.39	29	16.52	12	25°	2.203	S36	28.45	10.96	15.18	15	35°	1.682
S12	31.88	18	16.18	14	30°	2.317	S37	33.35	19.25	15.45	14	30°	2.5
S13	25.67	26	15.79	14	30°	2.327	S38	44.15	9.51	16.18	14	30°	2.707
S14	20.45	24	15.49	14	30°	1.972	S39	5.88	43.77	15.79	12	25°	2.593
S15	20.1	25	15.79	11	20°	2.893	S40	10.69	36.61	15.49	14	30°	1.962
S16	21.2	29	16.87	11	20°	3.181	S41	18.54	30	15.64	11	20°	3.046
S17	31.65	22	16.97	11	20°	3.594	S42	41.27	8	16.38	11	20°	3.774
S18	3.98	34	16.77	15	35°	1.305	S43	43.38	13	17.95	18	45°	1.336
S19	33.57	23	16.97	15	35°	2.211	S44	32.47	22	16.67	12	25°	3.13
S20	2.95	35	17.65	15	35°	1.293	S45	30.97	20	17.26	14	30°	2.275
S21	3.92	34	17.26	15	35°	1.303	S46	13.35	32.78	17.46	11	20°	2.749
S22	46.49	19	17.95	15	35°	2.529	S47	2.45	34.89	17.97	11	20°	1.889
S23	19.81	28	17.95	15	35°	1.782	S48	49.34	13.7	17.02	17	40°	2.156
S24	30.8	18	16.97	17	40°	1.593	S49	15	24.23	15.89	17	40°	1.268
S25	43.38	24	16.48	17	40°	2.256	S50	31.39	26.84	16.52	15	35°	2.291

sites S11, S2, S20, S8, and S43 represent slope angles of 25°, 30°, 35°, 40°, and 45°, respectively, as illustrated in figures 4.3(a) through 4.3(f). The resulting Factor of Safety across the various slopes ranged from 1.046 to 3.594, with the highest FoS observed at site S17 and the lowest at site S8. According to IS 14243:1995, sites with a FoS greater than 1.5 were considered stable, while those with a FoS less than 1.5 were deemed to be in a critical condition. The high FoS at site S17 can be primarily attributed to its lower slope angle and slope height, whereas the low FoS at site S8 is largely due to its higher slope angle and greater slope height.

In addition to slope geometry, soil properties significantly play a critical role in determining the Factor of Safety (FoS). This is evident in sites S47 and S11, with slope angles of 20° and 25°, respectively (Figures 4.3a and 4.3b). Although S47 has a gentler slope, S11 shows a higher FoS, primarily due to its greater soil cohesion and slightly higher unit weight (Table 4.2). Cohesion enhances stability by increasing shear strength, while unit weight contributes to normal stress but may act as a destabilizing factor in clayey soils with low friction angles. This comparison underscores the point that while slope angle is a critical factor, soil properties such as cohesion and internal friction angle often play a more decisive role in slope stability under static (free slope) conditions. It also highlights the need to consider multiple geotechnical parameters rather than relying solely on geometry. However, factors like seismic occurrences, or long-term changes in soil parameters may not be accounted in free slope stability analysis.

4.4.2 Stability of slope with step back building

The findings of the slope stability study with step back building loads under static and seismic conditions are presented in this section. To consider the building loads under static analysis, the RCC building model designed for various slope angles are shown in figure 4.2. The column loads obtained from those RCC model for various slope angle shown in Table 4.1 were taken into account as a concentrated load at 2.5m depth from the surface of the slope in each site depending on their slope angle. Moreover, to perform the analysis under seismic conditions, the seismic

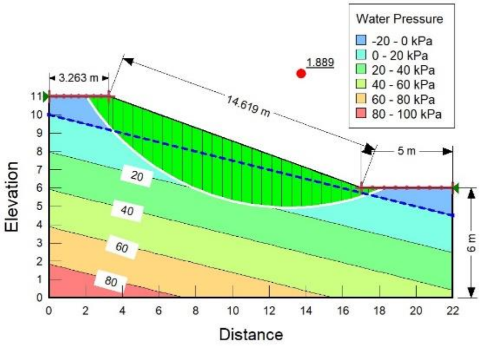

a) S47 of 20° slope (FoS=1.889)

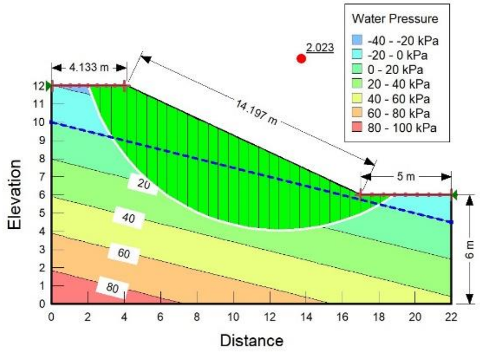

b) S11 of 25° slope (FoS=2.023)

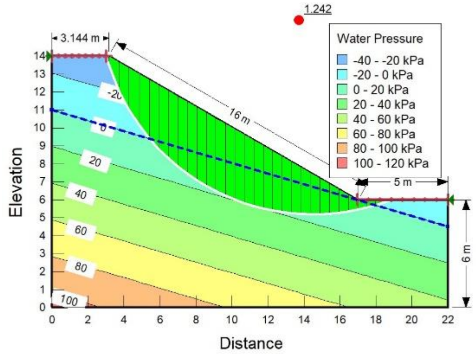

c) S2 of 30° slope (FoS=1.242)

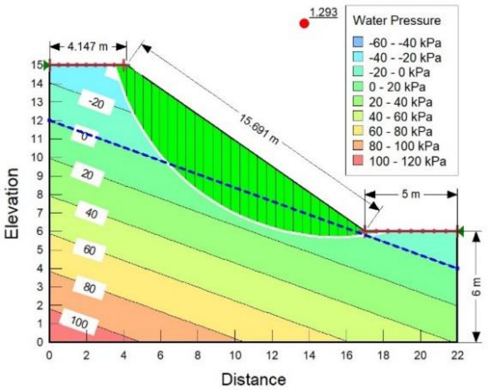

d) S20 of 35° slope (FoS=1.293)

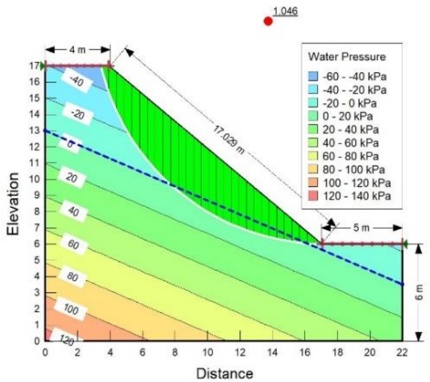

e) S8 of 40° slope (FoS=1.046)

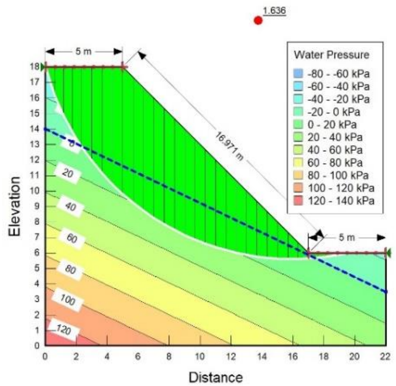

f) S43 of 45° slope (FoS=1.636)

Fig:4.3 Free slope analysis showing its factor of safety for various slope such as a) 20° b) 25° c) 30° d) 35° e) 40° f) 45°

coefficient for Zone-V (as per IS 1893 part I:2016) such as 0.36 (horizontal coefficient) and 0.24 (vertical coefficient) was employed in the analysis.The derived FoS for all sites under static and seismic conditions with various slope angles such as β =20°, 25°, 30°, 35°, 40° and 45° respectively are presented in Table 4.3. The obtained Factor of Safety spans from 0.511 to 1.524 across different slopes when only column loads are considered, with the maximum FoS observed at site S39, and the minimum at site S43. When both column and seismic loads are considered, the FoS values vary between 0.471 and 1.388 respectively. This indicates a decrease in FoS upon incorporating seismic loads, resulting in more susceptibility of the slope failure compared to scenarios where only column loads are considered. Furthermore, consistent with the analysis performed on free slopes, the results demonstrate that the higher FoS observed at site S39 can primarily be attributed to its lower slope angle and slope height. Conversely, the lower FoS observed at site S43 can be attributed to its steeper slope angle and slope height.

In slope stability analysis with building loads, the sites with the highest and lowest FoS changed from S17 to S39 and from S8 to S43, respectively, compared to the free slope analysis. This shift is mainly due to differences in the angle of internal friction of the soils, as shown in Table 4.3. Sites S39 and S43 have higher internal friction angles than S17 and S8, which improves shear resistance and slope stability under identical building loads. Thus, a higher angle of internal friction results in a higher FoS. Figures 4.4 and 4.5 show the analytical results of slopes with building loads under static and seismic conditions, respectively. Seismic effects were incorporated using a seismic coefficient. The most critical sites were selected to represent various slope angles: S42 (20°), S9 (25°), S40 (30°), S36 (35°), S7 (40°), and S43 (45°). As shown in Table 4.3, some steeper slopes exhibited higher FoS due to higher angles of internal friction. This highlights that while slope angle is important, soil properties particularly the angle of internal friction also play a critical role in slope stability under building and seismic loads.

Table 4.3: FoS obtained with step back building

Sites	Slope height (m)	Slope angle (β)	Factor of safety (FoS)		Sites	Slope height (m)	Slope angle (β)	Factor of safety (FoS)	
			column loads	column loads with seismic loads				column loads	column loads with seismic loads
S1	14	30°	1.01	0.914	S26	17	40°	0.9	0.822
S2	14	30°	0.958	0.874	S27	17	40°	0.886	0.808
S3	14	30°	0.836	0.762	S28	17	40°	0.616	0.562
S4	14	30°	0.679	0.619	S29	17	40°	0.909	0.832
S5	14	30°	0.603	0.546	S30	15	35°	1.118	0.994
S6	17	40°	0.692	0.626	S31	15	35°	0.87	0.769
S7	17	40°	0.545	0.495	S32	15	35°	0.847	0.759
S8	17	40°	0.894	0.821	S33	14	30°	1.117	1.021
S9	12	25°	0.562	0.518	S34	14	30°	0.782	0.714
S10	12	25°	0.835	0.765	S35	14	30°	0.869	0.776
S11	12	25°	0.953	0.871	S36	15	35º	0.545	0.497
S12	14	30°	0.762	0.693	S37	14	30º	0.811	0.74
S13	14	30°	0.933	0.851	S38	14	30°	0.619	0.57
S14	14	30°	0.822	0.751	S39	12	25°	1.524	1.388
S15	11	20°	1.000	0.918	S40	14	30°	0.597	0.552
S16	11	20°	1.166	1.065	S41	11	20°	1.17	1.076
S17	11	20°	1.018	0.927	S42	11	20°	0.629	0.574
S18	15	35°	0.888	0.796	S43	18	45°	0.918	0.837
S19	15	35°	0.917	0.814	S44	12	25°	0.94	0.858
S20	15	35°	0.911	0.811	S45	14	30°	0.809	0.732
S21	15	35°	0.889	0.795	S46	11	20°	1.237	1.129
S22	15	35°	0.927	0.834	S47	11	20º	1.211	1.04
S23	15	35°	0.897	0.793	S48	17	40º	0.716	0.648
S24	17	40°	0.668	0.608	S49	17	40º	0.702	0.643
S25	17	40°	0.926	0.845	S50	15	35º	0.995	0.902

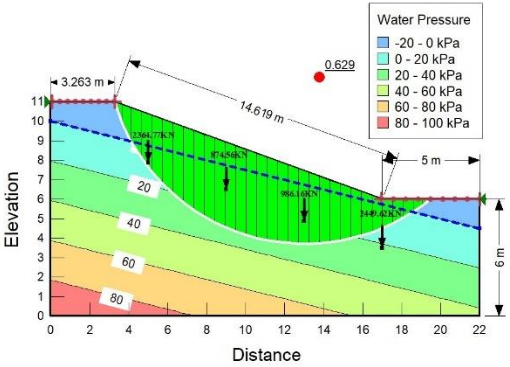

a) S42 of 20° slope (FoS=0.629)

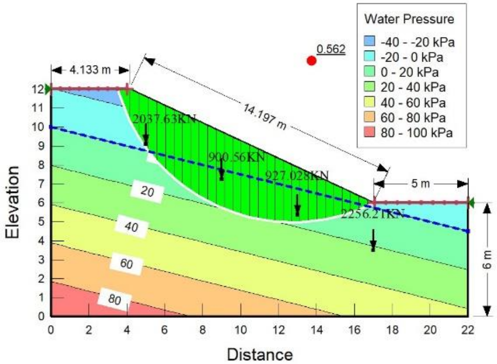

b) S9 of 25° slope (FoS=0.562)

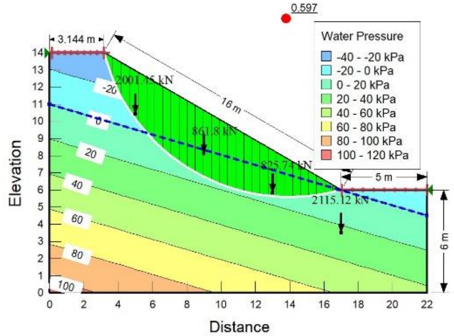

c) S40 of 30° slope (FoS=0.597)

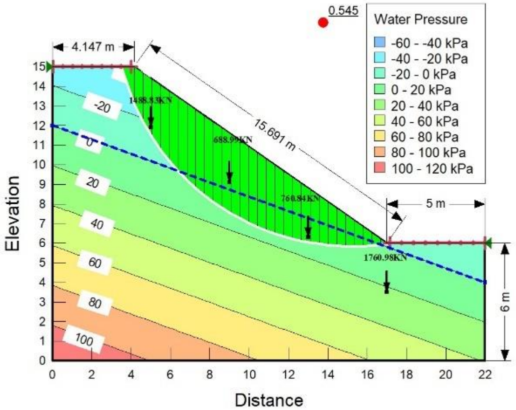

d) S36 of 35° slope (FoS=0.545)

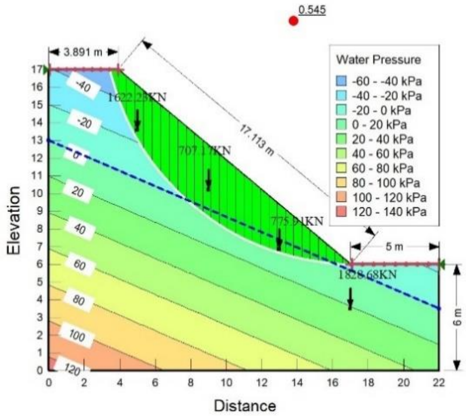

e) S7 of 40° slope (FoS=0.545)

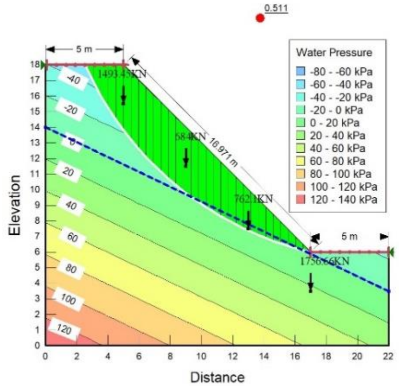

f) S43 of 45° slope (FoS=0.511)

Fig:4.4 Slope stability analysis with step back building under static condition showing its factor of safety for various slope such as a) 20° b) 25° c) 30° d) 35° e) 40° f) 45°

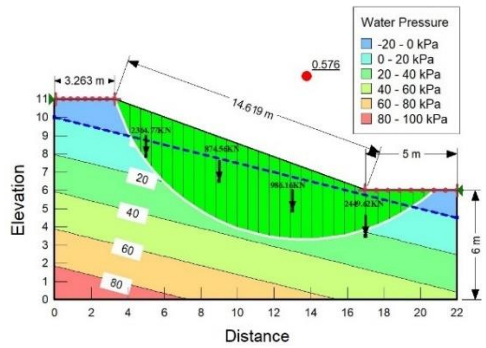

a) S42 of 20° slope (FoS=0.576)

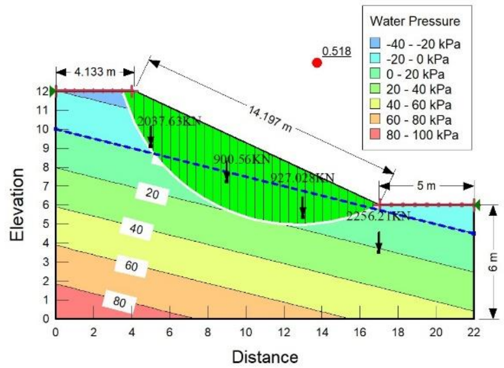

b) S9 of 25° slope (FoS=0.518)

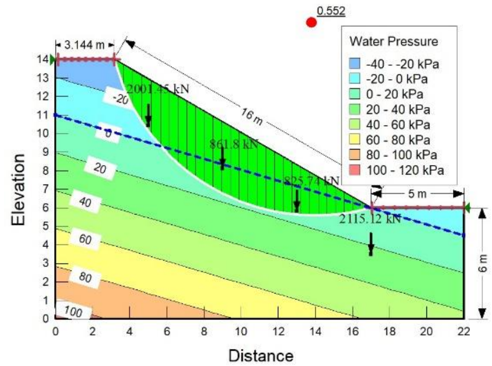

c) S40 of 30° slope (FoS=0.552)

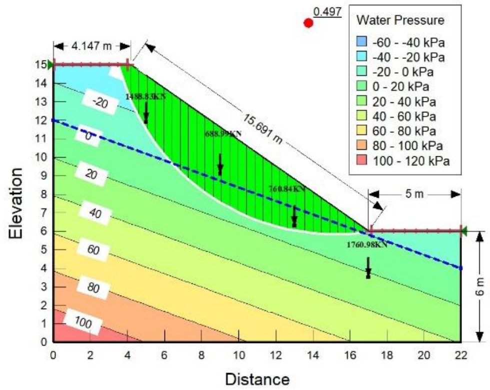

d) S36 of 35° slope (FoS=0.497)

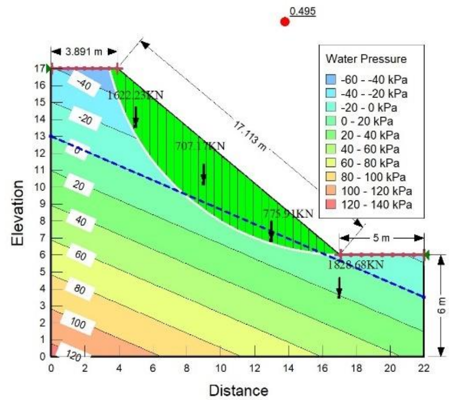

e) S7 of 40° slope (FoS=0.495)

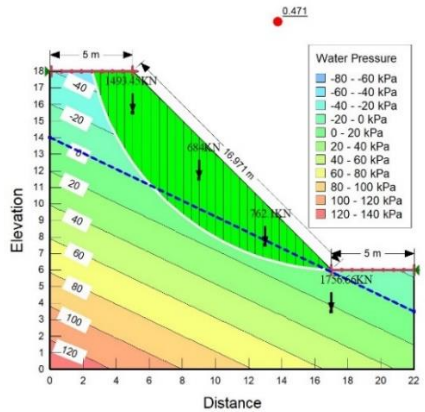

f) S43 of 45° slope (FoS=0.471)

Fig.4.5: Slope stability analysis with step back building under seismic conditions showing its factor of safety for various slope such as a) 20° b) 25° c) 30° d) 35° e) 40° f) 45°

4.4.3 Stability of slope with step back setback building

This section presents the slope stability analysis for step back setback buildings under static and seismic conditions, with the corresponding FoS values summarized in Table 4.4. The Factor of Safety (FoS) obtained varies from 0.488 to 2.480 under static conditions, with the lowest FoS observed in S36 and the highest in S47. Similarly, under seismic conditions, the FoS ranges from 0.46 to 2.183, with S36 having the lowest FoS and S47 the highest. The column loads taken as concentrated load in each selected site was given in Table 4.1. The FoS obtained were higher in each selected sites for step back setback building when compared with step back building alone, leading to more stability of the slopes. The main factors of the stability improvement of slope for this type of building can be due to the reduction of the column loads as the reduced in building loads minimize the risk of overloading the slope and mitigate the potential for slope failure. As the building with the step back topology results in uneven column heights leading to unequal distribution of load which impacts the structural integrity of the building and may leads to the failure of slope. Therefore, the step back setback mechanism was performed to compensate for the uneven column heights to maintain equal distribution of load. The results from Table 4.4 shows that the analysis of slope with step back setback building under static conditions (include column loads only) . higher FoS when compared with the analysis performed under seismic conditions (include both column and seismic loads).

Figure 4.6 and 4.7 represents the analytical results of slope with step back setback building under static and seismic conditions. To represent the various slopes angle for each site, critical sites were selected. For instance, S42 represents 20° slope angle. Likewise, S9, S40, S36, S7 and S43 represents 25°, 30°, 35°, 40° and 45° slope angle respectively as illustrated in figure 4.6 and figure 4.7. The analytical findings indicate that with this building configuration, the column located at the highest point on the slope bears more weight compared to the column situated at the lowest point on the slope. Consequently, a greater portion of the building weight is concentrated on the upper side of the slope, thereby enhancing its stability and mitigating the risk of sliding. Additionally, step-back setback building topology reduces the vulnerability of slopes to failure when subjected to seismic loads with

Table 4.4: FoS obtained with step back setback building

Sites	**Slope height (m)**	**Slope angle (β)**	**Factor of Safety (FoS)**		**Sites**	**Slope height (m)**	**Slope angle (β)**	**Factor of Safety (FoS)**	
			column loads	**column loads with sesimic loads**				**column loads**	**column loads with sesimic loads**
S1	14	30°	1.041	0.934	S26	17	40°	0.977	0.884
S2	14	30°	0.978	0.885	S27	17	40°	0.934	0.845
S3	14	30°	0.878	0.793	S28	17	40°	0.66	0.596
S4	14	30°	0.716	0.647	S29	17	40°	0.948	0.86
S5	14	30°	0.633	0.572	S30	15	35°	1.138	1.009
S6	17	40°	0.743	0.665	S31	15	35°	0.888	0.782
S7	17	40°	0.555	0.501	S32	15	35°	0.863	0.772
S8	17	40°	0.917	0.838	S33	14	30°	1.153	1.045
S9	12	25°	0.602	0.555	S34	14	30°	0.819	0.74
S10	12	25°	0.88	0.8	S35	14	30°	0.9	0.806
S11	12	25°	0.984	0.892	S36	15	35º	0.589	0.53
S12	14	30°	0.801	0.721	S37	14	30º	0.852	0.77
S13	14	30°	0.971	0.878	S38	14	30°	0.658	0.601
S14	14	30°	0.854	0.774	S39	12	25°	1.55	1.41
S15	11	20°	1.035	0.942	S40	14	30°	0.631	0.578
S16	11	20°	1.204	1.09	S41	11	20°	1.206	1.1
S17	11	20°	1.061	0.958	S42	11	20°	0.667	0.605
S18	15	35°	0.903	0.807	S43	18	45°	0.556	0.504
S19	15	35°	0.936	0.828	S44	12	25°	0.987	0.893
S20	15	35°	0.926	0.822	S45	14	30°	0.847	0.759
S21	15	35°	0.904	0.806	S46	11	20°	1.271	1.15
S22	15	35°	0.947	0.849	S47	11	20º	1.236	1.04
S23	15	35°	0.914	0.805	S48	17	40º	0.761	0.685
S24	17	40°	0.704	0.636	S49	17	40º	0.73	0.665
S25	17	40°	0.977	0.884	S50	15	35º	1.016	0.917

building loads, as opposed to employing a step-back building design alone. Consequently, implementing the step-back setback building topology enhance slope stability in both static and seismic conditions.

4.4.4 Sensitivity analysis of soil properties (cohesion and angle of internal friction)

As soil properties play an important role in analysis of slope stability. Therefore, due to the extensive data set, the parametric analysis of shear strength parameters of soil i.e., 'c' and 'ϕ' has been conducted to understand their influence on factor of safety (FoS). A sensitivity analysis of the shear strength parameters was performed under two scenarios: free slope and slope with step-back building under static and seismic condition. To assess the effect of cohesion, the original soil cohesion value was systematically increased to 2c and 3c while keeping the angle of internal friction constant. Similarly, to examine the influence of frictional resistance, the angle of internal friction was increased to $2 \tan \phi$ and $3 \tan \phi$ while maintaining constant cohesion. Two representative sites S47 and S42 of similar slope geometry were selected for the analysis due to their contrasting soil properties. Site S47 is characterized by low cohesion and higher friction angle, while site S42 exhibits high cohesion and low friction angle. This contrast allows for a comprehensive understanding of how different soil types respond to changes in shear strength parameters under various loading conditions with similar slope geometry. The FoS variations with changes in 'c' and 'ϕ' for site S42 are shown in figures 4.8(a) and 4.8(b), and for site S47 in figures 4.9(a) and 4.9(b).

Figure 4.8 (a) & (b) indicate that for Site S42 (a soil with high cohesion and low internal friction angle), the sensitivity analysis revealed that increasing cohesion (c) significantly improves the factor of safety (FoS) across all loading conditions—free slope, building loads under static and seismic conditions. Although increasing the angle of internal friction (ϕ, represented as $\tan \phi$) also improves FoS, its influence is comparatively less than that of cohesion. This demonstrates that in cohesive soils like S42, cohesion is the dominant parameter influencing slope stability under all loading scenarios.

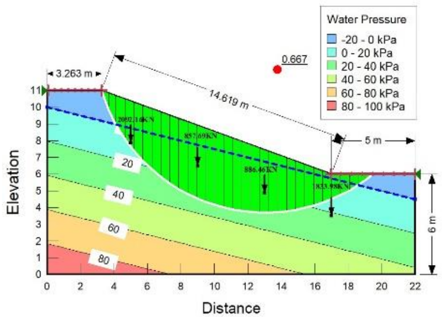

a) S42 of 20° slope (FoS=0.667)

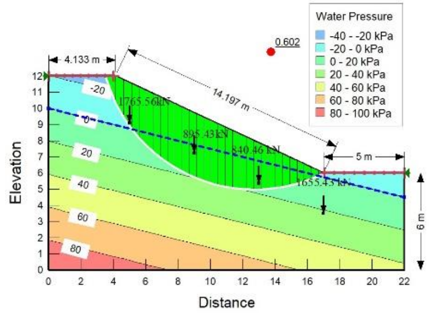

b) S9 of 25° slope (FoS=0.602)

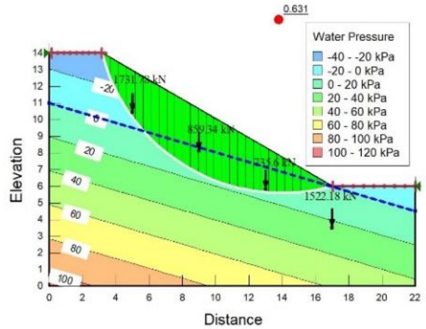

c) S40 of 30° slope (FoS=0.631)

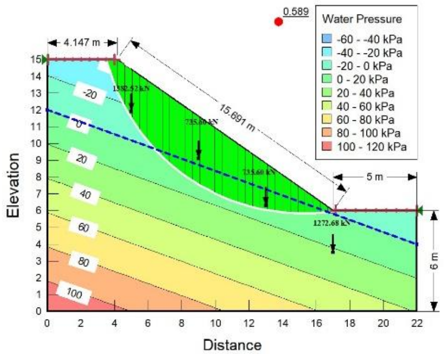

d) S36 of 35° slope (FoS=0.589)

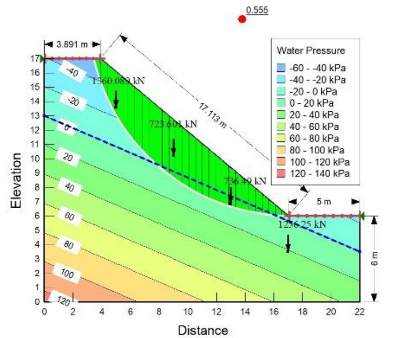

e) S7 of 40° slope (FoS=0.555)

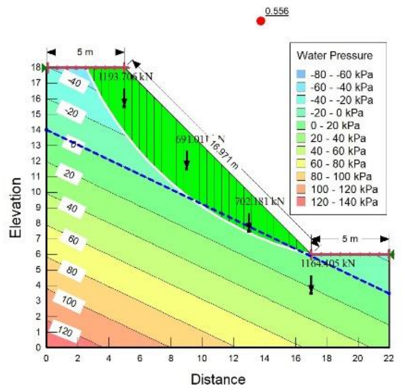

f) S43 of 45° slope (FoS=0.556)

Fig.4.6: Slope stability analysis with step back setback building under static condition showing its factor of safety for various slope such as a) 20° b) 25° c) 30° d) 35° e) 40° f) 45°

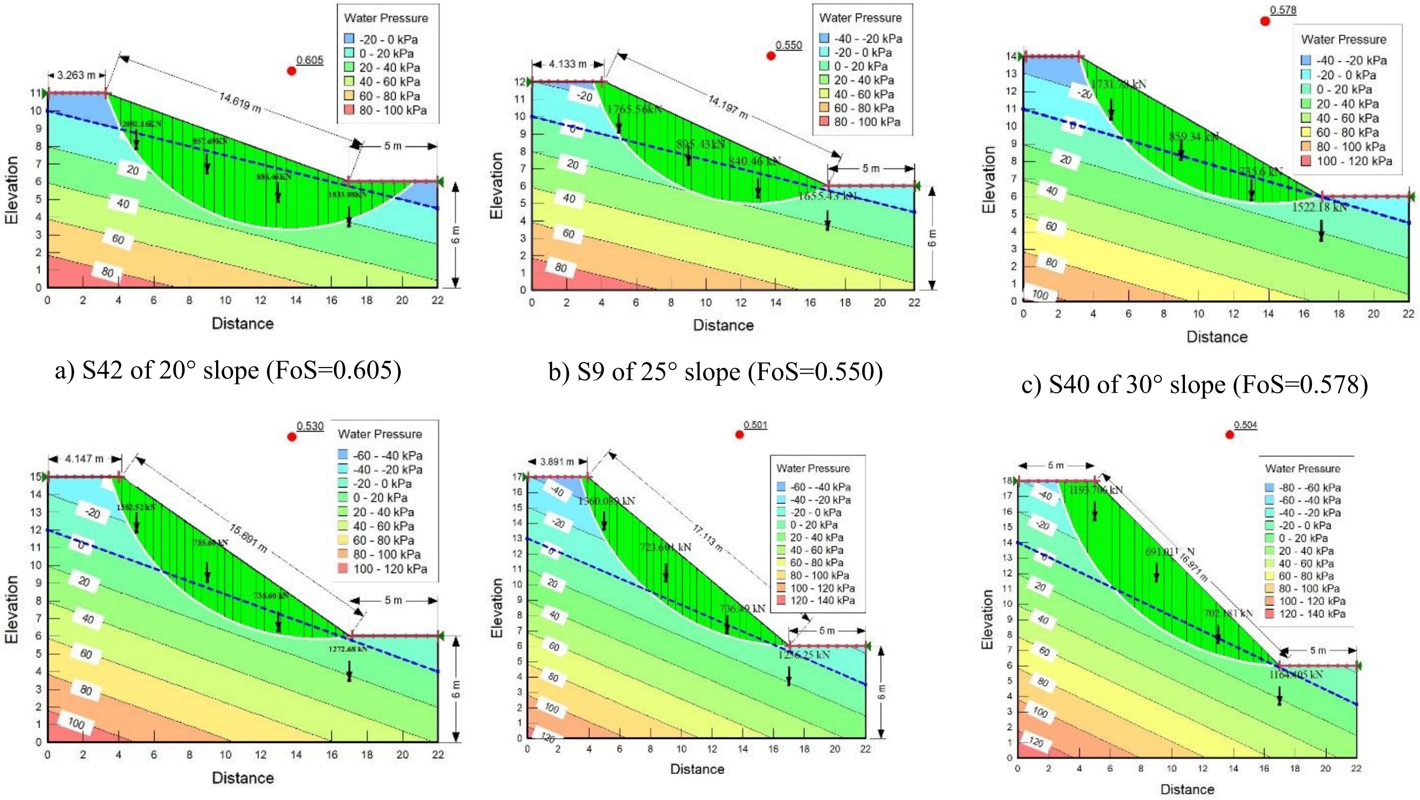

a) S42 of 20° slope (FoS=0.605)

b) S9 of 25° slope (FoS=0.550)

c) S40 of 30° slope (FoS=0.578)

d) S36 of 35° slope (FoS=0.530)

e) S7 of 40° slope (FoS=0.501)

f) S43 of 45° slope (FoS=0.504)

Fig.4.7: Slope stability analysis with step back setback building under seismic conditions showing its factor of safety for various slope such as a) 20° b) 25° c) 30° d) 35° e) 40° f) 45°

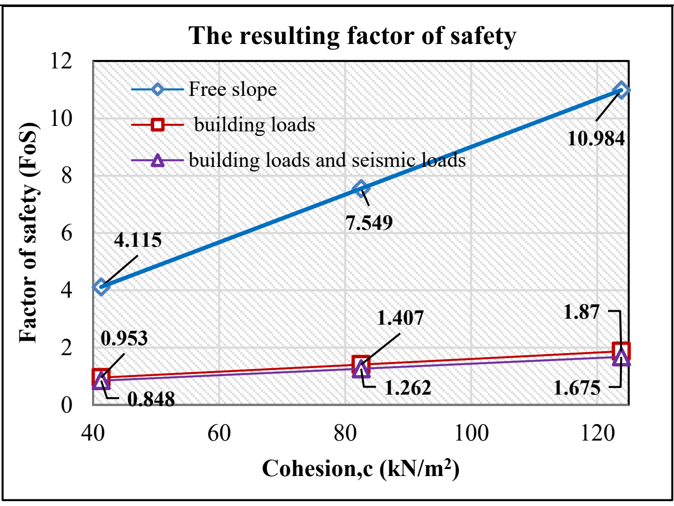

Fig.4.8 (a) The resulting factor of safety for S42 with β =20°, ϕ=8° and c = (41.27,82.54,123.81) kN/m²

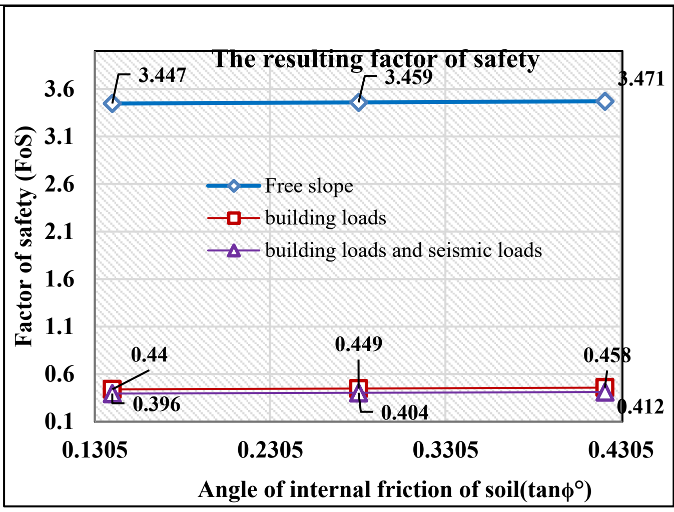

Fig. 4.8(b): The resulting factor of safety for S42 when β =20°, c=41.27 kN/m² and tan ϕ= (0.141,0.281,0.423) °

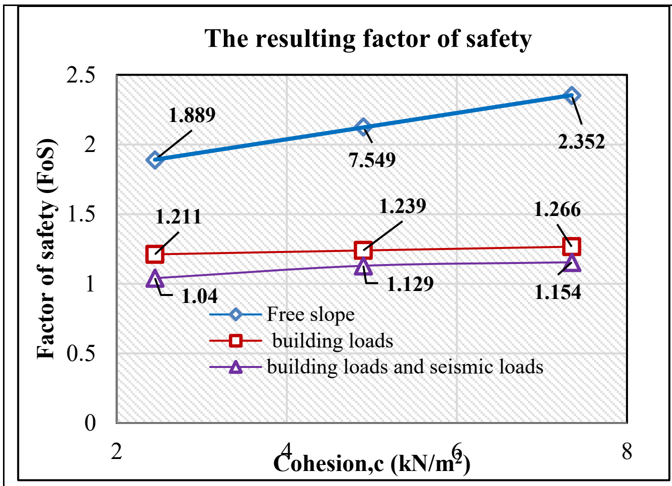

Fig.4.9 (a) The resulting factor of safety for S47 with β =20°, ϕ=34.89° and c = (2.45,4.9,7.35) kN/m²

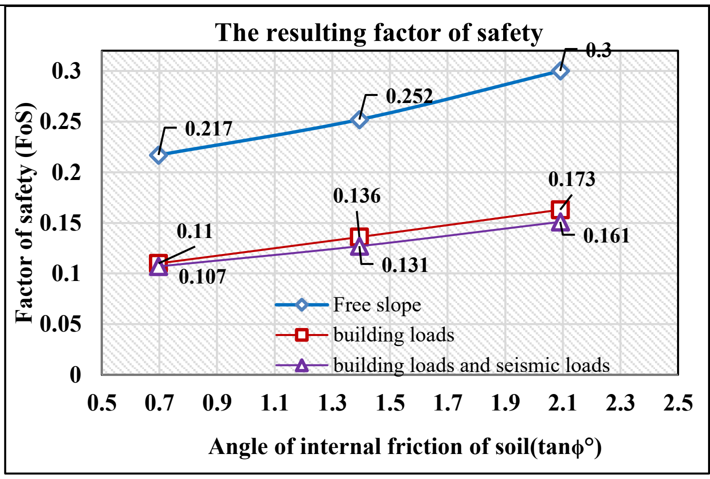

Fig.4.9(b) The resulting factor of safety for S47 when β =20°, c=2.45 kN/m² and tan ϕ= (0.697,1.394,2.091) °

Figure 4.9 (a) & (b) show that for Site S47 (a soil with low cohesion and high friction angle), the sensitivity analysis revealed that increasing cohesion (c) does improve FoS, particularly under free slope conditions. However, under building and seismic loading conditions, the angle of internal friction (ϕ) exerts a more significant influence on FoS. This suggests that in granular soils, ϕ becomes more critical under applied loads, while cohesion has a relatively limited effect.

4.4.5 Comparison of step back and step back setback building in the analysis of slope stability.

A study was conducted to determine the best building topology for hilly terrain, which results in better slope stability. Two building topologies, step back and step back setback, which are common existing building practices in Aizawl city, were used for this study. This section compares the analysis of slope with step back and step back setback building to determine which building topology will provide better stability to the slope. For assessing the impact of two building topologies, the most critical sites with varied slope angles of 20°, 25°, 30°, 35°, 40°, and 45° respectively were assumed to have similar soil properties such as c= 41.27 kN/m^2, ϕ=8° and γ=16.38 kN/m^3. With the two building topologies i.e., Step back building and Step back setback building considered, the obtained FoS for various slopes with similar soil properties are presented in Table 4.5.

Table 4.5: Comparison of FoS obtained with two building topologies

SL/No.	Sites	Slope angle (β)	FoS obtained in Step back building		FoS obtained in Step back setback building	
			Static condition	Seismic condition	Static condition	Seismic condition
1	S42	20°	0.629	0.576	0.667	0.605
2	S9	25°	0.602	0.549	0.643	0.584
3	S40	30°	0.551	0.507	0.588	0.536
4	S36	35°	0.574	0.519	0.589	0.53
5	S7	40°	0.517	0.47	0.56	0.521
6	S43	45°	0.511	0.471	0.526	0.488

Based on the results presented in Table 4.5, it is evident that the factor of safety (FoS) obtained for both step back and step back setback building topologies is higher under static conditions compared to seismic conditions. Furthermore, figures 5.1(a) and 5.1(b) provide graphical representation of the analysis conducted on both building topologies considering static and seismic conditions across various slope angles. These figures illustrate that the step back setback building consistently achieved a higher factor of safety compared to the step back building at each site analyzed. Overall, the results indicate that the step back setback building topology generally exhibits better performance in terms of factor of safety under both static and seismic conditions for different slope angles when compared to the step back building topology.

As a result, it is clear that in hilly areas such as Aizawl city, employing a step back setback building design offers significant advantages over a step back building design alone in terms of slope stability and minimizing the risk of slope failure. The setback feature, resembling terraced or stepped structures, plays a crucial role in enhancing slope stability by redistributing the building load more uniformly. This redistribution helps in reducing concentrated pressure points on specific areas of the slope, thereby minimizing the overall load acting on the slope as indicated in Table 4.1. Additionally, the setback design reduces shear stress on the slope by mitigating the forces acting parallel to it. By stepping back the building, the forces exerted on the slope are dispersed more evenly, thus reducing the risk of slope failure. In conclusion, for areas with sloping terrain like Aizawl city, building designs incorporating both step back and setback features are highly recommended for improving slope stability and mitigating the potential for slope failure.

4.4.6 Influence of building types on the shape of the critical slip surface of the slope.

The majority of sites in the selected area are dominated by a slope angle of 30°. Consequently, site S40, with a slope angle of 30° and a height of 14 meters, was used to demonstrate how different building types influence the shape of the critical slip surface. The analytical models for both building types under static conditions are depicted in figures 4.4(e) and 4.6(e). Despite variations in factor of safety (FoS) due

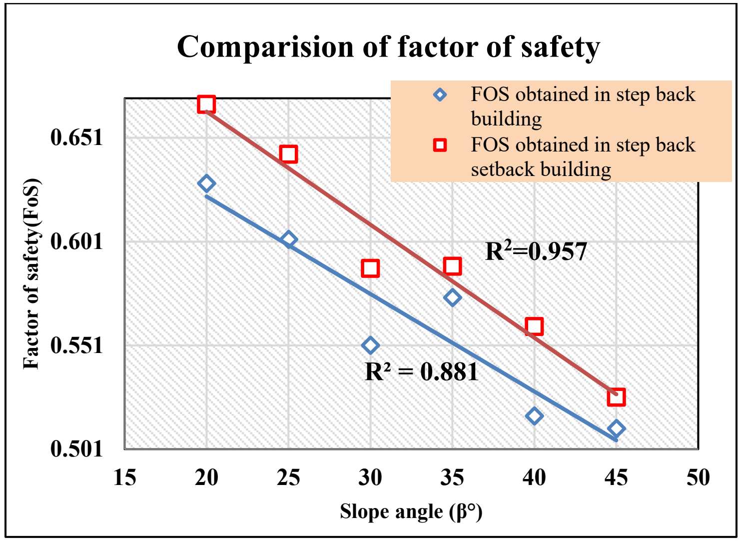

(a) FoS obtained with building loads under static conditions.

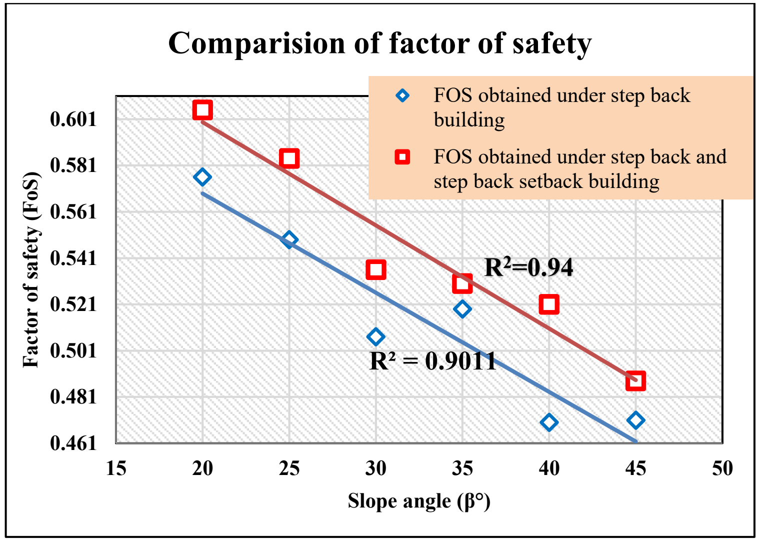

(b) FoS obtained with building loads under seismic conditions.

Fig.5.1: Comparison of the Factor of Safety obtained with step back building and step back setback building (a) FoS obtained with building loads under static conditions (b) FoS obtained with building loads under seismic conditions.

to changes in building loads, the shape of the critical slip surface remains consistent and rotational for both building types. Similarly, under seismic analysis, the shape of the slip failure remains same under two types of building load, as shown in figures 4.5(e) and 4.7(e).

The above statement clarifies that the variations of step back and step back setback building loads within the same slope geometry and soil properties has no influence on the shape of the critical slip surface. However, the FoS obtained on the critical slip surface depending on the building load may vary due to the variation of base normal stress and frictional strength. The graphical representation on how the FoS vary on the lowest five critical slip surface depending on the building loads under static and dynamic conditions has been illustrated in figure 5.2.

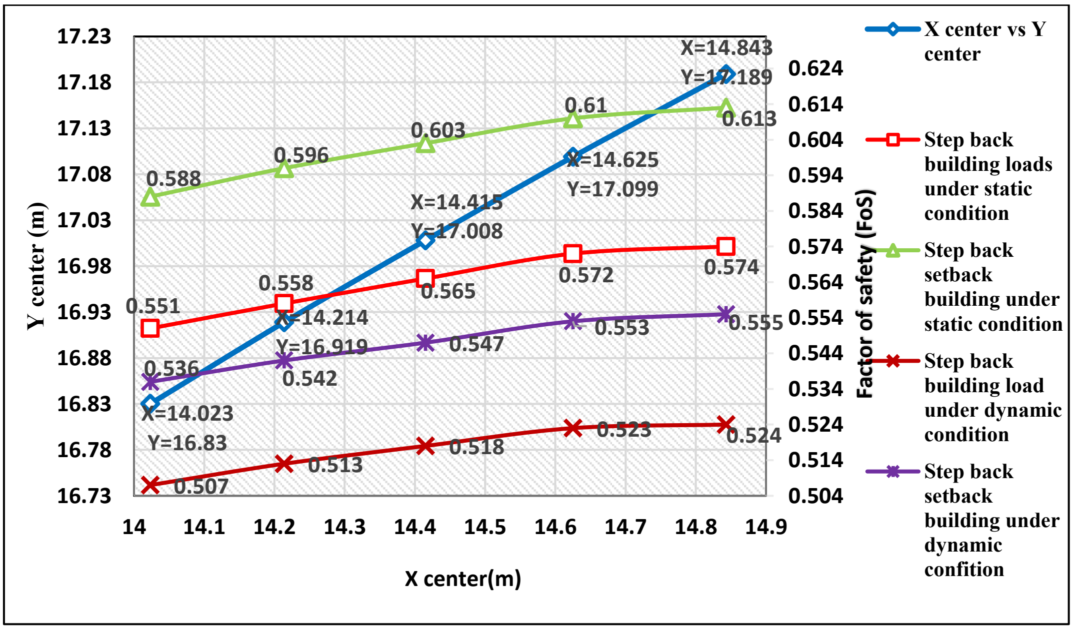

Fig.5.2: Impact of varying factor of safety on the lowest five critical slip surface due to step back and step back setback building loads under static conditions and seismic conditions.

4.4.7 Influence of slope geometry on the shape of the critical slip failure.

The study investigates how different slope angles affect the shape of the circular critical slip failure surface. The slopes such as S42, S9, S40, S36, S7, and S43 respectively represents varied slope angle of 20°, 25°, 30°, 35°, 40°, and 45° respectively which were assumed to have similar soil properties (c= 41.27 kN/m², ϕ=8°, and γ=16.38 kN/m³).

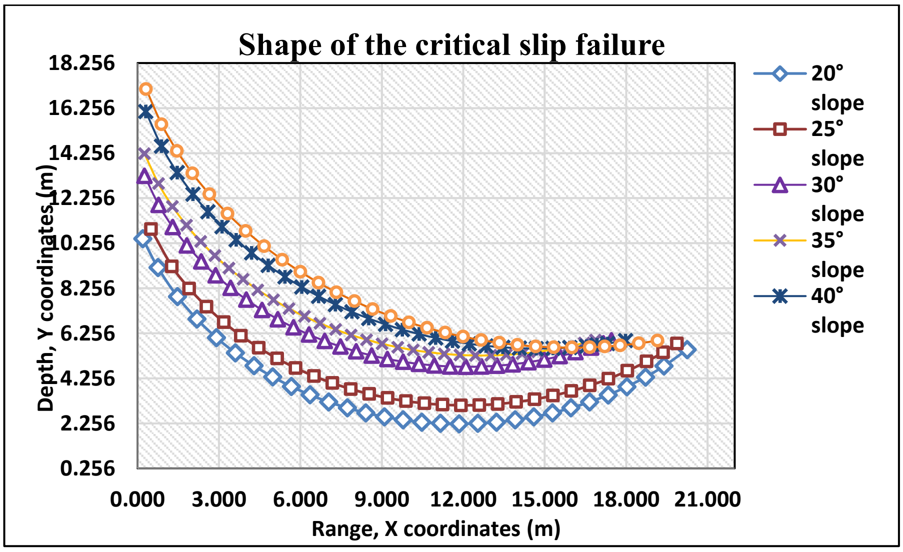

Fig.5.3: Comparison of shape of the critical slip surface for varied slope angle with similar soil properties.

Analysis of the slope stability at each site produced critical slip surface. Figure 5.3 illustrates the varying effects of slope geometry on the critical slip surfaces.

Figure 5.3 indicates that slope geometry, including slope angle and height, significantly affects the shape of the critical slip failure surface. When soil properties are kept consistent across slopes, higher slope angles and height increases the depth but decreases the range of the slip surfaces. This deeper and narrower configuration reduces the factor of safety (FoS), thus resulting in instability of the slope.

4.5 Summary:

The present study analyzed the effects of two building configurations, namely step back and step back setback buildings, on the stability of hill slopes. A comprehensive analysis was conducted on 50 slopes with varying slope angles from different locations within Aizawl city. The input variables for determining the factor of safety (FoS) in each selected site included slope geometry (slope height and slope angle) and soil parameters such as unit weight of soil (γ) and shear parameters (c & ϕ). Following general conclusions were made from the present study:

i) Results of the sensitivity analysis suggest that in cohesive soils, cohesion (c) has a greater influence on the factor of safety (FoS) than the angle of internal friction (ϕ) under all loading conditions. In contrast, for non-cohesive soils, although an increase in cohesion also improves the FoS, the angle of internal friction (ϕ) has a more significant effect on slope stability, particularly under building loads of static and seismic conditions. Similar findings have been reported in previous studies [115,116].

ii) A comparison of two building topologies proves that with the consideration of both static and seismic conditions, step back setback building obtained higher factor of safety than step back building alone in each site. Therefore, in hilly places like Aizawl city, RCC structures with a step back setback building is preferable owing to its superior FoS value (less susceptibility to slope failure) over step back building.

iii) The study concludes that varying building types under similar slope geometry and soil properties do not affect the shape of the critical slip surface as only circular failure alone is considered. However, changing the slope height and slope angle influence the shape of the critical slip failure surface in terms of its range and depth. This conclusion aligns with findings from other literature sources. [117,118]

iv) From the analytical results, the majority of selected sites in Aizawl city are less susceptible to slope failure without external loads. This suggests that under natural conditions, the slopes exhibit a certain level of stability. However, when subjected to external loads, specifically 21m building height with seismic loads, many of these sites become prone to slope failure.

v) All the conclusions are based on a limited range of soil parameters ($c = 7$–$45\ kN/m^2$, $\phi = 6°$–$25°$) and slope angles (20°–45°). These reflect site-specific conditions and may not apply to broader scenarios. These parameters were selected based on critical site conditions observed in the study area. Therefore, the findings should be interpreted within these bounds and may not be directly applicable to slopes with significantly different geotechnical or geometric conditions

CHAPTER 5

ZONATION MAPPING OF SLOPE VULNERABILITY WITH BUILDING LOADS IN AIZAWL CITY

5.1 Introduction

Landslide hazard zonation is a method used to evaluate risk in areas susceptible to landslides. This technique involves classifying an area into various zones, where each zone represents a different level of risk. The classification is based on several causative factors, which are weighted according to their potential impact on slope failure. In case of Aizawl city, a hilly region prone to frequent landslides, this study is particularly crucial due to the significant problems caused by landslides, including loss of life and property, road blockages, communication disruptions, and economic impacts. The objective of this study was to generate a slope vulnerability map, also called a landslide hazard zonation (LHZ) map subjected to building loads in Aizawl city. In this regard, the study has been carried out by following the procedures outlined in IS 14496 (Part 2): 1998, which provides guidelines for preparing landslide hazard zonation maps in mountainous areas.

Previous research, as outlined in the literature review, has largely concentrated on creating landslide zonation maps using geo-environmental factors including land use, land cover, natural drainage, bedrock etc. However, these maps often neglect the impact of building loads, which is critical in areas like Aizawl city where construction literally took place on slopes or near slope with the slope ranging from 15° to 45°. In Aizawl city, most slope failures have been attributed to inadequate slope management and improper building construction, often carried out without proper site investigation or assessment of critical soil properties, including bearing capacity and shear strength.

To address this gap, the current study aims to develop a vulnerability map that incorporates the loads from G+6 story buildings. Slope stability analysis was performed considering soil properties and slope morphology, with the findings expressed in terms of the factor of safety (FoS). The development of the vulnerability map takes into account various causative factors affecting slope stability, including soil bearing capacity (SBC), factor of safety (FoS), lithology, rainfall, bedrock and topographic features. Both the qualitative and quantitative methods were implemented for the assessment of vulnerability which includes heuristic (expert evaluation) techniques, statistical (data-driven) method and deterministic method. These methods integrate the various factors to produce a detailed vulnerability map for Aizawl city.

5.2 Study area

The random selected sites in the municipal areas of Aizawl city have been identified and studied. A total of 182 sites (S1 to S182) were selected as the study area to represent the Aizawl city after investigating and assessing the history of each site. These selected sites are built-up area where people are residing and the area of each selected site ranges from 200sqm to 500sqm. Laboratory tests were conducted on the collected soil samples for determination of geotechnical properties and shear strength parameters of soil as per American Society for Testing and Materials (ASTM). This soil parameters obtained from the laboratory tests were adopted for determining the safe bearing capacity (SBC) of the soil and factor of safety (FoS) of the slope in each selected site. A map showing the selected sites is provided in Figure 1.3, and detailed information about the location and characteristics of these sites are described in Table 1.1 in chapter-1.

5.3 Materials and methods

5.3.1 Data used

In the present study, a vulnerability map for Aizawl city has been generated using an outlined map of the Aizawl Municipal Area, prepared by the Aizawl Municipal Corporation (AMC) as the based map. The vulnerability assessment incorporates various factors, including:

- Safe Bearing Capacity (SBC) of Soil
- Factor of Safety (FoS) of Slope Analysis with step back building (G+6).
- Structural features (bedrock).

- Slope morphology.
- Lithology.
- Rainfall.

Some of the causative factors—SBC map, FoS map, and bedrock map—were developed through statistical methods based on field investigations and subsequent analyses. Other factors, like lithology map and slope map of the study area was generated using the base map generated from MIRSAC (Mizoram Remote Sensing Application Centre). Rainfall map of the study area was collected from State Meteorological Centre (Sc & Tech).

To generate the final vulnerability map, these individual maps were integrated through weighted overlay analysis using ArcGIS 10.4.1 software. This process involved combining all the causative factors to produce a comprehensive vulnerability map of the study area.

Thematic layers

Slope vulnerability is influenced by multiple factors. In a hilly region like Aizawl city, where land use is predominantly for construction, six critical causative factors were identified and organized into thematic layers using satellite data and field studies. These layers were then employed to map slope vulnerability. The different layers are:

(i) Bearing capacity of soil:

In this study, the safe bearing capacity (SBC) for square footings was evaluated across all selected sites. The methodology for calculating SBC is detailed in Chapter 3. The study area was categorized into three classes based on the SBC values obtained: High, Moderate, and Low. Table 5.1 depicted the area covered by each class measured in square kilometers.

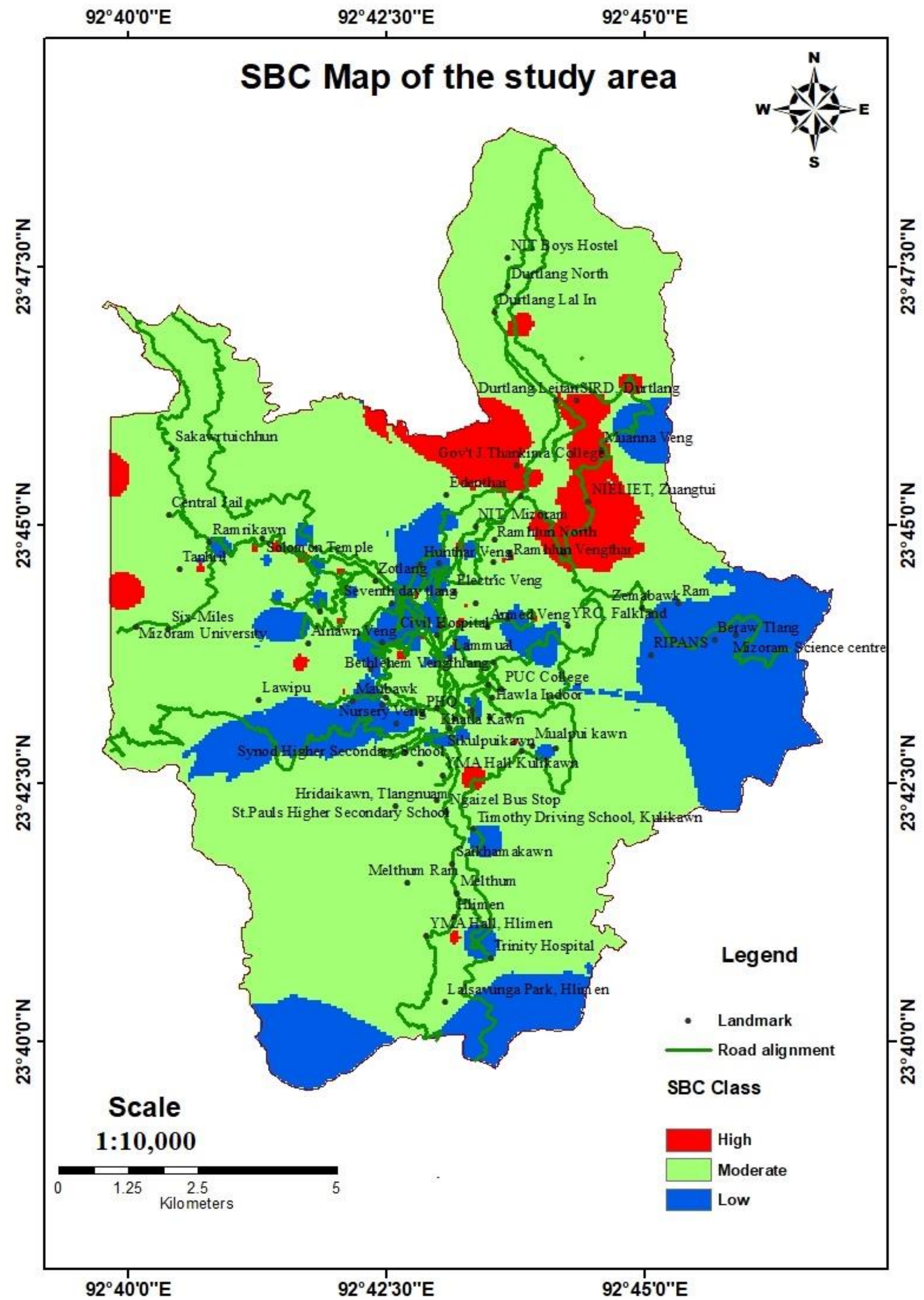

Fig.5.4: SBC map of the study area.

- **High Class**: SBC values less than 200 kN/m².
- **Moderate Class**: SBC values between 200 kN/m² and 300 kN/m².
- **Low Class**: SBC values above 300 kN/m².

Each class was assigned a weightage value. The High class, which has the lowest SBC values, was given the highest weightage of vulnerability, followed by the Moderate and Low classes. Using these classifications and corresponding weightages, a map was generated to depict slope vulnerability based on the SBC values obtained as given in Figure 5.4.

Table 5.1: Statistics of SBC values obtained in the study area

SBC class	Area (sq.km)	Percentage (%)
High	6.89	5.31
Moderate	88.55	68.16
Low	34.47	26.53
Total	129.91	100

(ii) Factor of Safety (FoS) with step back building:

Despite the fact that the slope stability analysis may not account for every possible vulnerability factor, it addresses many critical elements, including surcharge loads, pore water pressure, seismic activity, soil types, slope height, and slope angle. This comprehensive approach helps to assess and ensure the stability of slopes by considering the most significant factors influencing their vulnerability. In this study, the FoS obtained from the analysis of slope with step back building (G+6) under seismic conditions in all the selected sites of the study area were implemented. The analysis performed has been detailed in chapter-4. The study area was classified into three categories based on the factor of safety (FoS) values such as High, Moderate, and Low. Table 5.2 illustrates the area covered by each classification, measured in square kilometers.

- **High Class**: FoS values less than 1.

- **Moderate Class**: FoS values between 1 to 1.5.
- **Low Class**: FoS above 1.5.

A weightage value based on its level of vulnerability was assigned for each class. The High Class, with a factor of safety (FoS) value less than 1, was assigned the highest weightage for vulnerability. This was followed by the Moderate Class, which includes FoS values ranging from 1 to 1.5, and the Low Class with FoS values greater than 1.5. A map was then created to represent slope vulnerability according to these FoS classifications and their associated weightages, as depicted in Figure 5.5.

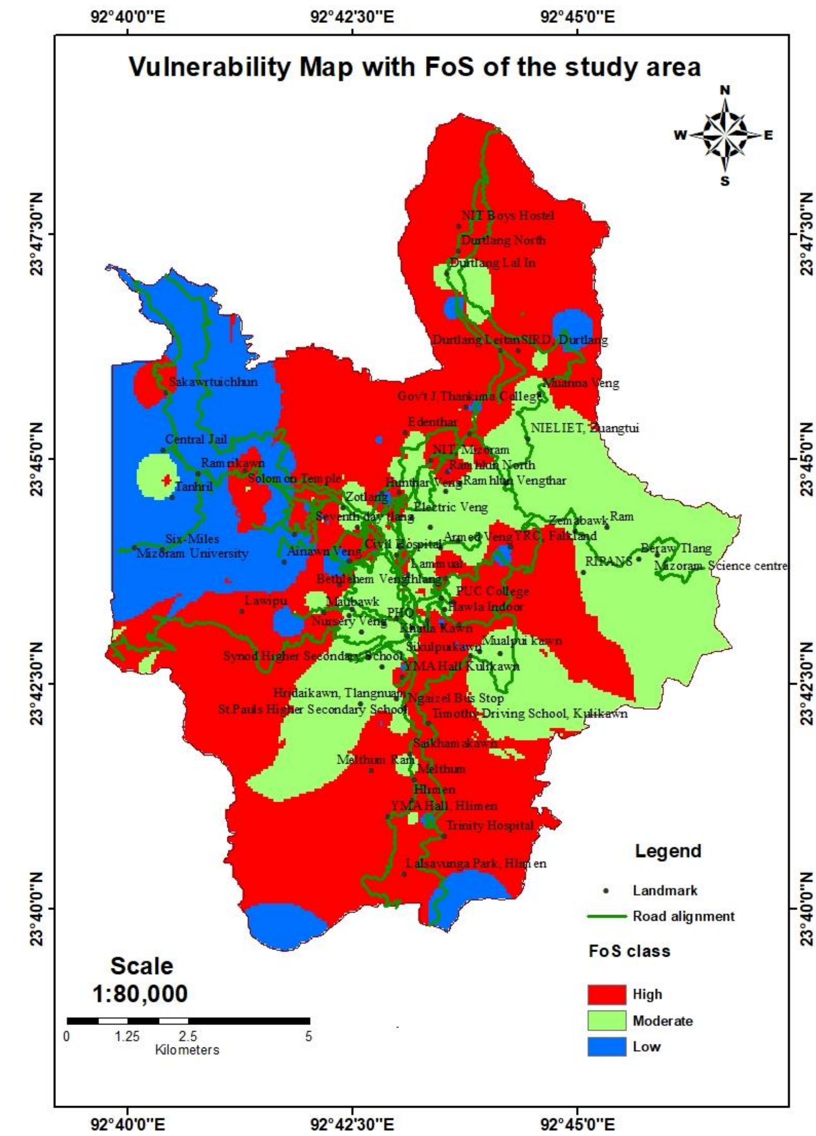

Fig.5.5: FoS map of the study area.Table

Table 5.2: Statistics of FoS value obtained in the study area

FoS class	Area (sq.km)	Percentage (%)
High	63.05	48.54
Moderate	34.50	26.56
Low	32.36	24.90
Total	129.91	100

(iii) Structural features (bedrock outcrop):

The stability of slopes is significantly influenced by the structural features of the underlying rock, particularly its bedding. To understand these influences, measurements are often taken using a clinometer to determine the orientation of the rock bedding. Based on the relationship between the slope and the bedrock orientation, the study area has been divided into four primary types of slopes such as:

- **Anti-dip Slope**: This occurs when the slope is oriented in the opposite direction to the dip of the rock beds. In other words, the slope faces away from the direction in which the rock layers are inclined. Anti-dip slopes can be relatively stable if the rock layers are well-cemented and the slope does not exceed critical angles.
- **Homo-clinal Slope (Dip Slope)**: In this case, the slope is oriented parallel to the bedding plane of the rock. Here, the slope runs in the same direction as the inclination of the rock layers. Dip slopes can be prone to sliding if the bedding planes are steep or if there are weaknesses within the rock layers.
- **Strike Slope**: A strike slope is oriented perpendicular to the bedding planes. This means the slope runs across the direction of the rock layers. The stability of strike slopes depends on the dip of the rock layers and the presence of any discontinuities that could affect slope stability.
- **Oblique Slope**: This type of slope is oriented at an angle that is neither parallel nor perpendicular to the bedding planes but instead intersects them at an oblique angle. The stability of oblique slopes can be complex to assess as it involves a combination of factors from both the dip and strike orientations, along with additional geological features.

Each slope type interacts with the underlying rock structure in distinct ways, impacting stability and the likelihood of slope failures. Based on these interactions, the homo-clinal slope was assigned the highest weightage in terms of its potential to influence slope instability. This was followed in descending order by oblique slopes, strike slopes, and anti-dip slopes. A map was subsequently created to represent the relationship between the slope and the rock bedding, as illustrated in Figure 5.6. The statistical details of the rock bedding measured in the study area are provided in Table 5.3.

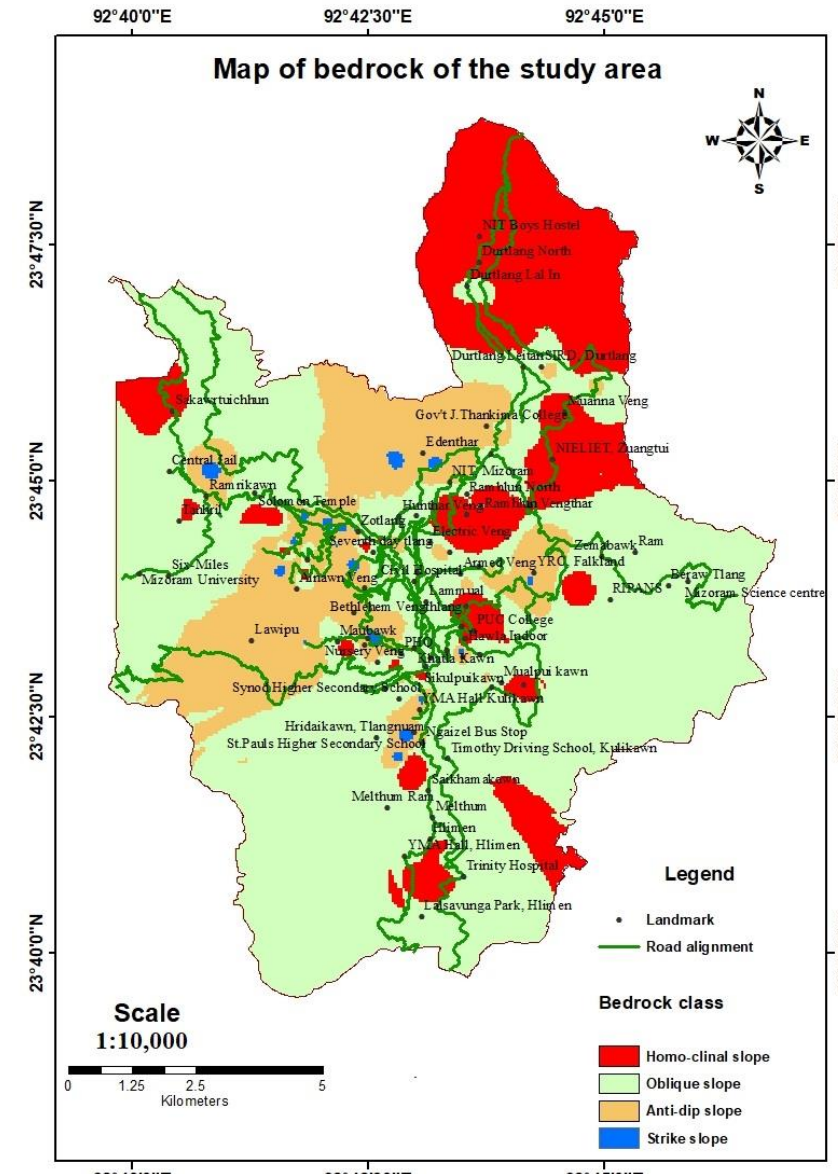

Fig. 5.6: A map showing relationship of bedrock with slope of the study area.

Table 5.3: Statistics of bedrock orientation with slopes in the study area

Bedrock orientation with slopes	Area (sq.km)	Percentage (%)
Homo-clinal slope	25.05	19.28
Oblique slope	73.46	56.55
Strike slope	23.88	18.38
Anti-dip slope	7.52	5.79
Total	129.91	100

(iv) Slope:

Shear stress in soil or other unconsolidated materials generally increases with the angle of the slope, making slope angle a critical factor in stability assessment and slope design. In this study, the slope map produced by MIRSAC was utilized and cross-verified with field investigations at all selected sites. The slope angles measured in the field closely matched those generated by MIRSAC, as illustrated in Figure 1.6 of Chapter 1. The slopes in the study area are categorized by degrees into five facets: 15° to 25°, 25° to 30°, 35° to 40°, 40° to 45°, and above 45° respectively. Weightage values were assigned based on the steepness of these slopes. The detailed slope statistics for the study area are presented in Table 5.4.

Table 5.4: Statistics of slope of the study area

Degrees of slope	Area (sq.km)	Percentage (%)
15° to 25°	0.353	0.27
25° to 30°	0.184	0.14
30° to 35°	7.958	6.13
35° to 40°	11.275	8.68
40° to 45°	47.06	36.23
>45°	63.08	48.56
Total	129.91	100

(v) Lithology:

Lithology, which refers to the physical and chemical characteristics of rock formations, plays a critical role in the vulnerability assessment of slopes due to its significant influence on slope stability and erosion processes. The study area, which is situated over the Bhuban and Bokabil formations of the Surma Group from the Tertiary period, the predominant rock types are arenaceous (sandy) and argillaceous (clayey) rocks. Based on the exposed rock formations observed at the site, five distinct lithology units have been identified and categorized according to their hardness. These units are listed as follows: sandstone, siltstone-sandstone, shale-sandstone and crumpled shale. The weightage value was assigned depending on the hardness of the rock. Therefore, the highest weightage value was assigned to the weakest rock such as crumpled shale which was followed by shale-sandstone, siltstone-sandstone and sandstone respectively. Using a lithology map of Aizawl generated by MIRSAC as a base map, a lithology map of the study area has been modified according to the classification of litho-unit shown in Figure 1.4. The statistics of the lithology observed at the study area are shown in Table 5.5

Table 5.5: Statistics of lithology of the study area

Types of rocks	Area (sq.km)	Percentage (%)
Crumpled shale	31.25	24.06
Shale-sandstone	33.25	27.13
Siltstone-sandstone	22.73	17.50
Sandstone	42.68	31.31
Total	129.91	100

(vi) Rainfall:

In hilly areas such as Aizawl city, where the majority of sites are characterized by clayey soil, rainfall becomes a critical factor in assessing slope vulnerability. Clayey soils, due to their low permeability, can become highly saturated during heavy rainfall. This saturation increases the pore water pressure within the soil, reducing its shear strength and making the slope more prone to failure. Additionally, prolonged or intense rainfall can lead to increased soil erosion and destabilization of the slope. Therefore, understanding and monitoring the annual rainfall is essential for accurately evaluating and managing the risk of landslides and slope instability in such regions. As a result, a map generated by State Meteorological Centre shown in Figure 1.7 of chapter 1 has been implemented for this study. The annual rainfall in the study area has been classified into five categories such as very low, low, moderate, high, and very high. The amount of rainfall for each category are as follows: very low (2061mm to 2205mm), low (2205mm to 2294mm), moderate (2294mm to 2376mm), high (2376mm to 2462mm), and very high (2462mm to 2611mm). The weightage value has been assigned according to the amount of annual rainfall. The highest weightage has been assigned to the category of very heavy rainfall followed by high, moderate, low and very low rainfall respectively. The statistics of the annual rainfall of the study area is illustrated in Table 5.6.

Table 5.6: Statistics of annual rainfall of the study area

Rainfall class	**Area (sq.km)**	**Percentage (%)**
Very High	3.72	2.86
High	19.9	15.32
Moderate	49.74	38.29
Low	43.75	33.68
Very Low	12.8	9.85
Total	129.91	100

5.4 Data Analysis

In the study area, the geology, morphology and human activity were found to be the most influential factors on slope failure. The six fundamental parameters such as bearing capacity (SBC), factor of safety (FoS), structural features (bedrock), slope morphology, lithology and rainfall significantly influence the occurrence of slope failure. These six factors are the fundamental parameters for assessment of vulnerability of slope and are categorized into specific classes for detailed analysis. Each class within these parameters was carefully examined to determine its relationship to slope vulnerability. A weightage value was assigned to each class, reflecting its potential impact on the occurrence of slope failure, with higher weightage indicating a greater influence on slope instability. The weightage values were assigned based on expert knowledge and their relative importance of each factor in triggering slope failure, referring to the weightage value given by National Remote Sensing Agency [119] and stability ratings devised by Joyce and Evans [120]

The thematic layers, along with their assigned weightages, are integrated and analysed using ArcGIS software (version 10.4.1), to create a slope vulnerability map with building loads (G+6) of the study area. A map of the study area was then generated by weighted overlay analysis providing a comprehensive assessment of slope vulnerability in the study area which is shown in Table 5.7. The evaluation scale used for generating the map is 1 to 9 by 1. The ratings of the influence of the parameters are also given in terms percentage (%) as shown in Table 5.7.

Table 5.7: Parameters and their ranking in terms of their influence to slope vulnerability.

Parameters	**Influence (%)**	**Category**	**Weightage**
Safe Bearing Capacity (SBC) of soil	20	High	6
		Moderate	4
		Low	2
Factor of Safety (FoS)	35	High	9
		Moderate	7
		Low	5
Structural features (bedrock)	10	Homo-clinal slope	6
		Oblique slope	5
		Strike slope	4
		Anti-dip slope	2
Slope	20	>45°	9
		40° to 45°	8
		35° to 40°	7
		30° to 35°	6
		25° to 30°	5
		15° to 25°	4
Lithology	5	Crumpled shale	4
		Shale-sandstone	3
		Siltstone-sandstone	2
		Sandstone	1
Rainfall	10	Very High	5
		High	4
		Moderate	3
		Low	2
		Very Low	1

5.5 Results and discussion

Integrating all the controlling parameters and assigning different weightings to each theme, the final map of vulnerability of slopes subjected to building loads in Aizawl city was developed and classified into the categories of 'Very High', 'High', 'Moderate' and 'Low' zones respectively. The output of this map was generated at a scale of 1:10,000 as shown in Figure 5.7. The vulnerability classes are defined as follows:

5.5.1 Very High Vulnerability Zone

Based on slope morphology, this zone is characterized by steep slopes of approximately 35° or greater. However, slope stability is influenced not only by the slope morphology, but also by soil properties, particularly its shear strength. Geologically, the area is highly unstable due to the type of soil and rock formations, which disrupt the relationship between the slope and the bedrock. This instability is compounded by the combination of building loads of G+6 and seismic activity. Rainfall intensity further contributes to slope instability in those areas. Human activities such as road cutting also contribute to the instability. The area typically features steep slopes with loose and unconsolidated materials and includes sites with evidence of recent or past landslides. This zone covers approximately 24.78 sq.km, representing 19.07% of the total study area. Soil bearing capacity in these regions is relatively low. Therefore, existing buildings should be maintained with appropriate measures to ensure slope stability and structural integrity.

5.5.2 High Vulnerability Zone

The study area within this zone features steep slopes typically ranging from 30° to 35°. The vulnerability of slope is influenced by various factors, including slope morphology, the factor of safety (FoS) from slope stability analysis, lithology, rainfall intensity, and the relationship between the slope and bedrock. Although most FoS values in this zone fall within the moderate range, they alone do not fully represent the vulnerability of slope. Field investigations revealed that the predominant rock formations are crumpled shale, shale-sandstone, and silt-sandstone, with crumpled shale being the dominate rocks. This rock composition places much of the area in a high vulnerability zone.

The slopes in this region are characterized by dip slopes and oblique slopes, and the rainfall intensity is classified as high to moderate. The soil bearing capacity (SBC) in these areas typically ranges from 100 to 250 kN/m^2. Consequently, constructing a G+6 building in this zone requires implementing effective slope stability measures and should be carried out under the supervision of experienced Engineer. This zone covers about 68.01 square kilometres, which constitutes 52.35% of the total study area, indicating that it encompasses the majority of the area. Engineers are advised to design buildings according to the specific geological and SBC conditions of the site.

5.5.3 Moderate Vulnerability Zone

The study area in this zone features steep slopes generally ranging from 25° to 30°. This slope morphology tends to reduce the vulnerability of slope, although it is not the sole factor determining classification of the area. The higher factor of safety (FoS) values in this zone contribute to a lower risk of slope failure. Despite the high intensity of rainfall in these areas, the relatively thin soil layer allows for noticeable bedrock exposure. The predominant rock formation is sandstone, and the slopes are characterized by an oblique relationship with the bedrock, resulting in a moderate vulnerability classification for the zone. The soil bearing capacity (SBC) in these areas ranges from 200 to 300 kN/m^2. Therefore, constructing a G+6 building in this zone is deemed feasible. However, engineers should design buildings based on the specific geological conditions and SBC of the site to ensure the stability of both the slope and the structure. The Moderate Vulnerability zone covers approximately 30.89 square kilometers, representing 23.78% of the total study area, as highlighted in Table 5.8.

5.5.4 Low vulnerability zone

This zone encompasses areas where a combination of factors typically does not negatively affect slope stability. Situated in a hilly region with residential and construction activities on or near slopes, this zone represents a very small portion of the study area with low vulnerability. The gentler slope angles here, generally below 25°, contribute to its low vulnerability status. A significant part of this zone is characterized by hard, compact rock types like sandstone. It includes flatlands and regions with gentle slopes and is primarily located where human activities are minimal or non-existent. There is no observed evidence of instability or expected mass movement within this zone, barring significant changes to the site. As such, this zone is considered suitable for development projects. It covers approximately 6.23 square kilometers, which is 4.8% of the total study area as shown in Table 5.8.

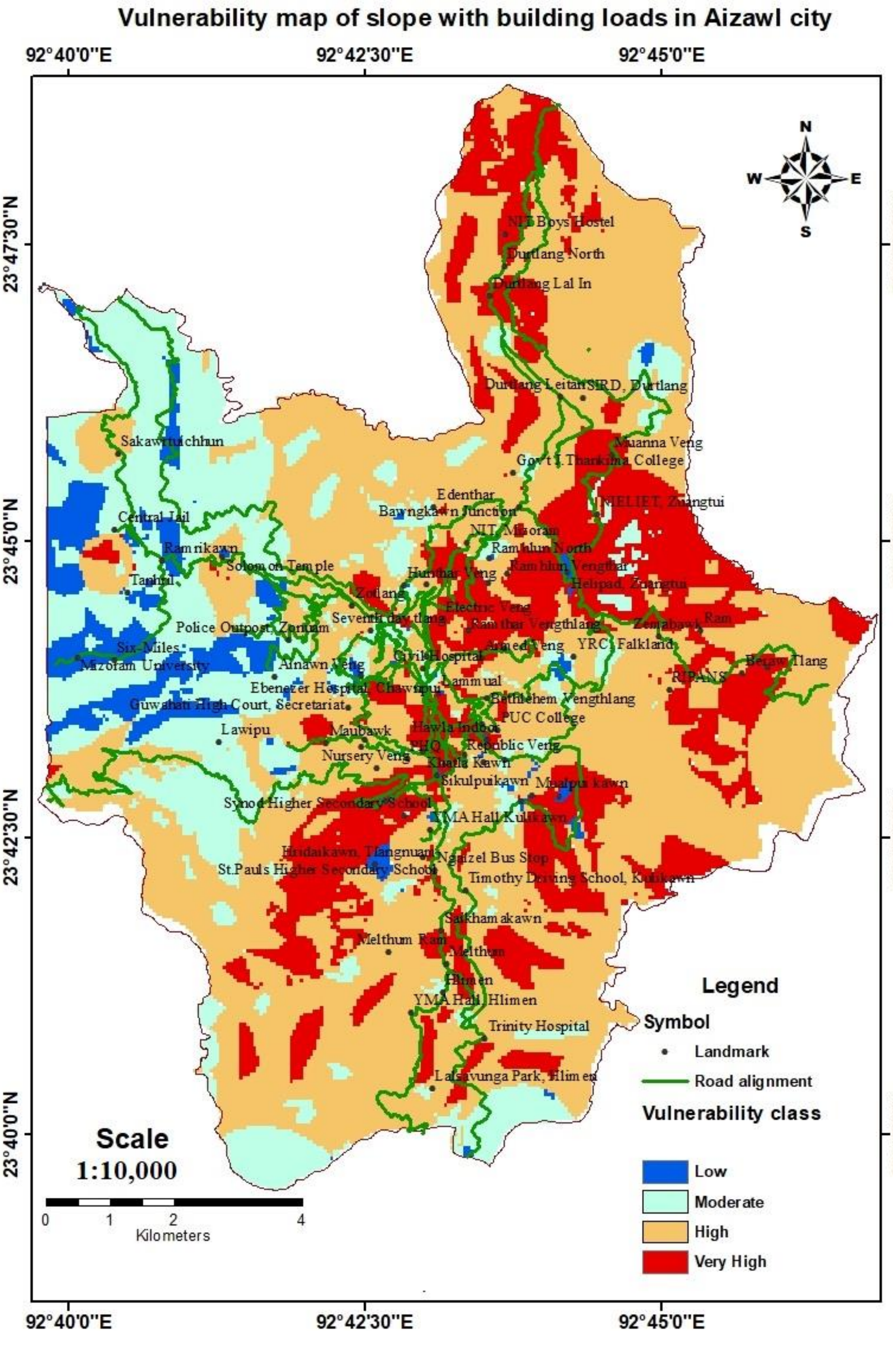

Fig.5.7: A map showing vulnerability of slopes with building loads (G+6) of the study area.

Table 5.8: Statistics of vulnerability class of the study area

Vulnerability class	Area (sq.km)	Percentage (%)
Very High	24.78	19.07
High	68.01	52.35
Moderate	30.89	23.78
Low	6.23	4.80
Total	129.91	100

5.6 Summary

The present study aims to create a map depicting slope vulnerability in relation to building loads. To develop this map, several critical factors were considered, including soil bearing capacity (SBC), factor of safety (FoS), slope, structural features (bedrock), lithology, and rainfall data. These factors were incorporated as thematic layers to produce a map categorizing vulnerability of the study area into four hazard zones: Very High, High, Moderate, and Low. The following general conclusions were drawn from the study:

1) The final map highlights that the majority of the municipal area falls within High and Very High vulnerability classes, driven by steep slope angles (>30°), weak lithologies (notably crumpled shale), low SBC in many locations, and elevated rainfall.
2) Slope stability is strongly affected by anthropogenic activities particularly construction without prior geotechnical investigation and slope modification (bench cutting) which are spatially correlated with the mapped high-risk zones. Moreover, incorporating building loads (G+6) and seismic effects into factor of safety (FoS) calculations substantially alters the vulnerability assessment, revealing high-risk locations that conventional geo-environmental zonation alone would underestimate.
3) The vulnerability map was qualitatively validated through field observations and historical landslide records wherever available. A substantial proportion of documented failures were found to occur within the High and Very High

vulnerability zones, thereby confirming the reliability of the map and supporting its utility for planning and mitigation purposes.

4) The vulnerability map, which includes considerations for G+6 building loads, generated by this study will serve as a critical resource for selecting appropriate sites for development. It will assist the decision makers, administrator like Aizawl Municipal Corporation (AMC) and developmental planner in identifying unstable areas for constructing G+6 buildings and in implementing suitable mitigation measures in landslide-prone zones.

CHAPTER 6

CONCLUSIONS

6.1 Conclusions

The study carried out in this thesis has successfully addressed the complex problem of slope vulnerability in Aizawl city under the influence of building loads, integrating geotechnical, geological, structural, and geospatial aspects into a unified framework. A total of 182 sites were systematically investigated through field surveys, laboratory testing, and advanced analytical methods. The research adopted a holistic approach by combining soil mechanics, slope stability analysis, machine learning–based regression modeling, and GIS-based spatial analysis, thereby ensuring a comprehensive understanding of slope vulnerability in an urban hilly terrain.

One of the significant achievements of this work is the development of a modified bearing capacity model equation using machine learning regression techniques, calibrated against IS 6403:1981. This represents a novel contribution, bridging conventional geotechnical design with modern data-driven approaches, and enhancing the reliability of safe bearing capacity estimation for complex soil conditions of Aizawl city.

The study also provides an in-depth evaluation of building typologies and their effect on slope stability. By analysing Step Back and Step Back–Set Back configurations under both static and seismic loading conditions, the research has generated valuable insights into structural-slope interaction, highlighting the safer performance of Step Back–Set Back configurations. This is of particular importance for urban planning and design in Aizawl, where unplanned construction continues to exert pressure on fragile slopes.

Another commendable outcome is the preparation of a Slope Vulnerability Hazard Zonation (SVHZ) map, which integrates multiple thematic layers such as lithology, slope morphology, structural features, rainfall, soil properties, and building loads. The resulting map classifies the study area into four vulnerability zones, providing a clear and practical tool for administrators, planners, and engineers. The successful use of remote sensing and GIS techniques, validated with field investigations, has demonstrated the power of combining modern spatial technologies with traditional geotechnical analysis.

This research further emphasizes the role of human-induced modifications, such as slope cutting, unplanned development, and road construction, as aggravating factors of slope failure. The findings serve as a strong technical foundation for policy-makers and regulatory bodies such as the Aizawl Municipal Corporation (AMC) to incorporate vulnerability considerations into building regulations and urban development strategies.

In summary, this work makes a substantial contribution to geotechnical and geo-environmental research in hilly urban areas. It not only advances the scientific understanding of slope vulnerability under building loads but also provides a practical framework for hazard assessment and sustainable urban planning in Aizawl. The meticulous fieldwork, rigorous laboratory testing, innovative application of machine learning, and the integration of GIS-based mapping reflect the depth and originality of this research.

The thesis demonstrates that a multidisciplinary approach, combining soil mechanics, structural engineering, geology, and spatial technology, can generate highly reliable and actionable outcomes. The work stands as a valuable reference for future research and a guiding framework for engineers, planners, and decision-makers working in landslide-prone urban hill environments.

Following important conclusions were derived from the present study:

1) The regression model for estimating soil bearing capacity indicates that square footings have the highest capacity, influenced by low Plasticity Index (PI), high unit weight of soil and shear strength parameters (cohesion ‘*c*’ and internal friction angle ‘ϕ’). Both stepwise and Lasso regression effectively predicted bearing capacity, ϕ showing high correlation with IS 6403:1981 guidelines.
2) Stepwise regression identified ‘ϕ’ as the most significant factor, followed by ‘*c*’, foundation depth (D), unit weight of soil (γ), and plasticity index (PI). While

stepwise regression had slightly better R^2 values and used fewer predictor terms (eight versus nine in Lasso), it neglected foundation width (B), which Lasso included. This suggests Lasso may offer a more realistic model for bearing capacity estimation. Overall, both of the methods yielded satisfactory results in predicting bearing capacity.

3) The sites with higher cohesion (c) value have more impact for determination of factor of safety (FoS) under free slope stability analysis. Meanwhile, the sites having higher angle of internal friction (ϕ) has more impact under the analysis carried out with consideration of building loads. This finding was also validated by the performing the sensitivity analysis of shear strength parameters of soil.
4) The study concludes that varying building types under similar slope geometry and soil properties do not affect the shape of the critical slip surface as only circular failure alone is considered. However, changing the slope height and slope angle influence the shape of the critical slip failure surface in terms of its range and depth.
5) The comparative analysis of two building typologies demonstrates that the implementation of a step-back setback configuration enhances slope stability to a greater extent than the conventional setback building configuration.
6) The slope vulnerability map generated highlights that the majority of the study area falls within High and Very High vulnerability classes, driven by steep slope angles (>30°), weak lithologies (notably crumpled shale), low SBC in many locations, and elevated rainfall.
7) Slope stability is strongly affected by anthropogenic activities particularly construction without prior geotechnical investigation and slope modification (bench cutting) which are spatially correlated with the high-risk zones in the slope vulnerability map.
8) Moreover, incorporating building loads, SBC and FOS for analyzing slope stability substantially alters the vulnerability assessment, revealing high-risk

vulnerable sites that conventional geo-environmental zonation alone may underestimate the risks.

9) This resource generated from the present study will aid the decision makers, administrator like Aizawl Municipal Corporation (AMC) and developmental planner in identifying unstable areas for constructing buildings storey and in implementing suitable mitigation measures in landslide-prone zones.

6.2 Scope for Further Studies

1) Future studies may extend the present work by expanding the geotechnical database through additional field investigations and geophysical surveys which will improve spatial resolution of the slope vulnerability maps.
2) By incorporating additional factors influencing slope vulnerability, the prediction of slope vulnerability maps can be improved, thereby providing a more realistic representation of site conditions.

APPENDICES:

Table 6.1 Soil properties and other related parameters of slope vulnerability assessment

Sites	Specific Gravity	Plasticity Index (PI) (%)	Liquid Limit (%)	Unit weight (kN/m3)	OMC (%)	Cohesion (*c*) kN/m2	Angle of internal friction (ϕ°)	Soil types (USCS)	Rock types	SBC (kN/m2) for square footing	FoS under static and seismic conditions	Bedrock orientation
S1	2.4	5.89	35.35	17.46	18	13.5	32	ML	Sandstone	592.89	1.329	Antidip
S2	2.47	1.25	30.52	15.4	20	0.8	35	ML or OL	Sandstone	426.78	1.018	Antidip
S3	2.56	16.053	30.42	15.59	22	33.84	20	CL	Sandstone	160.39	1.137	Antidip
S4	2.49	11.832	36.25	15.69	20	31.68	15	ML	Sandstone	513.2	0.893	Antidip
S5	2.51	12.76	30.79	17.51	16	32.43	12	CL	Crumpled Shale	98.34	0.757	Homoclinal
S6	2.55	18.5	37.96	17.97	14	55.034	11	CL	Crumpled Shale	93.63	0.577	Homoclinal
S7	2.56	15.306	27.65	15.18	20	47.87	7	CL	Crumpled Shale	133.65	0.48	Homoclinal
S8	2.57	1.51	33.55	17.02	18	0.76	35	ML or OL	Crumpled Shale	148.62	0.627	Oblique
S9	2.4	14.66	34.29	15.89	18	40.64	7	CL	Crumpled Shale	461.42	0.463	Oblique
S10	2.47	13.63	37.906	15.45	20	34.5	18	CL	Crumpled Shale	139.07	0.725	Oblique
S11	2.49	6.23	38.9	16.52	18	10.39	29	ML	Sandstone	148.75	0.839	Homoclinal
S12	2.72	13.796	45.01	16.18	22	31.88	18	ML	Sandstone	410.73	0.87	Homoclinal
S13	2.4	10.25	46.84	15.79	22	25.67	26	ML	Sandstone	162.9	1.154	Homoclinal
S14	2.47	10.15	47.34	15.49	18	20.45	24	ML	Sandstone	215.86	1.031	Homoclinal
S15	2.5	10.45	49.35	15.79	18	20.1	25	ML	Sandstone	169.13	1.658	Homoclinal
S16	2.54	10.25	42.46	16.87	20	21.2	29	ML	Sandstone	179.54	1.938	Homoclinal
S17	2.53	11.895	35.93	16.97	20	31.65	22	CL	Crumpled Shale	633.87	1.554	Antidip
S18	2.56	2.15	34.12	16.77	19	3.98	34	ML or OL	Crumpled Shale	199.92	0.846	Antidip
S19	2.6	12.95	33.63	16.97	19	33.57	23	CL	Crumpled Shale	678.01	0.766	Oblique
S20	2.51	1.15	29.19	17.65	16	2.95	35	ML or OL	Crumpled Shale	128	0.867	Oblique
S21	2.6	1.45	32.72	17.26	18	3.92	34	ML or OL	Crumpled Shale	221	0.844	Oblique
S22	2.63	16.91	34.24	17.95	16	46.49	19	CL	Crumpled Shale	754.55	0.761	Antidip
S23	2.63	8.253	34.34	17.95	16	19.81	28	ML	Crumpled Shale	693.51	0.791	Antidip

Sites	Specific Gravity	Plasticity Index (PI) (%)	Liquid Limit (%)	Unit weight (kN/m3)	OMC (%)	Cohesion (*c*) kN/m2	Angle of internal friction (ϕ°)	Soil types (USCS)	Rock types	SBC (kN/m2) for square footing	FoS under static and seismic conditions	Bedrock
S24	2.6	10.59	30.62	16.97	18	30.8	18	CL	Crumpled Shale	250.99	0.55	Homoclinal
S25	2.5	14.15	36.36	16.48	18	43.38	24	CL	Crumpled Shale	310.18	0.764	Homoclinal
S26	2.54	13.95	33.51	16.48	18	33.38	24	CL	Crumpled Shale	676.25	0.731	Homoclinal
S27	2.8	16.8	40	16.18	22	41.69	23	CL	Crumpled Shale	184.85	0.515	Oblique
S28	2.78	10.12	43.82	16.38	18	44.99	11	ML	Crumpled Shale	307.94	0.741	Oblique
S29	2.6	9.45	50.27	16.87	18	23.93	29	MH	Crumpled Shale	282.57	0.867	Oblique
S30	2.8	10.34	34.76	17.85	16	20.69	35	ML	Crumpled Shale	228.29	0.726	Oblique
S31	2.51	4.52	18.84	15.4	12	31.88	22	CL	Crumpled Shale	170.21	0.754	Oblique
S32	2.57	0.43	30.42	15.59	18	18.84	26.65	ML or OL	Siltstone-Sandstone	761.68	0.955	Antidip
S33	2.61	18.59	40.2	15.64	16	17.76	34	CL	Crumpled Shale	1383.19	1.083	Antidip
S34	2.49	10.55	36.25	15.69	18	28.203	20	ML	Siltstone-Sandstone	232.45	0.937	Oblique
S35	2.49	12.71	47.93	17.51	20	33.35	21	ML	Siltstone-Sandstone	204.87	1.129	Homoclinal
S36	2.57	13.8	38.53	15.18	16	28.45	10.96	CL	Crumpled Shale	577.5	0.451	Homoclinal
S37	2.61	15.05	30.05	15.45	18	33.35	19.25	CL	Crumpled Shale	344.95	1.067	Antidip
S38	2.51	12.76	39.207	16.18	21.17	44.15	9.51	ML	Crumpled Shale	690.33	0.746	Oblique
S39	2.4	2.93	24.23	15.79	12	5.88	43.77	ML or OL	Crumpled Shale	139.4	1.346	Oblique
S40	2.41	11.06	38.09	15.49	20	10.69	36.61	ML	Crumpled Shale	157.13	0.743	Oblique
S41	2.45	8.816	40.2	15.64	22	18.54	30	ML	Crumpled Shale	189.88	1.92	Oblique
S42	2.5	16.56	34.89	16.38	20	41.27	8	CL	Crumpled Shale	701.7	0.846	Oblique
S43	2.634	16.15	32.54	17.95	16	43.38	13	CL	Crumpled Shale	113.1	0.49	Oblique
S44	2.61	12.65	41.34	16.67	18	32.47	22	ML	Crumpled Shale	186.53	0.816	Oblique
S45	2.7	11.23	34.65	17.26	16	30.97	20	CL	Crumpled Shale	147.6	1.066	Oblique
S46	2.91	3.31	32.78	17.46	14	13.35	32.78	ML or OL	Crumpled Shale	210.51	2.046	Oblique

Sites	Specific Gravity	Plasticity Index (PI) (%)	Liquid Limit (%)	Unit weight (kN/m3)	OMC (%)	Cohesion (*c*) kN/m2	Angle of internal friction (ϕ°)	Soil types (USCS)	Rock types	SBC (kN/m2) for square footing	FoS under static and seismic conditions	Bedrock
S47	2.47	2.67	42.13	17.97	18	2.45	34.89	ML	Siltstone-Sandstone	599.06	2.083	Homoclinal
S48	2.46	8.05	30.6	17.02	20	49.34	13.7	CL	Siltstone-Sandstone	155.31	0.593	Homoclinal
S49	2.47	7.01	35.3	15.89	20	15	24.23	ML	Shale-Sandstone	1121.18	0.572	Oblique
S50	2.44	7.43	26.6	16.52	16	31.39	26.84	CL	Shale-Sandstone	1267.1	0.851	Oblique
S51	2.62	12.41	31	18.25	16	44.8	11.68	CL	Siltstone-Sandstone	544.882	0.52	Oblique
S52	2.63	18.08	36.77	16.38	20	44.15	15.96	CL	Crumpled Shale	236.83	0.93	Oblique
S53	2.642	9.14	30.6	16.68	16	28.73	27.72	CL	Crumpled Shale	233.29	0.744	Antidip
S54	2.52	7.62	32.2	16.16	18	27.95	25.64	ML	Crumpled Shale	236.072	1.348	Antidip
S55	2.52	8.96	36.35	16.68	22	28.74	22	ML	Crumpled Shale	208.952	1.174	Antidip
S56	2.51	1.36	32.85	16.97	10	18.84	26.65	ML	Siltstone-Sandstone	230.508	1.318	Homoclinal
S57	2.59	4.99	24.87	17.26	16	53.93	8	CL-ML	Sandstone	427.99	0.561	Homoclinal
S58	2.52	12.91	34.2	15.91	18	31.39	24	CL	Shale-Sandstone	254.545	0.682	Homoclinal
S59	2.52	12.82	36.2	15.58	18	36.05	17.021	CL	Crumpled Shale	248.34	1.014	Oblique
S60	2.55	12.02	35.4	15.66	18	36.06	18	CL	Crumpled Shale	249.652	0.668	Oblique
S61	2.55	12.02	35.4	15.66	18	36.06	15.5	CL	Crumpled Shale	249.652	0.61	Oblique
S62	2.54	4.23	30.407	17.46	12.17	2	44.71	CL-ML	Siltstone-Sandstone	400	0.649	Strike
S63	2.48	6.2	36.35	17.16	16	32.37	26.86	CL-ML	Siltstone-Sandstone	425.56	1.439	Strike
S64	2.56	5.44	26.065	18.64	14	25.5	26.65	CL-ML	Shale-Sandstone	251.69	0.69	Strike
S65	2.42	9.38	34.709	18.25	14	51.9	8.26	ML	Siltstone-Sandstone	249.82	0.664	Oblique
S66	2.38	7.73	28.445	17.15	18	39.534	20.556	CL	Crumpled Shale	279.84	1.193	Oblique
S67	2.39	5.98	26.17	18.44	14	18.15	35.48	CL-ML	Shale-Sandstone	349.019	1.161	Oblique
S68	2.41	14.48	31.89	17.75	14	28.45	29.72	CL	Sandstone	395.86	0.903	Oblique
S69	2.5	7.77	24.88	18.15	14	20.6	37.68o	CL	Sandstone	502.56	1.949	Oblique

Sites	Specific Gravity	Plasticity Index (PI) (%)	Liquid Limit (%)	Unit weight (kN/m3)	OMC (%)	Cohesion (*c*) kN/m2	Angle of internal friction (ϕ°)	Soil types (USCS)	Rock types	SBC (kN/m2) for square footing	FoS under static and seismic conditions	Bedrock
S70	2.4	11.25	30.94	17.26	16	43.16	7.68	CL	Sandstone	161.43	0.482	Oblique
S71	2.48	21.77	46.23	16.48	18	35.193	18.352	CL	Siltstone-Sandstone	221.96	0.589	Antidip
S72	2.33	8.26	40.2	17.44	14	22.396	20.76	ML	Sandstone	378.855	0.801	Oblique
S73	2.65	9.94	31.4	16.38	18	29.82	27.72	CL	Crumpled Shale	238.73	1.073	Antidip
S74	2.65	9.94	31.4	16.38	18	29.82	27.72	CL	Crumpled Shale	253.55	1.073	Homoclinal
S75	2.52	5.16	26.4	16.99	12	19.37	37.361	CL-ML	Crumpled Shale	251.961	1.929	Strike
S76	2.6	23.49	51.46	15.6	24	32.37	29.03	CH	Crumpled Shale	280.545	1.107	Antidip
S77	2.49	12.71	36.85	16.18	20	33.35	21	CL	Sandstone	197.91	0.631	Antidip
S78	2.65	17.59	40.85	16.38	20	34.335	11.98	CL	Crumpled Shale	160	0.777	Oblique
S79	2.63	7.75	29.75	16.68	18	13.94	32.13	CL	Siltstone-Sandstone	360.14	1.572	Antidip
S80	2.49	22.44	45	15.59	20	41.2	6.84	CL	Siltstone-Sandstone	156	0.412	Oblique
S81	2.31	7.69	36.105	15.107	19	18.64	24.23	ML	Crumpled Shale	235.64	0.937	Oblique
S82	2.67	10.58	35.75	16.58	16	22.56	30.96	ML	Crumpled Shale	425.86	1.579	Oblique
S83	2.59	9.4	31.87	15.59	16	20.601	27.68	CL	Siltstone-Sandstone	265.49	1.394	Strike
S84	3	8.74	37	15.49	18	7.35	44.03	ML	Shale-Sandstone	409.58	2.315	Antidip
S85	2.49	1.69	32.89	15.4	14	16.18	23.84	ML	Shale-Sandstone	190.315	1.166	Oblique
S86	2.52	11.68	29.44	17.15	18	42.15	17.9	CL	Shale-Sandstone	218	0.626	Antidip
S87	2.59	7.79	32.3	16.48	16	25.5	29.19	ML	Crumpled Shale	310.56	1.17	Antidip
S88	2.66	9.76	22.83	18.14	14	29.43	24.17	CL	Crumpled Shale	276.046	0.762	Homoclinal
S89	2.7	15.93	51.05	15.2	24	44.64	24.85	MH	Crumpled Shale	276.63	0.903	Strike
S90	2.5	11.42	38.63	15.7	20	20.64	25.45	ML	Siltstone-Sandstone	256	1.28	Strike
S91	2.52	12.35	30.165	16.58	18	26.24	28.025°	CL	Shale-Sandstone	257.805	1.452	Antidip
S92	2.62	4.28	30.58	16.97	17	28.15	19.815°	CL-ML	Siltstone-Sandstone	157.47	0.842	Strike

Sites	Specific Gravity	Plasticity Index (PI) (%)	Liquid Limit (%)	Unit weight (kN/m3)	OMC (%)	Cohesion (c) kN/m2	Angle of internal friction (ϕ°)	Soil types (USCS)	Rock types	SBC (kN/m2) for square footing	FoS under static and seismic conditions	Bedrock
S93	2.44	10.43	28.72	17.44	16	10.49	35°	CL	Crumpled Shale	379.44	1.706	Oblique
S94	2.62	4.62	30.185	16.68	18	20.6	28.23o	CL-ML	Crumpled Shale	324.96	0.806	Antidip
S95	2.47	25.61	53.43	15.4	24	54.54	10.54°	CH	Crumpled Shale	170.95	0.637	Antidip
S96	2.49	1.69	32.89	15.4	14	16.18	23.84°	ML	Crumpled Shale	190.315	0.661	Strike
S97	2.62	14.76	31.9	16.18	18	47.09	14.26°	CL	Sandstone	275.52	0.676	Strike
S98	2.52	10.67	34.2	17.16	16	39.48	22.42°	CL	Crumpled Shale	207.57	0.796	Strike
S99	2.56	4.61	27.97	15.79	17.23	3.04	41.63o	CL-ML	Crumpled Shale	350	1.236	Oblique
S100	2.4	19.94	41.79	16.18	18	37.76	16.31o	CL	Siltstone-Sandstone	183.42	0.64	Homoclinal
S101	2.53	3.6	29.62	15	18	13.73	27.9o	ML	Siltstone-Sandstone	177.313	0.749	Oblique
S102	2.68	3.8	20.2	17.26	14	30.41	24°	ML	Crumpled Shale	405.085	0.93	Strike
S103	2.5	10.23	25.96	17.27	16	50	13.33°	CL	Siltstone-Sandstone	455.552	0.658	Strike
S104	2.54	7.12	34.2	15.83	18	28.69	9.35°	ML	Shale-Sandstone	269.324	0.372	Strike
S105	2.52	14.3	48.115	16.78	16	18.64	32.21o	ML	Siltstone-Sandstone	345.16	0.904	Homoclinal
S106	2.49	16.99	42.87	15.3	22	51.49	15o	CL	Crumpled Shale	238.26	1.056	Homoclinal
S107	2.54	2.73	27.915	16.58	14	53.93	15.9°	ML	Siltstone-Sandstone	189.2	1.113	Oblique
S108	2.42	5.25	23.85	16.97	16	24.48	15.1°	CL-ML	Crumpled Shale	119.59	0.449	Antidip
S109	2.65	4.91	30.2	17.06	16	23.94	29.48°	CL-ML	Crumpled Shale	202.14	1.507	Oblique
S110	2.61	10.68	27.085	17.658	17	51.79	5.64°	CL	Sandstone	330	0.475	Antidip
S111	2.54	9.97	38.46	16.28	16	32.53	10.92°	ML	Sandstone	298.056	0.718	Homoclinal
S112	2.51	5.96	30.2	13.04	16	33.108	28.37°	CL-ML	Shale-Sandstone	259.516	1.554	Oblique
S113	2.68	11.07	35.1	15.79	18	34.53	27.24°	CL	Crumpled Shale	258.18	0.887	Oblique
S114	2.642	5.95	28.3	17.85	14	22.66	32.68°	CL-ML	Crumpled Shale	273.7	1.667	Antidip
S115	2.678	11.07	35.1	15.79	18	26.32	27.24°	CL	Crumpled Shale	258.18	0.825	Oblique

Sites	Specific Gravity	Plasticity Index (PI) (%)	Liquid Limit (%)	Unit weight (kN/m3)	OMC (%)	Cohesion (c) kN/m2	Angle of internal friction (ϕ°)	Soil types (USCS)	Rock types	SBC (kN/m2) for square footing	FoS under static and seismic conditions	Bedrock
S116	2.52	15.04	40.16	16.2	22	30.79	19.03°	CL	Crumpled Shale	206.595	1.057	Homoclinal
S117	2.42	8.42	26.67	17.76	12	32.99	29°	CL	Siltstone-Sandstone	579.411	1.55	Antidip
S118	2.44	6.78	27.27	16.58	25	34.43	11.47°	CL-ML	Shale-Sandstone	230.508	0.755	Oblique
S119	2.43	7.29	28.42	18.64	16	43.098	0.92°	CL	Sandstone	174.425	0.344	Oblique
S120	2.54	2.22	24.205	16.48	17.24	18.64	18.80°	ML	Siltstone-Sandstone	153.5	0.664	Antidip
S121	2.52	6.81	32.2	17.04	16	28.99	37.36°	CL-ML	Crumpled Shale	367.905	1.143	Oblique
S122	2.56	3.34	34.95	16.75	16	1.962	40.53°	ML	Siltstone-Sandstone	454.871	0.894	Oblique
S123	2.52	3.49	30.185	16.57	16	37.67	21.39°	ML	Shale-Sandstone	183.45	0.668	Oblique
S124	2.37	9.62	26.67	16.58	16	29.92	18.62°	CL	Siltstone-Sandstone	206.93	0.634	Homoclinal
S125	2.56	18.29	36.6	19.13	12	32.37	21.65°	CL	Shale-Sandstone	297.664	0.63	Homoclinal
S126	2.46	7.89	29.34	17.65	16	13.3	32.37°	CL	Siltstone-Sandstone	445.36	0.745	Antidip
S127	2.52	2.17	30.05	13.73	14	41.202	18.035°	ML	Sandstone	256.76	1.114	Homoclinal
S128	2.52	14.79	34.2	17.25	18	48.06	20.93°	CL	Shale-Sandstone	194.26	0.728	Antidip
S129	2.52	4.81	26.2	17.29	16	32.61	28.70°	CL-ML	Shale-Sandstone	264.028	1.535	Oblique
S130	2.52	0.96	22.45	13.43	14	33.84	28.025°	ML	Shale-Sandstone	356.352	0.798	Oblique
S131	2.53	7.61	28.6	12.65	16	35.316	7.36°	CL	Crumpled Shale	250.312	0.408	Oblique
S132	2.52	12.35	30.165	16.58	18	26.24	28.025°	CL	Shale-Sandstone	257.805	0.844	Oblique
S133	2.52	6.84	32.165	16.7	16	44.39	26.68°	CL-ML	Crumpled Shale	358.781	1.532	Oblique
S134	2.4	14.55	33.033	15.89	20	14.7	19.39°	CL	Crumpled Shale	201.59	0.539	Oblique
S135	2.53	8.4	28.05	17.9	14	28.45	19.79°	CL	Siltstone-Sandstone	216.508	0.647	Homoclinal
S136	2.15	8.54	28.59	17.75	14	9.9	35.29°	CL	Crumpled Shale	389.148	0.929	Oblique
S137	2.52	5.48	30.44	14.54	16	42.91	27.36°	CL-ML	Crumpled Shale	250.997	0.843	Oblique
S138	2.52	9.59	34.2	15.13	18	31.39	20.7°	ML	Crumpled Shale	254.257	0.699	Oblique

Sites	Specific Gravity	Plasticity Index (PI) (%)	Liquid Limit (%)	Unit weight (kN/m3)	OMC (%)	Cohesion (c) kN/m2	Angle of internal friction (ϕ°)	Soil types (USCS)	Rock types	SBC (kN/m2) for square footing	FoS under static and seismic conditions	Bedrock
S139	2.654	3.44	30.2	17.66	14	23.94	32.87°	ML	Crumpled Shale	285.71	0.961	Antidip
S140	2.53	12.71	32.37	17.55	16	44.39	24°	CL	Shale-Sandstone	305.11	0.767	Antidip
S141	2.45	4.23	22.99	17.46	14	12.94	35.45°	CL-ML	Crumpled Shale	307.85	0.958	Antidip
S142	3	8.27	35.99	17.15	18	42.18	17.69°	ML	Crumpled Shale	283	0.876	Strike
S143	2.52	7.12	34.2	15.83	18	28.69	29.35°	ML	Crumpled Shale	269.324	0.901	Strike
S144	2.43	10.91	43.36	15.3	22	29.9	17.06°	ML	Siltstone-Sandstone	192.65	0.53	Oblique
S145	2.64	4.53	35.2	15.99	18	6	49.9°	CL-ML	Siltstone-Sandstone	678.36	2.603	Oblique
S146	2.46	15.62	39.05	15.49	18	12.95	22.04°	CL	Siltstone-Sandstone	119.32	0.591	Antidip
S147	2.45	18.83	36.19	16.38	14	38.26	26.08°	CL	Sandstone	168.95	1.453	Strike
S148	2.55	2.88	32.88	17.85	17	1.95	49.48°	ML	Siltstone-Sandstone	489.56	0.976	Homoclinal
S149	2.66	16.05	42.71	15.2	18	53.76	3.49°	ML	Siltstone-Sandstone	229.802	0.921	Homoclinal
S150	2.43	15.13	30.44	16.57	20	32.94	13.6°	CL	Shale-Sandstone	259.86	0.834	Homoclinal
S151	2.65	17.1	44.3	14.72	22	42	24.52°	ML	Shale-Sandstone	254.26	1.074	Homoclinal
S152	2.45	14.8	39.31	15.18	20	55.92	7.7°	CL	Crumpled Shale	352.23	0.758	Oblique
S153	2.44	4.59	22.73	18.25	14	46.1	12.82°	CL-ML	Crumpled Shale	221.73	0.9	Oblique
S154	2.53	9.35	36.51	15.3	16	36.1	13.65°	ML	Crumpled Shale	183.44	0.506	Oblique
S155	2.8	10.73	33.21	17.75	14	23.67	37.56°	CL	Crumpled Shale	499.78	1.97	Oblique
S156	2.52	15.86	36.2	15.86	18	39.24	12.41°	CL	Crumpled Shale	207.48	0.557	Homoclinal
S157	2.53	8.37	36.28	16.08	20	30.9	28.035°	ML	Crumpled Shale	257.625	1.495	Strike
S158	2.52	4.76	30.52	15.4	20	34.34	20.7°	CL-ML	Crumpled Shale	254.7	0.931	Oblique
S159	2.55	7.13	29.476	17.85	16	20.6	22.78°	CL	Siltstone-Sandstone	414.802	0.662	Strike
S160	2.44	13.21	35.58	16.87	12	39.27	10.96°	CL	Crumpled Shale	245.18	0.472	Oblique

Sites	Specific Gravity	Plasticity Index (PI) (%)	Liquid Limit (%)	Unit weight (kN/m3)	OMC (%)	Cohesion (*c*) kN/m2	Angle of internal friction (ϕ°)	Soil types (USCS)	Rock types	SBC (kN/m2) for square footing	FoS under static and seismic conditions	Bedrock
S161	2.54	10.46	33.25	15.59	20	35.32	19.2°	CL	Siltstone-Sandstone	210	0.852	Oblique
S162	2.49	14.55	33.033	15.89	20	24.7	19.39°	CL	Crumpled Shale	201.59	0.539	Oblique
S163	2.52	5.62	25	17.85	14	19.67	21.27°	CL-ML	Crumpled Shale	419.46	0.692	Homoclinal
S164	2.55	1.33	29.232	16.48	16	29.43	26.61°	ML	Siltstone-Sandstone	304.61	0.724	Oblique
S165	2.26	16.89	40.28	17.15	20	51.93	6.86°	CL	Crumpled Shale	390.93	0.626	Homoclinal
S166	2.05	9.88	45.59	16.48	18	9.71	48.56°	ML	Shale-Sandstone	663.034	1.445	Oblique
S167	2.41	6.57	30.51	16.85	18	30.83	28.56°	CL-ML	Crumpled Shale	173.99	1.516	Antidip
S168	2.6	7.55	30.2	17.06	16	21.18	31.44°	CL	Crumpled Shale	236.49	0.9	Oblique
S169	2.51	10.18	38.51	16.68	20	27.76	19.59°	ML	Sandstone	216.83	1.055	Homoclinal
S170	2.59	7.63	34.316	16.08	20	40.74	11.99°	ML	Sandstone	146.715	0.564	Homoclinal
S171	2.59	8.69	30.745	17.17	16	24.52	31.59°	CL	Shale-Sandstone	402.5	1.626	Oblique
S172	2.54	17.29	50.75	16.97	22	42.67	15.64°	MH	Shale-Sandstone	205.45	1.001	Oblique
S173	2.47	9.92	27.05	17.95	16	24.27	27.36°	CL	Siltstone-Sandstone	244.31	0.702	Homoclinal
S174	2.52	12.35	30.165	16.58	18	26.24	28.025°	CL	Siltstone-Sandstone	257.805	1.456	Strike
S175	2.605	8.83	31.4	16.08	18	27.86	26.96°	CL	Crumpled Shale	216.32	0.722	Oblique
S176	2.52	11.01	32.16	15.91	18	37.76	27.7°	CL	Crumpled Shale	254.55	1.121	Oblique
S177	2.52	11.98	40.4	15.7	18	29.43	27.02°	ML	Crumpled Shale	248.37	1.433	Oblique
S178	2.52	11.02	36.165	16.58	18	31.63	26.67°	ML	Crumpled Shale	245.59	0.848	Oblique
S179	2.683	14.65	40.1	16.68	20	39.04	17.48°	ML	Crumpled Shale	285.94	0.598	Oblique
S180	2.628	4.16	25.4	17.26	16	20.01	32.74°	CL-ML	Crumpled Shale	291.19	1.653	Strike
S181	2.628	4.7	26.3	16.58	16	23.94	28.93°	CL-ML	Shale-Sandstone	215.76	0.739	Strike
S182	2.645	1.65	23.2	17.66	14	19.13	35.54°	ML	Crumpled Shale	349.09	1.176	Oblique

References:

1. A. Indira, N. Chandrasekaran, Infrastructure development in India: A systematic review, Lett Spat Resour Sci 16 (35) (2023), https://doi.org/10.1007/s12076-023-00357-5.
2. S.O. Ryding, ISO 14042 Environmental management• Life cycle assessment• life cycle impact assessment, Int. J. Life Cycle Assess 4 (1999) 307. [Google Scholar] [CrossRef].
3. H. Wang, X. Wang, C. Zhang, C. Wang, S. Li, Analysis on the susceptibility of environmental geological disasters considering regional sustainable development, Environ. Sci. Pollut. Res. 30 (2023) 9749–9762. [Google Scholar] [CrossRef] [PubMed].
4. M. Kumar, V. Krishnaveni, S. Muthukumar, Geotechnical Investigation and Numerical Analysis of Slope Failure: A Case Study of Landslide Vulnerability Zone in Kolli Hills, Tamil Nadu, J Geol Soc India 97 (2021) 513–519. https://doi.org/10.1007/s12594-021-1717-z.
5. A. Jaiswal, A.K. Verma, T.N. Singh, A critical review of rock mass classification systems for assessing the stability condition of rock slopes, Environ Earth Sci 83 (2024) 245. https://doi.org/10.1007/s12665-024-11532-2.
6. J.S. Thounaojam, S. Ibotombi, Influence of Clay on Soil Erodibility and Landslides: Some Examples from Manipur, Northeast India, Indian Geotech J (2024). https://doi.org/10.1007/s40098-023-00845-x.
7. H.M. Shiferaw, Study on the influence of slope height and angle on the factor of safety and shape of failure of slopes based on strength reduction method of analysis, Beni-Suef Univ J Basic Appl Sci 10 (31) (2021). https://doi.org/10.1186/s43088-021-00115-w
8. Y. Li, X. Wang, H. Mao, Influence of human activity on landslide susceptibility development in the Three Gorges area, Nat Hazards 104 (2020) 2115–2151. https://doi.org/10.1007/s11069-020-04264-6.

9. D.K Paul, Satish Kumar, Stability analysis of slope with building loads, Soil Dynamics and Earthquake Engineering 16 (6) (1997) 395-405. https://doi.org/10.1016/S0267-7261(97)000 08-0.
10. Dhiraj Singh, Yogendra Singh, Effects of building loads on the stability of hill slopes. Geo-Chicago (2016) 638-647. https://doi.org/10.1061/9780784480144.063.
11. Onglin Zhang, Runqiang Zeng, Xingmin Meng, Shufen Zhao, Shixin Wang, Jianhua Ma, Hong Wang, Effects of changes in soil properties caused by progressive infiltration of rainwater on rainfall-induced landslides, CATENA 233 (2023) 107475, https://doi.org/10.1016/j.catena.2023.107475.
12. X. Yang, L. Shuang, W. Huanran, S. Jinquan, L. Hanlong, Strength and Infinite slope stability of unsaturated soils, Int.J. of Geomech. 23 (12) (2023). https://doi.org/10.1061/IJGNAI.GMENG-90.
13. W. Huang, Ji Jian, Upper bound seismic limit analysis of shallow landslides with a new kinematically admissible failure mechanism, Acta Geotechnica 18 (6) (2022) 1-13. DOI:10.1007/s11440-022-01731-1
14. L. Zheng, L. Lin, L.Jingpei, Development of three-dimensional failure mechanisms and genetic algorithm for limit analysis of two-layer slopes, Natural Hazards 103 (11) (2020). DOI:10.1007/s11069-020-04126-1
15. J. Zeng, T. Chen, Y. Chen, New method and insight for stability analysis of compound slopes, Computer and Geotechnics (2024), DOI:10.1016/j.compgeo.2023.105874
16. A. Ahmadi, B. Abbasi, Comprehensive Analysis of Geoengineering Approaches for Unstable Slopes: A Real Case Study Investigating Geology and Geophysics, Utilizing Photogrammetry, and Assessing Potential Failures, Affiliation: Politecnico di Milano (2022), DOI:10.13140/RG.2.2.24050.27844
17. A. Ardestani, M. Amini, K. Esmaeili, A two-dimensional limit equilibrium computer code for analysis of complex toppling slope failures, Journal of Rock Mechanics and Geotechnical Engineering (2020),

DOI:10.1016/j.jrmge.2020.04.006

18. La Touche THD, Records of the Geological Survey of India, Geological Survey of India (GSI) 24(2) (1891).
19. R. Hack, Geomorphological and geological influences on the stability of slopes, Engineering Geology 57(1) (2000), 137–147. https://doi.org/10.1016/S0013-7952(00)00022-1.
20. L. Prandtl, Über die Härte plastischer Körper.” Nachr. Ges. Wiss. Goettingen, Math.-Phys. Kl. (1920) 74-85.
21. Terzaghi K, Theoretical soil mechanics, John Wiley and Sons, New York, London (1943), https://doi.org/10.1002/9780470172766
22. A.W. Skempton, The bearing capacity of clays, Building Research Congress, London 1 (1951) 180-189. https://doi.org/10.1680/sposm.02050.0008
23. G.G. Meyerhof, The ultimate bearing capacity of foundations, Geotechnique 2 (4) (1951) 301-332. https://doi.org/10.1680/geot.1951.2.4.301.
24. J.B. Hansen, A revised and extended formula for bearing capacity, Bulletin of the Danish Geotechnical Institute 28 (1970) 5–11.
25. A. Vesic, Analysis of ultimate loads of shallow foundations, Journal of the Soil Mechanics and Foundations Division, ASCE 99 (1) (1973) 45-73.
26. S. Yang, C. Wei, B. Leshchinsky, C. Kai, F. Zhang, Scale effects on the ultimate bearing capacity of rectangular footings placed on slopes, Comput Geotech 137 (5) (2021) 104254.
27. G.G. Meyerhof, Some recent research on the bearing capacity of foundations, Can Geo Tech J 1 (1) (1963) 16–26. https://doi.org/10.1139/t63-00.
28. O. Kusakabe, T. Kimura, H. Yamaguchi, bearing capacity of slopes under strip loads on the top surfaces. Soils Found 21(4) (1981) 29–40. https://doi.org/10.3208/sandf1972.21.4_29.
29. K. Georgiadis, Undrained bearing capacity of strip footings on slopes. J Geotech Geo Environ Eng 136 (5) (2010) 677–685. https://doi.org/10.1061/(ASCE)GT.1943-5606.0000269.

30. K. Georgiadis, An upper-bound solution for the undrained bearing capacity of strip footings at the top of a slope. Geotechnique 60(10) (2010) 801–806. https://doi.org/10.1680/geot.09.T.016.
31. B. Leshchinsky, bearing capacity of footings placed adjacent to c′-ϕ′ slopes. J Geotech Geo Environ Eng. (2015). https://doi.org/10.1061/(ASCE)GT.1943-5606.00013
32. B. Leshchinsky, Y. Xie, Bearing capacity for spread footings placed near c′-ϕ′ slopes. J Geotech Geoenviron Eng. (2017). https://doi.org/10.1061/(ASCE)GT.1943-5606.00015
33. H. Zhou, G. Zheng, X. Yin, R Jia, X Yang, The bearing capacity and failure mechanism of a vertically loaded strip footing placed on the top of slopes. Comput Geotech 94 (2018) 12–21.
34. S. Yang, B. Leshchinsky, K. Cui, F. Zhang, Y. Gao, Unified approach toward evaluating bearing capacity of shallow foundations near slopes. J Geotech Geoenviron Eng (2019). https://doi.org/10.1061/(ASCE)GT.1943-5606.000217.
35. A.W. Skempton, The $\phi_u = 0$ analysis for stability and its theoretical basis. In: Proceeding 2nd International Conference of Soil Mechanics and Foundation Engineering 1 (1948) 72-77.
36. G.G Meyerhof, The ultimate bearing capacity of foundations on slopes. In: 4th International conference on soil mechanics and foundation engineering 3 (1957) 384–386.
37. G.G Meyerhof, Ultimate bearing capacity of footings on sand layer overlying clay. Canadian Geotech J 11 (1974) 223–229. https://doi.org/10.1139/t74-018
38. A.S Vesic, Bearing capacity of shallow foundations. In: Winterkorn HF, Fang HY (eds) Foundation engineering handbook, Chap 3, 1st edn. Van Nostrand Reinhold Co., New York (1975).

39. IS 6403:1981, Code of practice for determination of bearing capacity of shallow foundations CED 43. Soil and Foundation Engineering.
40. W.J.M. Rankine, On the stability of loose earth, Philosophical Transactions of the Royal Society, London 147 (1885).
41. Eurocode: 7. BS-EN 1997-1:2004. Geotechnical design
42. C.C. Huang, F.Y. Menq, Deep-footing and wide-slab effects in reinforced sandy ground. J Geotech Geoenviron Eng 123 (1) (1997) 30–36.https://doi.org/10.1061/(ASCE)1090-0241(1997)123:1(30)
43. S. Oloo, D.G. Fredlund, J.K.M. Gan, Bearing capacity of unpaved roads. Canadian Geotech J 34 (3) (1997)398–407. https://doi.org/10.1139/t96-084
44. M.H. Wayne, J. Han, K. Akins, The design of geosynthetic reinforced foundations. In: Proceedings of ASCEs annual convention & exposition 76 (1998) 1–18.
45. X.L. Yang, H.Y. Jian, Upper bound solution for ultimate bearing capacity with modified Hoek-Brown failure criterion, Int J Rock Mech Mining Sci 42 (4) (2005) 550–560. https://doi.org/10.1016/j.ijrmms.2005.03.002
46. A.B. Cerato, A.J. Lutenegger, Bearing capacity of square and circular footings on a finite layer of granular soil underlain by a rigid base. J Geotech Geoenviro Eng ASCE 132(11) (2006)1496–1501. https://doi.org/10.1061/(ASCE)1090-0241(2006)132:11(1496)
47. S.K Vanapalli, F.M.O Mohamed, Bearing capacity of model footings in unsaturated soils, Exp Unsatur Soil Mech (2007) 483–493. https://doi.org/10.1007/3-540-69873-6_48.
48. E. Sherif, N. Gary, P. Vimalaraj, A simple bearing capacity equation, Geo-Denver conference (2007). https://doi.org/10.1061/40915(234)4
49. Q. Chen, An experimental study on characteristics and behavior of reinforced soil foundation. PhD thesis, Louisiana State University, USA (2007).

50. A. Kalinli, M.C. Acar, G. Zeki, New approaches to determine the ultimate bearing capacity of shallow foundations based on artificial neural networks and ant colony optimization. Eng Geol 117(1-2) (2011) 29–38. https://doi.org/10.1016/j.enggeo.2010.10.002
51. S. Ullah, M. khan, G. Rehman, A brief review of the slope stability analysis methods, Geological behavior 4 (2) (2020) 73–77, https://doi.org/10.26480/gbr.02.2020.73.77.
52. Talha Nalgire, Prasad Dahale, Aashish Mehta, Prashant Hiwase, Slope stability analysis by GeoSlope, Helix 10 (2020) 71–75, https://doi.org/10.29042/2020-10-1-71-75.
53. Ika Juliantina, Yulindasari Sutejo, Ratna Dewi, Bimo Adhitya, Reffanda Kurniawan, Identification of slope stability analysis, Int. J. Adv. Sci. Eng. Inf. Technol. 8 (3) (2018) 671–677, https://doi.org/10.18517/ijaseit.8.3.2685.
54. L. Chen, L. Mei, B. Zeng, et al., Failure probability assessment of landslides triggered by earthquakes and rainfall: a case study in Yadong County, Tibet, China,Sci. Rep. 10 (2020) 16531, https://doi.org/10.1038/s41598-020-73727-4.
55. Z.F. Xu, W.C. Cheng, L. Wang, Effect of straw reinforcement on the shearing and creep behaviors of Quaternary loess, Sci. Rep. 11 (2021) 19926, https://doi.org/10.1038/s41598-021-99318-5.
56. IS 14243 (part 2), "Selection and development of site for building in hill areas" (1995).
57. P. Digvijay, C. Guruprasd, N. Rupa, R. Pooja, An overview on methods for slope stability analysis, Int. J. Eng. Res. 6 (3) (2017), https://doi.org/10.17577/IJERTV6IS030496.
58. D.V. Griffiths, P.A. Lane, Slope stability analysis by finite elements, Geotechnique 49 (3) (1999) 387–403.

59. Shovon Halder, M. Imam, Md Basir, A detailed analysis of slope stability using finite element method (FEM), CUET, Bangladesh (2016).
60. X. Liu, M. Su, Double strength reduction method for slope stability analysis based on water content variation: a study and engineering application, Water 15 (6) (2023) 1194, https://doi.org/10.3390/w15061194.
61. W.J. Xu, S. Wang, M. Bilal, LEM-DEM coupling for slope stability analysis, Sci.China Technol. Sci. 2019 (2019) 62, https://doi.org/10.1007/s11431-018-9387-2.
62. Y. Wang, Y. Li, J. Chen, Comprehensive analysis method of slope stability based on the limit equilibrium and finite element methods and its application, Open J. Civ. Eng. 13 (2023) 555–571, https://doi.org/10.4236/ojce.2023.134040.
63. P. Sudani, K.A. Patil, Y.A. Kolekar, Parametric study of the slope stability by limit equilibrium finite element analysis, Recent Trends in Construction Technology and Management 260 (2023) 767–777, https://doi.org/10.1007/978-981-19-2145-2_58.
64. H. Slavka, K. Kamila, K. Eva, H. Iveta, Analysis of slope stability, Civ. Environ. Eng. 0 (0) (2021), https://doi.org/10.2478/cee-2021-0020.
65. Amir Reza Beyabanaki, LEM stability analysis of landslides induced by earthquakes: impact of a weak layer, American Journal of Engineering Research 10 (5) (2021) 257–268.
66. T.K. Koca, M.Y. Koca, Comparative analysis of finite element and limit equilibrium method for heavily fractures rock slope, J. Earth Syst. Sci. 129 (49) (2020), https://doi.org/10.1007/s12040-019-1314-3.
67. J.M. Duncan, Soil slope stability analysis, Landslides: Investigation and Mitigation. Chapter, 13 (1996) 337–371.
68. W. Fellenius, Erdstatische Berechnungen mit Feng of Reibung und Kohasion, Ernst, Berlin, (1927).

69. A.W. Bishop, The use of the slip circle in the stability analysis of earth slopes, Geotechnique 5 (1) (1955) 7–17.
70. N. Janbu, Slope Stability Computations. (Geoteknikk, NTH), Soil Mechanics and Foundation Engineering, Technical University of Norway, 1968.
71. N.R. Morgenstern, V.E. Price, The analysis of the stability of general slip surfaces, Geotechnique 15 (1) (1965) 77–93.
72. E. Spencer, A method of analysis of the stability of embankments, assuming parallel interslice forces, Geotechnique 17 (1967) 11–26.
73. S.K. Sarma, Stability analysis of embankment and slopes, Geotechnique 23 (3) (1973) 423–433. Series, No. 46.
74. S.Y. Liu, L.T. Shao, H.J. Li, Slope stability analysis using the limit equilibrium method and two finite element methods, Comput. Geotech. 63 (2015) 291–298.
75. J.M. Duncan, State of the art: limit equilibrium and finite-element analysis of slopes, J. Geotech. Eng., ASCE 122 (7) (1996) 577–596.
76. R.S. Bidreddy, S.H. Sanni, Seismic analysis of multi-storey building on sloping ground with ground, middle and top soft storey, Sustainability Trends and Challenges in Civil Engineering 162 (2022) 149–165, https://doi.org/10.1007/978-981-16-2826-9_11.
77. B.G. Birajdar, S.S. Nalawade, Seismic analysis of buildings resting on sloping ground. 13th World Conference on Earthquake Engineering Vancouver, B.C, 2004. Paper No. 1472.
78. P. Roshan, S. Pal, Structural challenges for seismic stability of buildings in hilly areas, Environ. Sci. Pollut. Res. 30 (2023) 99100–99126, https://doi.org/10.1007/s11356-022-23263-7, 2023.
79. L. Pachuau, Zonation of Landslide Susceptibility and Risk Assessment in Serchhip town, Mizoram. J Indian Soc Remote Sens 47 (2019) 1587–1597. https://doi.org/10.1007/s12524-019-00996-6
80. Andsera Adugna Mekonnen, Tarun Kumar Raghuvanshi, Karuturi Venkata Suryabhagavan, Tibebu Kassawmar, GIS-based landslide susceptibility zonation

and risk assessment in complex landscape: A case of Beshilo watershed, northern Ethiopia, Environmental Challenges 8 (2022) 100586. https://doi.org/10.1016/j.envc.2022.100586.

81. S. Das, S. Sarkar, D.P. Kanungo, A critical review on landslide susceptibility zonation: recent trends, techniques, and practices in Indian Himalaya. Nat Hazards 115 (2023) 23–72. https://doi.org/10.1007/s11069-022-05554-x
82. L. Shano, T.K. Raghuvanshi, M. Meten, Landslide susceptibility evaluation and hazard zonation techniques – a review. Geoenviron Disasters **7** (18) (2020). https://doi.org/10.1186/s40677-020-00152-0
83. Irjesh Sonker, Jayant Nath Tripathi, Anil Kumar Singh, Landslide susceptibility zonation using geospatial technique and analytical hierarchy process in Sikkim Himalaya, Quaternary Science Advances 4 (2021) 100039, https://doi.org/10.1016/j.qsa.2021.100039.
84. Shano, Leulalem, Landslide susceptibility evaluation and hazard zonation techniques -a review. 7 (19) (2020).
85. F. Guzzetti F, A. Carrara, M. Cardinali, P. Reichenbach, Landslide hazard evaluation: a review of current techniques and their application in a multiscale study, Central Italy. Geomorphology 31 (1999) 181–216.
86. S. Sarkar, D.P Kanungo, G.S Mehrotra, Landslide hazard zonation: a case study in Garhwal Himalaya, India. Moun Res Dev 15 (4) (1995) 301–309.
87. D.P. Kanungo, M.K Arora, S. Sarkar, R.P Gupta RP, A comparative study of conventional, ANN black box, fuzzy and combined neural and fuzzy weighting procedures for landslide susceptibility zonation in Darjeeling Himalayas. Eng Geol 85 (2006) 347–66.
88. T.K Raghuvanshi, J. Ibrahim, D. Ayalew, Slope stability susceptibility evaluation parameter (SSEP) rating scheme—an approach for landslide hazard zonation. J Afr Earth Sci 99 (2014a) 595–612.

89. P. Aleotti, R. Chowdhury, Landslide hazard assessment: summary review and new perspectives. Bull Eng Geol Environ 58 (1) (1999) 21–44.
90. J. Corominas, C.J Van Westen, P. Frattini, L. Cascini, J.P Malet, S. Fotopoulou S, Catani F, van den Eeckhaut M, Mavrouli OC, Agliardi F, Pitilakis K, Winter MG, Pastor M, Ferlisi S, Tofani V, Hervás J, Smith JT (2014) Recommendations for the quantitative analysis of landslide risk: bull Eng. Geol Environ 73(2) (2014) 209–63.
91. P. Reichenbach, M. Rossi, B.D Malamu, M. Mihir, F. Guzzetti, A review of statistically-based landslide susceptibility models. Ear Sci Revs 180 (2018) 60–91.
92. H. Laldintluanga, F. Lalbiakmawia, F. Lalbiaknungi, Landslide hazard zonation along state highway between Aizawl city and Aibawk town, Mizoram, India using geospatial techniques. 5 (2018) 342-355.
93. J. Barman, B. Biswas, J. Das, Mizoram, the Capital of Landslide: A Review of Articles Published on Landslides in Mizoram, India. In: Das, J., Bhattacharya, S.K. (eds) Monitoring and Managing Multi-hazards. GIScience and Geo-environmental Modelling. Springer, Cham (2023) https://doi.org/10.1007/978-3-031-15377-8_6
94. Z.D Laltanpuia, C. Lalrokima, F. Lalbiakmawia, Landslide Hazard Zonation (LHZ) Of Saiha District, Mizoram, India Using Remote Sensing and GIS. International Journal of Engineering Science Advanced Computing and Bio-Technology, (2016) 8724.
95. R. Lallianthanga, Z.D. Laltanpuia, Landslide Hazard Zonation of Lunglei Town, Mizoram, India Using High Resolution Satellite Data (2013) 148-159.
96. Lalramngheta, A. Kumar, S. Dangayach, D. Raj, Landslide Hazard Zonation Mapping of Champhai District of Mizoram, India. In: Shukla, S.K. Raman, S.N. Bhattacharjee, B. Singh, (eds) Recent Developments in Geotechnics and Structural Engineering. TRACE 2022. Lecture Notes in Civil Engineering, (2023) 338. Springer, Singapore.

https://doi.org/10.1007/978-981-99-1886-7_19

97. A.S. Ibrahim, A.A Mus, A.Y Abdulfata, Developing soft-computing regression model for predicting soil bearing capacity using soil index properties. Model Earth Syst Environ 9 (2023) 1223–1232. https://doi.org/10.1007/s40808-022-01541-0
98. H. Fattahi, F. Malekmahmoudi, H. Ghaedi, Lateral bearing capacity of piles in soft saturated clay by two optimization algorithms. Iran J Eng Geol 16 (1) (2023) 17–30.
99. H. Fattahi, Applying computational intelligence methods to evaluate lateral load capacity for a pile. Soft Comput 27 (13) (2023) 8919–8929. https://doi.org/10.1007/s00500-022-07801-6.
100. F. Hattahi, H. Ghaedi, Improving predictions of geogrid-reinforced stone column bearing capability: a comparative analysis of RES and regression methods. Int J Optim Civ Eng 13 (4) (2023) 497–518.
101. R.A Mozumder, A.S. Laskar, M. Hussain, Empirical approach for strength prediction of geopolymer stabilized clayey soil using support vector machines. Constr Build Mater 132 (2017) 412–424. https://doi.org/10.1016/j.conbuildmat.2016.12.012.
102. R.A. Mozumder, A.S. Laskar, Prediction of unconfined compressive strength of geopolymer stabilized clayey soil using artificial neural network. Comput Geotech 69 (2015) 291–300. https://doi.org/10.1016/j.compgeo.2015.05.021
103. NDMA, Catalogue of building typologies in India: seismic vulnerability assessment of building types in India. A report submitted by the Seismic Vulnerability Project Group of IIT Bombay, IIT Guwahati, IIT Kharagpur, IIT Madras and IIT Roorkee to the National Disaster Management Authority (2013).
104. P. Sultana, A.K Dey, D. Kumar, Empirical approach for prediction of bearing pressure of spread footings on clayey soil using artificial intelligence (AI) techniques. Results Eng 15 (2022) 100489.

https://doi.org/10.1016/j.rineng.2022.100489

105. M. Das, A.K. Dey, Prediction of bearing capacity of stone columns placed in soft clay using ANN model. Geotech Geol Eng 36 (6) (2018) 1845–1861. https://doi.org/10.1007/s10706-017-0436-0

106. J. Yao, Precision analysis and parameter inversion in the stepwise deployment of a mixed constellation. Open J Stat 3 (6) (2013) 390–397. https://doi.org/10.4236/ojs.2013.36046.

107. A. Saltelli, M. Ratto, T. Andres, F. Campolongo, J Cariboni, Global Sensitivity analysis: the primer. John Wiley & Sons, Chichester, (2008) https://doi.org/10.1111/j.1751-5823.2008.00062_17.x.

108. M.O Akinwande, G.D. Hussaini, S.U Gulumbe, Identifying the limitation of stepwise selection for variable selection in regression analysis, Am J Theor Appl Stat 4 (5) (2015) 414–419. https://doi.org/10.11648/j.ajtas.20150405.22

109. H. Akaike, Information theory and an extension of the maximum likelihood principle. In: Akaike H, Parzen E, Tanabe K, Kitagawa G (eds) Selected papers of hirotugu akaike. Springer, New York, (1998) 199–213. https://doi.org/10.1007/978-1-4612-1694-0_15.

110. R. Tibshirani, Regression Shrinkage and Selection via the Lasso. Journal of the Royal Statistical Society: Series B (Methodological), 58 (1996) 267-288. https://doi.org/10.1111/j.2517-6161.1996.tb02080.x.

111. T. Hastie, R. Tibshirani, R and J. Friedman, The Elements of Statistical Learning: Data Mining, Inference, and Prediction (2nd ed.). Springer (2009).

112. G. James, D. Witten, T. Hastie and R. Tibshirani, An Introduction to Statistical Learning: With Applications in R. Springer (2013).

113. IS: 1893 (part 1), Criteria for Earthquake Resistant Design of Structures, (2016).

114. AMC Building Regulations, Building Requirements, 28 (2012), Chapter - II.

115. H. Slavka, P. Eva, Impact of shear strength parameters on slope stability, MATEC Web of Conferences 310 (2020) 00040, https://doi.org/10.1051/matecconf/202031000040.

116. S. Hany, D. Braja, Slope stability analysis under external static surcharge,Advanced Research on Shallow Foundations (Proceedings of the 2nd GeoMEast International Congress and Exhibition on Sustainable Civil Infrastructures, Egypt 2018 – The Official International Congress of the Soil-Structure Interaction Group in Egypt (SSIGE)) 5 (8) (2019) 89–102, https://doi.org/10.1007/978-3-030-01923-5_8.

117. H.M. Shiferaw, Study on the influence of slope height and angle on the factor of safety and shape of failure of slopes based on strength reduction method of analysis, Beni-Suef Univ J Basic Appl Sci 10 (31) (2021), https://doi.org/10.1186/s43088-021-00115-w.

118. B. Yang, J. Hou, Z. Zhou, Influence of different soil properties on the failure behavior of deposit slope under earthquake after rainfall, J. Mt. Sci. 20 (2023) 65–77, https://doi.org/10.1007/s11629-021-7243-z.

119. NRSA, Atlas on Landslide Hazard Zonation mapping in the Himalayas of Uttaranchal and Himachal Pradesh States using remote sensing and GIS, Hyderabad: National Remote Sensing Agency, (2001).

120. E. B. Joyce, R. S. Evans, Some areas of landslide activity in Victoria, Australia. Proceedings, Royal Society, Victoria, 88 (1& 2) (1976) 95–108.

121. Bureau of Indian Standards IS 2132: Methods of sampling soils for soil investigations. New Delhi: Bureau of Indian Standards (1972).

122. ASTM International, ASTM D1587/D1587M-15, Standard Practice for Thin-Walled Tube Sampling of Fine-Grained Soils for Geotechnical Purposes, ASTM International, West Conshohocken, PA (2015).

123. ASTM International, ASTM D4767-11, Standard Test Method for Consolidated Undrained Triaxial Compression Test for Cohesive Soils, ASTM International, West Conshohocken, PA (2020).

124. ASTM International, ASTM D698-12, Standard Test Methods for Laboratory Compaction Characteristics of Soil Using Standard Effort, ASTM International, West Conshohocken, PA (2021).

125. ASTM International, ASTM D854-23, Standard Test Methods for Specific Gravity of Soil Solids by Water Pycnometer, ASTM International, West Conshohocken, PA (2023).

126. ASTM International, ASTM D4318-17e1, Standard Test Methods for Liquid Limit, Plastic Limit, and Plasticity Index of Soils, ASTM International, West Conshohocken, PA (2018).

127. Bureau of Indian Standards, IS 1498:1970 — Code of Practice for Classification and Identification of soils for general Engineering Purposes, BIS, New Delhi, India (1970).

128. Bureau of Indian Standards, IS 6403:1981 — Code of Practice for Determination of Bearing Capacity of Shallow Foundations, BIS, New Delhi, India (1981).

BRIEF BIO-DATA

PERSONAL DETAILS

Name : K. Zirsangzeli

Father Name : K. Lalchhuanthanga

Contact : 91+8794013624

ziri.kingbawl@gmail.com

Present Address : H-No: K-243

Locality: Mualpui Bethel, ITI Veng

PO: Tlangnuam

Dist: Aizawl

Pin: 796001, Mizoram

Sex : Female

Nationality : India

Marital Status : Single

Educational Background

(a) B. E : Dr. Ambedkar Institute of Technology, VTU, Karnataka, India

(b) M.Tech : Bharath University, Chennai, Tamil Nadu, India

(c) Ph. D. Course work: SGPA of 9.00.

Present Occupation Details

Organization : Mizoram University

Rank : Guest Faculty, Department of Civil Engineering

Job Profile : Teaching and management of B.Tech. Courses of Department of Civil Engineering, Mizoram University

LIST OF PUBLICATIONS

Journal Publications

1. **K. Zirsangzeli**, R. Ramhmachhuani, R.A. Mozumder, Application of regression techniques for bearing capacity prediction in Aizawl, Indian Geotech. J. (2024). [SCI, Scopus]**.** https://doi.org/10.1007/s40098-023-00861-x
2. **K. Zirsangzeli**, Rebecca Ramhmachhuani, Ruhul Amin Mozumder, H. Laldintluanga, Impact of building topologies on hill slope stability in Aizawl city, Results in Engineering, Volume 23,2024,102744, ISSN 2590-1230 [SCI, Scopus] https://doi.org/10.1016/j.rineng.2024.102744.
3. **K. Zirsangzeli**, Rebecca Ramhmachhuani, Assessment of different methods for determining bearing capacity for shallow foundation on hill slope, IJESE , Vol. 12(2), 12-18.10.35940/ijese.A3823.13020125
4. **K. Zirsangzeli**, Rebecca Ramhmachhuani, Ruhul Amin Mozumder, H. Laldintluanga, F.Lalbiakmawia, Zonation mapping of vulnerability of slope with building loads in Aizawl city, Tanz research journal, Vol.11 (9), 114-136. DOI:10.6084/doi.25.11.9.TANZ2202890

Conference Publications

1. **K. Zirsangzeli**, Rebecca Ramhmachhuani, "Assessment of Selected Hill Slopes Stability," 2nd International Conference on Innovative Research in Engineering & Technology (ICIRET-22) organized by Institute for Engineering Research and Publication (IFERP) held during 15th -16th July, 2022. **(Paper presented)**

2. **K. Zirsangzeli**, Rebecca Ramhmachhuani, "Assessment of different methods for determining bearing capacity for shallow foundation on hill slope," International Conference Sustainable Infrastructure: Innovations, Opportunities, and Challenges (SIIOC 2023) held on 20th -21st April, 2023 at NITK, Surathkal. **(Paper presented)**

3. **K. Zirsangzeli**, Rebecca Ramhmachhuani, "Impact of building topologies on hill slope stability in Aizawl city" International Conference on Geo-disasters and Construction Engineering (ICGCE) held on 7th -8th June, 2024 at Waterloo, Ontario, Canada. **(Paper presented)**

PARTICULARS OF THE CANDIDATE

NAME OF THE CANDIDATE	: K. ZIRSANGZELI
DEGREE	: Ph.D
DEPARTMENT	: CIVIL ENGINEERING
TITLE OF THESIS	: VULNERABILITY OF SLOPES WITH BUILDING LOADS IN AIZAWL
DATE OF ADMISSION	: 31st AUGUST, 2019
APPROVAL OF RESEARCH PROPOSAL	:
1. DRC	: 30th APRIL, 2021
2. BOS	: 07th MAY, 2021
3. SCHOOL BOARD	: 20th MAY, 2021
MZU REGISTRATION NO	: 1900352
PHD REGISTRATION NO & DATE	: MZU/PhD/1616 of 01.08.2019
EXTENSION (IF ANY)	: NO

HOD

Civil Engineering Department

Mizoram University

VULNERABILITY OF SLOPES WITH BUILDING LOADS IN AIZAWL

AN ABSTRACT SUBMITTED IN PARTIAL FULFILMENT OF THE REQUIREMENTS FOR THE DEGREE OF DOCTOR OF PHILOSOPHY

K. ZIRSANGZELI

MZU REGISTRATION NO: 1900352

Ph.D REGISTRATION NO: MZU/PhD/1616 of 01.08.2019

DEPARTMENT OF CIVIL ENGINEERING
SCHOOL OF ENGINEERING AND TECHNOLOGY

NOVEMBER, 2024

VULNERABILITY OF SLOPES WITH BUILDING LOADS IN AIZAWL

By
K. Zirsangzeli
Department of Civil Engineering

Supervisor
Dr. Rebecca Ramhmachhuani

Co-Supervisor
Dr. Ruhul Amin Mozumder

SUBMITTED
IN PARTIAL FULFILMENT OF THE REQUIREMENT OF THE DEGREE OF DOCTOR OF PHILOSOPHY IN CIVIL ENGINEERING,
MIZORAM UNIVERSITY, AIZAWL

Aizawl, the capital and most populus city of Mizoram state has regularly witnessed failure of slopes characterized by its steep slope and erosive nature of slope forming material. In most of the cases these failures can be attributed to inadequate slope management and improper construction practices, often undertaken without comprehensive site investigations or assessments of soil properties, including bearing capacity and shear strength. Several works have been carried out in previous studies where zonation maps for slope vulnerability in hilly areas was generated by considering geo-environmental factors such as land use, land cover, natural drainage, bedrock etc. However, the existing studies often neglect the critical triggering factors such as building loads, earthquake loads, bearing capacity of soil and soil characteristics of the site. This omission is particularly crucial for areas like Aizawl, which lies in seismic zone V and has slopes ranging from 15° to 45° where building construction occurs on or near the slopes. In order to address the above identified research gap, the primary objective of this study was to develop a zonation map of slope vulnerability for the study area. This map takes into account various factors, including safe bearing capacity (SBC) of soil, factor of safety (FoS), slope morphology, annual rainfall data, lithology, and structural features such as bedrock.

A comprehensive study has been conducted to assess the vulnerability of slopes subjected to building loads in Aizawl city, spanning in an area of 129.91 sq.km and is under the jurisdiction of the Aizawl Municipal Corporation (AMC). Situated in a hilly region, Aizawl has experienced significant construction activity on or near the slopes with inclination ranging from 15° to 45°. This topographical and geological setting has led to numerous slope failures, primarily exacerbated by construction practices. Therefore, evaluating the vulnerability of slopes subjected to building load under both static and seismic conditions is of key importance. To this end, 182 different sites were identified in Aizawl city for detailed analysis of slope stability and subsequent evaluation of vulnerability of the slopes subjected to building load. Various factors influencing slope vulnerability such as topography, building loads, soil bearing capacity and characteristics, lithology, structural features, and rainfall were examined through a combination of field investigations, laboratory testing, and by collection of existing data. Soil samples from all 182 selected sites were collected and subjected to laboratory tests to determine essential engineering parameters related to slope stability. The data from laboratory tests, along with field observations of slope morphology, were used for prediction of the bearing capacity of soil based on a data driven regression technique. To this end, two different methods namely stepwise linear regression and Lasso regression were adopted for developing the bearing capacity prediction model using MATLAB software. Performance comparison of stepwise regression with Lasso regression suggested that stepwise regression performed marginally better than Lasso regression in terms model complexity. However, based on the input parameters included in the model equation, it may be concluded that Lasso regression has an edge over stepwise regression in simulating the physical process in bearing capacity prediction for the data set.

In hilly regions like Aizawl city, wherein houses are mostly built on slopes, the layout of building plays a crucial role in slope stability. Building failures in Aizawl often results from a) non-engineered alterations of slopes b) faulty foundation construction without soil investigation or design. Many residents build and reside on slopes without considering the soil characteristics. To address this, a study was conducted to examine the impact of two common building types - step-back buildings and step-back setback buildings on slope stability in Aizawl. The study evaluated slope stability under the conditions of free slope and slope stability with building loads under static and seismic conditions using Slope/W software. To account for building loads, a reinforced cement concrete (RCC) model with a G+6 story configuration was developed for both building types. The building loads were determined through analysis using structural software “STAAD Pro.vi8”. The study found that sites with lower slope angles generally demonstrated better stability, but there were cases where steeper slopes showed better stability due to superior shear strength values for identical slope geometry parameters. Sites with higher cohesion values exhibited better stability in free slope analysis, while those with higher internal friction angles showed better stability under building loads of both static and seismic condition. To validate the above findings, a sensitivity analysis of shear strength parameters of soil was performed.

Moreover, a sensitivity analysis along with a comparative analysis between step-back and step-back setback building types were also conducted. The results indicated that step-back setback buildings offered better stability compared to step-back buildings alone. This suggests that implementing step-back setback buildings could significantly improve slope stability in a hilly area like Aizawl.

To investigate the rock characteristics of the selected sites, a geological structural assessment survey was conducted, wherein the dip of the bedrock was measured to understand its relative orientation w.r.t that of the slope. The lithology of the sites was determined based on the rock exposure pattern observed in the study area, corroborated by existing lithological data of the study area prepared by Mizoram Remote Sensing Application Centre (MIRSAC). To study the impact of rainfall infiltration on slope vulnerability, annual average rainfall data of the study area collected from the Mizoram State Meteorological Centre (Sc. & Tech.) was incorporated in the study. The slope vulnerability assessment includes both the qualitative and quantitative methods, incorporating heuristic techniques (expert evaluations), statistical methods (data-driven approaches), and deterministic methods. In addition to field and laboratory investigations, numerical validation was performed using statistical analyses and appropriate numerical tools. Considering the various factors having significant impact on slope vulnerability, a final zonation map illustrating slope vulnerability subjected to building loads was generated for the study area by using ArcGIS software. Integrating all the controlling parameters and assigning different weightage to each class, the final zonation map of slope vulnerability with building loads in Aizawl city was developed and classified into the vulnerability categories such as ‘Very High’, ‘High’, ‘Moderate’ and ‘Low’ vulnerability zones. Furthermore, the statistics of each area occupied by different vulnerability zone were given in the form of sq.km and percentage (%). The zonation map of slope vulnerability indicates that 24.78 sq.km of the study area with “Very High vulnerability”. On the other hand, areas categorized as High, Moderate, and Low vulnerability cover 68.01 sq.km, 30.89 sq.km, and 6.23 sq.km, respectively.